NASA CR-54189
Astro Met 9-1-0032

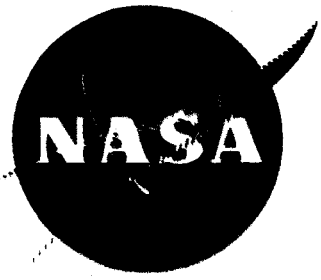

DEVELOPMENT OF LARGE SIZE FINISHED POROUS TUNGSTEN IONIZERS

by

John W. Graham and Raj K. Malik

prepared for

NATIONAL AERONAUTICS AND SPACE ADMINISTRATION

CONTRACT NAS 3-4115

Astro Met Associates Inc.

5390 GLENDALE-MILFORD ROAD
CINCINNATI 15, OHIO PHONE 772-1848

NASA CR-54189
Astro Met 9-I-0032

FINAL REPORT

DEVELOPMENT OF LARGE SIZE FINISHED POROUS TUNGSTEN IONIZERS

by

John W. Graham
Raj K. Malik

prepared for

NATIONAL AERONAUTICS AND SPACE ADMINISTRATION

March 18, 1965

Contract NAS 3-4115

Technical Management
NASA Lewis Research Center
Cleveland, Ohio

Spacecraft Technology Division
Albert E. Anglin, Jr.

ASTRO MET ASSOCIATES INC.
500 Glendale-Milford Road
Cincinnati, Ohio 45215

ACKNOWLEDGEMENT

This work was conducted on Contract NAS 3-4115 by Astro Met Associates Inc. of Cincinnati, Ohio, for the National Aeronautics and Space Administration, Electrical Propulsion Procurement Office, Lewis Research Center, under the direction of Albert E. Anglin, Jr., Project Manager, and Thomas Riley, Project Engineer.

The work was conducted under the technical direction of John W. Graham, with Raj K. Malik as project engineer. Acknowledgement is made to Robert E. Fogle for his major contributions in specimen processing, to Gladstone Laboratory for metallographic work, to LeDoux Company for spectrographic analysis, and to the Abar Corporation for scale-up vacuum sintering.

ABSTRACT

DEVELOPMENT OF LARGE SIZE FINISHED POROUS TUNGSTEN IONIZERS

by

John W. Graham
and
Raj K. Malik

25276

Several large size porous tungsten emitter plates almost 4 square inches in area were prepared for NASA evaluation as a result of extensive powder metallurgy and chemical processes. The tungsten structural characteristics met, and in some cases exceeded, contract objectives. The structures exhibited mean pore diameters from 1.1 to 1.7 microns in discrete levels with very narrow desirable ranges, open pore volume between 19 and 24%, pore count between 0.9 to 4 x 10^7 pores/cm^2 and transmission coefficient between 11 & 22 x 10^{-5} plus thermal stability to at least 2750°F.

The process consists of milling uniformly ultra fine tungsten, copper and nickel powders, hydrostatically pressing, liquid phase sintering at 2150 to 2250°F for periods from 5 to 25 hours, hydrochloric and then nitric acid leaching to efficiently remove the copper and nickel phase, reducing in wet hydrogen at 1800°F and vacuum bleaching at 2750°F. The process allows close control of grain size, pore diameter and pore volume. In addition, it results in almost spherical tungsten grains and is believed to be easily reproducible.

TABLE OF CONTENTS

LIST OF FIGURES

LIST OF TABLES

1.0 Introduction

The development of a stable micro porosity in sintered tungsten compacts has become very important for cesium propellant ionizers in ion propulsion systems[1-7]. Low density emitter components with 1 micron diameter pores result from closely controlled powder metallurgy approaches. Those approaches which have been most important in the sintered tungsten industry, involve technical steps which directly produce structures which continue to densify with time at cesium ionizer temperature[8-14]. High density sintered hydrogen reduced tungsten compacts result from close attention to such factors as pH, chemical purity and resulting compound particle size in the chemical purification processes; to time-temperature and atmospheric conditions[12] in the reducing cycle; to agglomerate size, particle size and shape, lubricants, binders, dies, rates, and degree of pressing in the forming cycle; and finally, to time-temperature and atmosphere in the sintering cycle. In addition, there are many interdependent relationships between most of these factors[13]. Until the past twelve months or so, most porous tungsten emitter structures were prepared using process factors described above. This resulted in high porosity sintered metal which was basically unstable and continued to sinter at temperatures above its recrystallization temperatures since such structures are at high energy levels[8-14].

Sintered porous tungsten at elevated temperatures continues to densify by three diffusion mechanisms. These are surface, grain boundary and volume diffusion mechanisms, each of which is governed by specific activation energy levels. As sintering temperature increases, these diffusion transport mechanism contributions shift toward the latter, ie, volume diffusion. In addition to these controlling factors, composition also highly influences diffusion constants. The continued sintering of porous tungsten is therefore dependent upon the diffusion rates which in turn are related to the above described factors and temperature as shown in the following Arrhenius equation[15].

$$D = Ae^{\frac{-Q_x}{RT}}$$

Where: D = diffusion constant
A = Dushman-Langmuir Factor (composition dependent)
Q_x = activation energy - surface, grain or volume
T = absolute temperature
e = natural logarithm
R = gas constant

Tungsten self diffusion activation energy levels Q_x are [16]:
surface -66, grain boundary -100, and volume -133 Kilo cal/mole.

According to Anglin[22] and Brophy[21], when porous sintered materials have been densified to 80% of above of their theoretical density (is) with less than 20% porosity, the densification controlling rate is probably by grain boundary diffusion with an activation energy of 90-100 Kilo calories/mole. Since volume diffusion activation energies are so high, densification at ion emitter temperature by this phenomenon should not be significant.

Grain boundary diffusion is, therefore, the predominate densification phenomenon for porous tungsten ion emitters and would be highly dependent upon metallurgical purity, vacancy levels and subgrain structures. These factors influence the diffusion rate by influencing both Q_{gh} activation energy and A, the Dushman-Langmuir factor.

Astro Met's approach toward developing a uniformily porous stable, low grain size - low pore diameter, sintered tungsten is that of decreasing the internal structural energy levels by two factors. One is that of producing uniform spherical grains. This would reduce the quantity of contact points as well as lower the contact angle. It is generally accepted that bonded spherical tungsten grains offer improved ion emitter stability[1, 3, & 18]. The other controlled factor in Astro Met's approach is that of lowering the internal lattice vacancy level. These two factors are brought about by the liquid phase sintering of tungsten using copper and nickel as the auxilliary liquid metal phase. This approach was originally developed by Smithell's[8,9,19,20] for producing high density tungsten compacts at relatively low sintering temperatures. The copper-nickel phase can dissolve tungsten to various saturation levels, dependent upon the ternary alloy ratios and temperatures. The finer particles are generally dissolved, and continuously precipitated upon intermediately sized tungsten grains. These tend to grow toward some average size which is proportioned to equilabrium levels that have not specifically been determined. Brophy[21] suggests that tungsten solubility in the molten copper-nickel phase would be directly related to solubility of tungsten in the available nickel, and the volume of copper nickel phase.

This liquid phase sintering produces spherical grains which can be nearly single crystal. Astro Met's hypothesis was that after such W structures were developed, the copper-nickel phase could be removed to relatively low levels, leaving a porous structure with relatively high activation energies. The higher activation energies would result, even in fine grain structures, by increasing the grain to grain contact angle by spheroidization and by lowering the lattice vacancy level by creating single crystal grains. By creating

this structure and then removing the copper-nickel phase, the surface and grain boundary diffusion mechanisms should be effectively terminated even if the structure was of low grain size and high pore volume.

A further critical factor in Astro Met's approach was that of reducing the copper and particularly the nickel concentrations to very low levels. This was important in order that the stable porous tungsten structure could be densified only by volume diffusion at the high activation energy level of 133 kilocalories/mole. This would, therefore, insure stability for thousands of hours at ion emitter temperatures. Small nickel concentrations have been shown[22] to lower tungsten grain boundary diffusion activation energy levels from variously reported levels of 90-100 to about 68 kilocalories/mole. The tungsten grain size after given sintering treatment was found to be inversely proportional to the square root of the nickel content.

Astro Met demonstrated the feasibility of this approach in 1963 on Contract NAS 3-2513[23]. A rather narrow W-Cu-Ni composition area and limited sintering conditions yielded porous tungsten structures in grain sizes ranging from 2 to 10 microns in diameter, and with mean pore diameters from 0.6 to 2 microns. That project further demonstrated that added copper and nickel concentrations, as well as most other elemental concentrations in the finished porous tungsten could be held below 100 parts per million.

The objectives of this current project were to refine procedures, create more uniform and more stable structures, and prepare emitter plate blanks of several square inches and in thicknesses of at least 1/8 inch.

2.0 Approach

Extremely fine tungsten, copper, and nickel, 0.80, 5 and -5 micron particle size respectively, are intimately blended and then hydrostatically pressed. The compact is cut into oversize specimens which are sintered in a hydrogen atmosphere at temperatures between 2100 and 2300°F for periods of 1 to 50 hours, which produces closely sized spherical tungsten structures.

The resulting sintered structures are acid leached with HCl, then HNO_3, to remove most of the Cu-Ni phase. If special specimens are machined before acid leaching, they must be briefly electro-etched in order to remove the worked tungsten structure which otherwise will later close at high process or operational temperatures.

Vacuum furnace bleaching removes the residual copper and nickel phases to levels generally below 30 parts per million.

The resulting purified structure is reinfiltrated with copper in order to become machinable, where precise components can be prepared. After another anodic etch to remove the thin worked tungsten surface, the copper is removed by vacuum bleaching - providing a porous emitter component. This component can be joined to a refractory metal retort by electron beam welding or by rhodium brazing.

3.0 Laboratory Procedures

NOTE:

The following section describes procedures which were generally used during the course of the project. Because the work was divided into two principal tasks (ie) Preliminary Studies and Improvement Studies, specific details of special studies conducted in these tasks are discussed in those respective sections of this report.

Various material and preparation procedures were modified during the project. The major variations are listed on Table 3-1 by specimen "Generation".

3.1 Mixing and Milling

First and second generations specimens were mixed by kneading 200 gram mixtures within polyethylene bags. The 3rd generation specimens were milled in a vibratory mill with tungsten carbide slugs for the purpose of providing more uniform particle and pore distribution. In order to eliminate carbon pickup, all subsequent generations (4th thru 6th) specimens were vibratory milled, using small sintered W-Cu-Ni slugs from previous grain size studies. Initial vibratory milling used trichloroethylene as a liquid vehicle, but excessive volatilization due to frictional mill heating caused milling to change unpredictably as the mix became pasty.

Xylene worked better as a milling liquid due to its higher boiling point, but powder separation due to splashing was a problem. Subsequently, 4th, 5th and 6th generation specimens were vibratory milled as 2# mixes for 16 hours within polyethylene containers. Four 2# milled mixes were subsequently wet blended in larger polyethylene containers in order to produce uniformly blended mixes for large slugs from which the large emitter slabs were cut.

3.2 Pressing

The 200 gm W-Cu-Ni slugs were sealed in small rubber balloons. These were placed in a small hand-pumped laboratory hydrostatic press with a 1-3/4" diameter by 2-1/2" long chamber. Pressing to 20,000 psi was done by hand pumping over a 3-4 minute period.

Following pressing, the slugs were strong enough to clamp and cut with a high speed abrasive wheel.

TABLE 3-1 POROUS TUNGSTEN ION EMITTER STRUCTURES

MATERIAL and PROCESS DISTINCTIONS FOR VARIOUS GENERATIONS

Generation	Tungsten Particle Size 0.80 μ / Copper Particle Size 44 μ	7.5 μ (a)	5 μ (b)	Milled	Acid Treatment HNO_3 130°F	HCl 70°F	then HNO_3 130°F	H_2 Reduction	Vacuum Bleaching (c) Temp. °F	Results (d)
1	X				X			X	3400	Good grain size control Large Cu-Ni lakes, wide pore range, Large pits
2		X			X			X	3400	Grain size control unchanged Finer mean pore diameter Large Cu-Ni lakes and pits
3		X		X	X			X	3400	Grain size and pore diameter dropped. Grain and pore distribution very uniform
4			X	X	X			X	3400	Grain size control good. Excellant pore distribution Medium size specimens cracked in acid leaching due to oxidation.
5			X	X		X			3000 & 2750	Grain and pore size control as in #4. Leaching took longer but did not oxidize specimen. Bleaching resulted in rapid pore closure
6			X	X		X	X	X	2750	Grain and pore size control as in #4 and #5. Scale-up specimens readily made. Leached 99.9% of Cu-and Ni. Produced high pore volume structures. Stable at 2750°F

NOTES: (a) Elutriated Sherrit Gordon copper powders. Contained agglomerates and some particles to 100 microns.

(b) Sharples Classified, Monsanto Chem. Co. Fines 10 microns & below, with 5 micron mean diameter.

(c) Vacuum bleaching for 4 hours in vacuum of 10^{-5} Torr.

(d) Grain size analysis & presence of W-Cu-Ni distribution including Cu-Ni lakes made metallographically on speci[illegible]

The large 10 pound 5th and 6th generation scale-up slugs were compacted in larger hydrostatic presses in a similar manner, to pressures of 20,000 psi. Emitter slab blanks were readily cut from the green slugs.

3.3 Pre-Sintering

Low temperature pre-sintering was found to be unnecessary in previous work.

However, the large 6th generation specimen slabs had to be pre-sintered in order to cause shrinkage so that the plates could be subsequently sintered under closely controlled temperatures in a 2" I.D. hydrogen tube furnace used for most of this work. The pre-sintering was done within a retort type furnace by heating at a rate of about 300°F/hour to 2100°F where they were held for 1 hour.

3.4 Sintering

All other sintering was done within a 2" I.D. x 12" long molybdenum wire would tube furnace. This furnace was constantly flushed (24 hrs./day) with -70°F dew point hydrogen with the flow rate adjusted to prevent internal oxidation and maintain a permanently low dew point.

Specimens were generally placed upon or within high purity /99% alumina boats, plates or specimen holders.

3.5 Temperature Measurements

A Leeds & Northrup optical pyrometer was used for all temperature measurements. Readings were made through the gas flame curtain in the hydrogen tube furnace which was determined to be more accurate than through a glass window which could be gradually clouded. Vacuum furnace readings were taken through a 1/4" glass window. Temperature readings are reported as read, with no corrections.

All temperature measurements were made by viewing into black body furnace environments; therefore, no corrections due to emissivity factors are necessary.

For exact interpretation, the following corrections can be made to those non-corrected temperatures reported as having been measured through the 1/4" glass window in the vacuum bleaching operations, 2500 to 2558, 2600 to 2660, 2750 to 2815, 3000 to 3070, 3400 to 3480 and 3600 to 3688°F.

3.6 Cutting & Machining

For composition and processing variation studies, the specimens were cut in the green non-sintered state where they exhibited a chalk like structure. Cutting was also done to sintered, acid leached, vacuum bleached and reinfiltrated specimens. An eight inch diameter 3/32" thick silicon carbide wheel was used to cut green slugs into slabs, as well as to cut sintered slugs into slices of varying thicknesses. A small hand held Dremel Moto-Tool, with alundum wheels, was used to cut smaller specimens into about 1 gram fragments for various sintering, leaching and bleaching trials and specimen evaluation. Sintered specimens were readily machinable and ground. Sintered disc type specimens .157" diameter x .020" thick (specified final dimensions) were made by cutting them oversize, using expected shrinkage factors. These were lathe turned from sintered specimens and sliced with the "Dremel Moto-Tool" using a dial indicator for traverse measurements.

Rough specimen blanks which were cut in the green state required no other surface treatment. Precision shaped ion emitter specimens cut after sintering required etching as one of the final steps to prevent subsequent pore closure. Detailed descriptions of emitter polishing and etching studies are described in Section 4.3.4 and 4.3.5 respectively.

3.7 Acid Leaching

As discussed previously, one most important step in Astro Met's approach is that of removing the copper nickel phase from the sintered ternary W-Cu-Ni compact. The potential residual nickel content, if high, could create further densification by activation sintering.

Technical grade acids and solutions were used for all leaching studies.

All specimens were acid leached in covered "Pyrex" beakers. Weighed specimens were isolated and used for determining total weight losses. Hot leaching was conducted on electric hot plates with variable transformer input control. Temperature was measured with sensitive laboratory thermometers. Specimen weights were measured on a "Metler" balance sensitive to 0.1 miligram. Detailed discussions of acid leaching studies are reported in Sections 4.3.6 and 5.2.2.

3.8 Vacuum Vaporization

Specimen vacuum vaporization (bleaching) was done on an experimental basis at temperatures varying from 2600°F to 3400°F in the Astro Met laboratory-constructed vacuum furnace, using a tantalum sheet element 2" dia.& 3" high. Initially, 1st generation specimens were bleached at a pressure level below 50 microns (10^{-3} Torr Hg) in the heating zone. The vacuum was measured by a McLeod gage. It was possible to attain the bleaching temperature in about 20 minutes. Later, 5th and 6th generation experimental specimens were processed below 1 micron (10^{-4} Torr) in this furnace by reducing the leak rate.

Vacuum vaporization of slabs and S.T.L. specimens for delivery to NASA was done on a service basis in an Abar furnace by Abar Corporation. This furnace used a square shaped, six-wall hot zone and operated at pressures below 10^{-5} Torr Hg as determined by an ionization gage. Temperatures were maintained within ±5°F by L & N optical pyrometer measurement and manual control of the power supply.

3.9 Chemical and Spectrographic Analyses

Chemical analysis for Cu and Ni contents after leaching the W-Cu-Ni specimens was done on a service basis with F. C. Broeman & Company, Cincinnati, Ohio. The results were claimed to have an accuracy of better than 0.01%.

Spectrographic analysis was done on a service basis by LeDoux Company, Teaneck, New Jersey, and Materials Testing Laboratory, Los Angeles, California. Sensitivities of 10 to 500 parts per million were determinable in these analyses, dependent upon the element. Duplicate specimen cross-check analyses were conducted which resulted in considerable variation from the earlier analyses, as is described in Section 4.4.2.1. This indicated that more thorough quantitative spectrographic analyses should have been requested. Such is possible by extensive standardization, more analysis time and resulting greater expense.

3.10 Metallographic Analysis

Metallographic analysis was done on a service basis on small sintered W-Cu-Ni specimen groups cemented together and cast into 1-1/8" dia. metallographic mounts. Porous (leached and bleached) tungsten samples were infiltrated with copper at 2300°F for 10 minutes in the hydrogen tube furnace before mounting. Polishing was done on an automatic polisher. Diamond polishing, or a combination of etching and

polishing with fine alumina suspension in alkaline potassium ferro cyanide was also used. An alkaline solution of potassium ferri cyanide was used as etchant to reveal grain boundaries. A Unitron Metallograph with a Polaroid back was used for viewing and photographing.

A Bausch & Lomb "Dynazoom" metallograph was used by Astro Met for more detailed examination of microstructures, surfaces, deposits etc. Both Polaroid and 35 mm cameras were used for photographing various structures.

3.11 Porosity Analyses

(a) By Mercury Intrusion:

Pore spectrum analyses were conducted using an Aminco-Winslow Porosimeter (mercury intrusion)[24]. For the mercury intrusion technique, the sample is evacuated to below 100 microns and then immersed in mercury. It is then incrementally pressurized. Non-wetting mercury can be forced into pores where the required pressure, P, is inversely proportional to the pore diameter, d. ($d = \frac{-4T \cos \theta}{P}$ where T = mercury surface tension and θ = contact angle between the liquid mercury and the test material). As pressure is increased by steps, a precise measurement of the mercury volumetric change in the feed stem (of penetrometer) indicates pore volume at the corresponding pressure increment, ie, corresponding pore diameter. A large internal pore interconnected to the surface by many smaller pores will appear equal to the largest of any channel constrictions feeding mercury to that pore.

By this method, precise specimen volume, open, closed and total pore volume and mean pore diameter can be measured. The relative pore concentration can be calculated by following formula:

$$\text{Average No. of } \frac{\text{Pores}}{\text{cm}^2} = \left(\frac{\% \text{ open porosity}}{100} \Big/ \frac{\pi d^2}{4} \right) \times 10^8$$

where d is mean pore diameter in microns.

Using the same formula, a statistical analysis of average no. of pores/cm^2 in each 10% of open pore volume range can be made.

(b) By Water Absorption:

In a few cases (before the Aminco-Winslow Porosimeter was procured by Astro Met) porosity was measured by water absorption method. Open porosity was determined by the following equation:

$$P = \frac{W_S - W_D}{W_S - W_{SS}}$$

where P = open porosity
W_D = dry specimen weight
W_S = saturated specimen weight
W_{SS} = suspended saturated weight

The specimens were boiled in distilled water for 1 hour and allowed to cool to room temperature in that water. The surplus water was wiped off with a damp cloth. The sample was then weighed, giving W_S; the weight of sample when suspended in distilled water with 1 mil wire (subtracted weight) gives W_{SS}.

The water absorption method is believed to be less accurate than the mercury intrusion technique, as a result of surface water variations on small specimens, and evaporation weight changes.

3.12 Transmission Coefficient and Permeability Measurements

3.12.1 Apparatus

Extreme care was taken to assure that proper transmission coefficient measurements were made on representative specimens. Reserve specimens were made at the same time and of the same dimensions as the S.T.L. emitter test specimens supplied to NASA for evaluation. Special attention was given to specimen mounting in order to prevent bypass nitrogen leakage, as well as to prevent occlusion. For measurement, a special relay and timer unit was designed which, when excited by electrical contacts through the mercury manometer, would precisely indicate the required time for a specific pressure drop. Details of these approaches are further discussed below.

One important detail for proper transmission coefficient measurements was that of providing for consistent specimen mounting and sealing. Initially, specimen sealing gaskets were prepared from soft rubber using a special cutting jig. The hole in the gasket was made 0.156" in diameter, which was about 0.001" less than the average specimen diameter. The thickness of the gasket was about 0.030", while the specimen thickness was 0.020". Since gasket thickness was difficult to control, small Buna-N rubber "O" rings were procured from Parker Seal Co. with the following dimensions: I.D. = .154 ± .005" and width = .032 ± .003".

Compression exerted by the mounting fixture pressed the gasket or "O" ring between the sample periphery and the congruent fixture wall and base. This sealed the specimen so that only the face area was exposed to the pressurized nitrogen gas.

The gas storage and flow apparatus consisted of a nitrogen tank, a valve, a mercury manometer, a chamber of known volume, the specimen holder and an electrical control circuit. These are shown schematically in Figures 3-1 and 3-2.

For operation, the nitrogen pressure was so adjusted that the mercury in the manometer was forced above the upper contact K_1. The valve was then closed so that no more N_2 entered the apparatus. Switch Sw_1 was then closed to activate the circuit. As the chamber pressure dropped due to specimen permeation, the mercury level in the manometer would lower from and break contact with the upper contact K_1, the relay R_1 was de-energized, making contact with its upper terminal - starting the timer. As the pressure dropped further and the mercury lost contact with K_2, relay R_2 was de-energized, breaking contact with its lower terminal, thereby interrupting the timer power. This provides an accurate measurement of the time necessary for the pressure to drop causing the mercury to drop from the K_1 to the K_2 level. K_1 and K_2 consists of a fine double insulated thermocouple wire with the insulation stripped back. The distance between K_1 and K_2 was established by terminating the two wire ends 25 mm apart. The double wire thermocouple was inserted in the top of the glass mercury manometer tube and adjusted up and down to the proper height relative to the zero line. The upper contact K_1 was 150 mm above the mercury level when resting at atmospheric pressure. This provides a 137.5 mm mean height, which indicates half the mean chamber pressure above atmospheric.

3.12.2 Nitrogen Permeability Test Procedure

The transmission coefficient is calculated by measuring the time, δt, required for the test chamber pressure to decay from 300 mm to 250 mm Hg and using the following formulae[25]:

Transmission Coeff. C = $\frac{\text{Mass Departure Rate}}{\text{Mass Arrival Rate}}$

$$C = \frac{8.428 \times 10^{-5} \; V \; P_{mm}}{A \; \delta t \; P_{mm}}$$

where V = Volume of gas in pressure chamber
= 75 c.c.

P_{mm} = Decrement of pressure in δt seconds
= 50 mm. Hg

P_{mm} = Mean absolute pressure of gas in the chamber
= 760 / 275 = 1035 mm. Hg

A = Area of porous ionizer perpendicular to gas flow
= $\frac{\pi (\text{dia.})^2}{4} = \frac{\pi (.157 \times 2.54)^2 \text{ c.m}^2}{4}$

$$C = \frac{8.428 \times 10^{-5} \times 75 \times 50}{\pi \frac{(.157 \times 2.54)^2}{4} \; \delta t \times 1035}$$

$$= \frac{245.7 \times 10^{-5}}{\delta t}$$

The volume of the pressure chamber was measured as follows:

The pressure chamber was dried by evacuating it with a mechanical vacuum pump, then weighed. Next, it was evacuated again and was allowed to be filled with water by the external atmospheric pressure and weighed again. The difference between the two weights corrected at 1 gram per c.c. gives the chamber volume. Suitable corrections were made for volume in the manometer tube and in specimen holder. The exact total volume was found to be 75.0 c.c.

The diameters of the porous ion emitters averaged 0.157". However, the diameter of each emitter was measured and the transmission coefficient was corrected as follows:

$$C^1 = C \left(\frac{0.157}{d}\right)^2$$

where C^1 = corrected transmission coeff.

d = diameter of emitter in inches

therefore $C^1 = \frac{245.7 \times 10^{-5}}{\delta t} \left(\frac{0.157}{d}\right)^2$

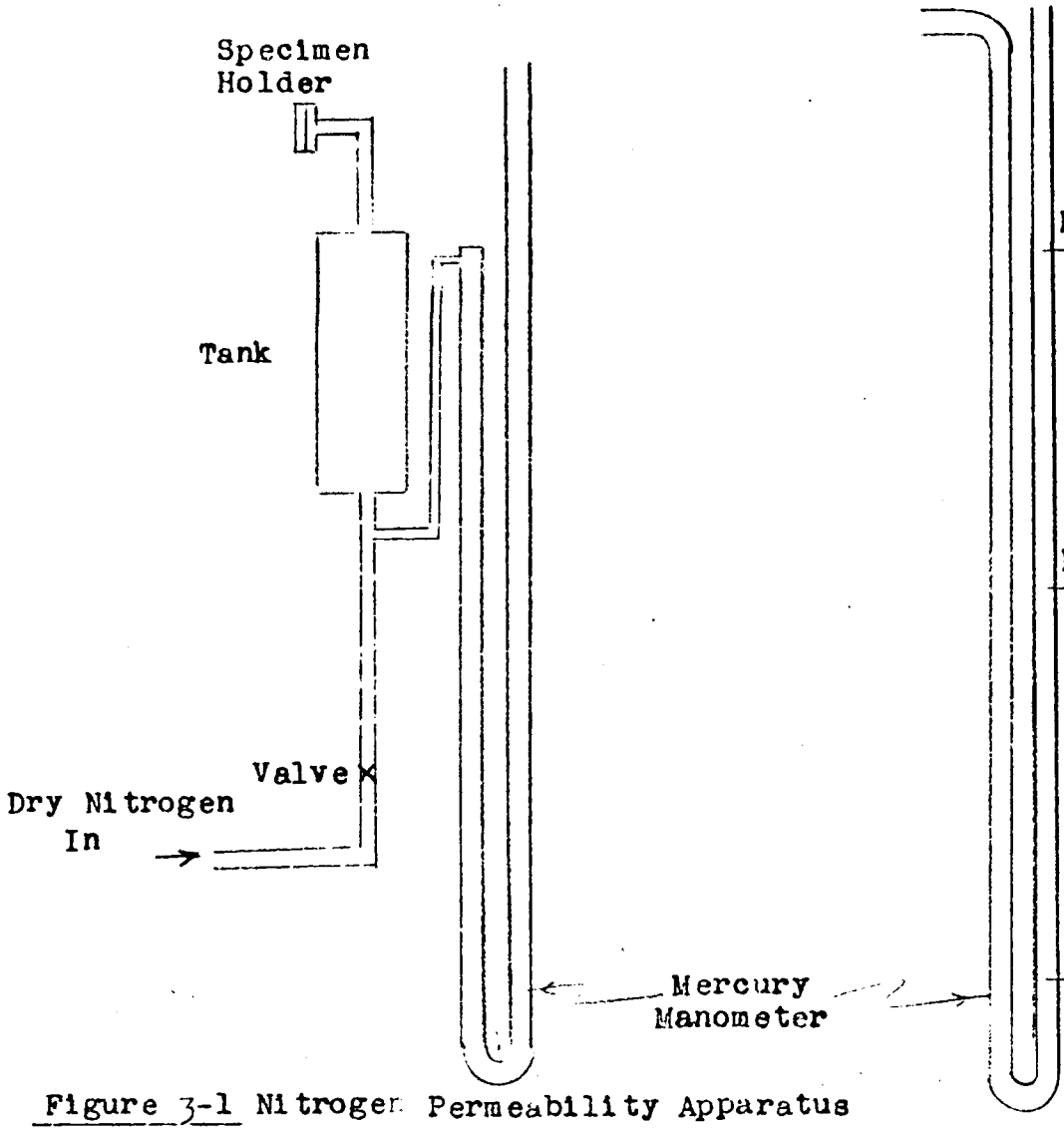

Figure 3-1 Nitrogen Permeability Apparatus

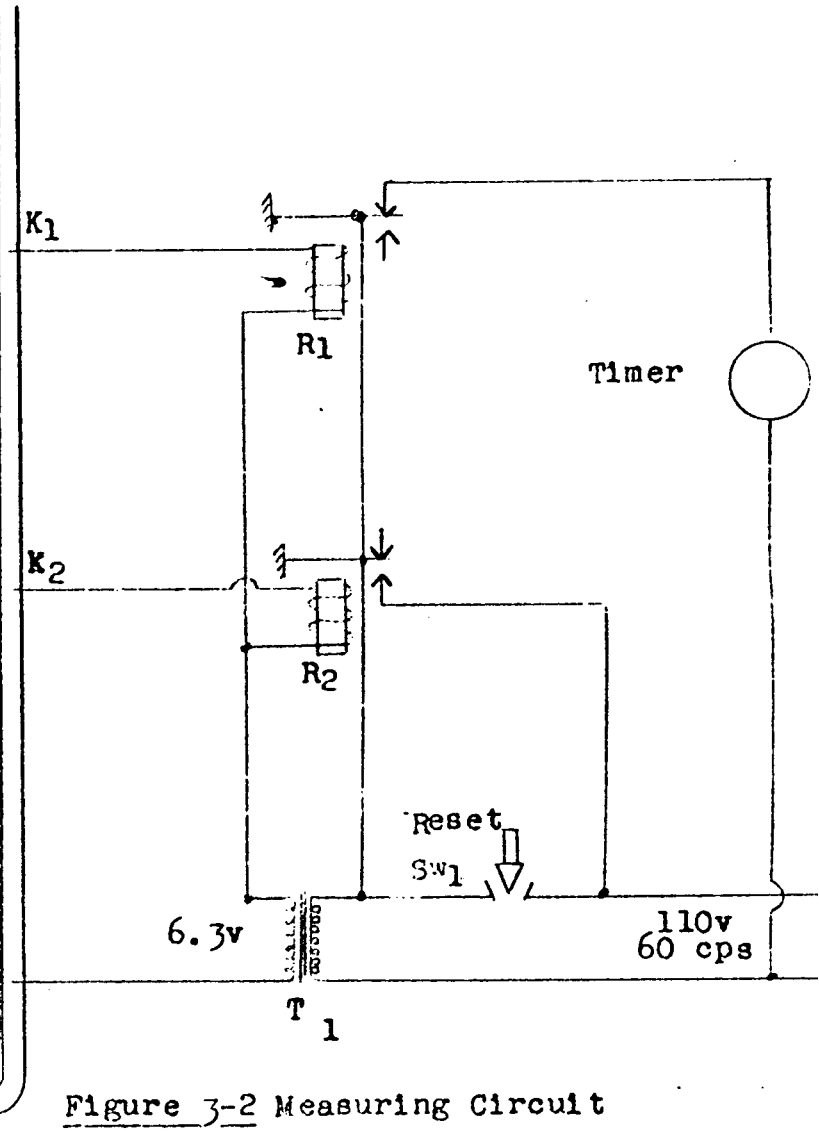

Figure 3-2 Measuring Circuit

3.13 X-ray Back Reflection

A few X-ray back reflection patterns were taken of the small diameter S.T.L. specimens using a G.E. X-ray diffraction unit. Copper radiation was used and operated at 35 K.V. and 23 m.a. The exposure time was ten minutes for DuPont Medical Type 508 film.

These patterns are expected to indicate non-destructively trends of grain growth (due to grain boundary diffusion) with aging.

The results of X-ray diffraction analyses are discussed in Section 4.4.5.2.

4.0 Preliminary Studies

4.1 Materials

4.1.1 Tungsten Powder

All tungsten powder used in this entire project was procured from General Electric as their .88 Grade. A report of their chemical and particle size analyses is reproduced as Table 4-1. Lot to lot variations were nil.

4.1.2 Copper Powder

Two micron average particle size chemically prepared copper powder was initially supplied by Charles Hardy Co. and used for 1st through 3rd generation emitter structures. The particle size was stated as being 2 micron average with 95% below 5 microns and the balance containing particles as large as 100 microns. The use of this powder without separation in 1st generation emitter specimens resulted in poor tungsten grain distribution which produces large Cu-Ni lakes and concomitant pits in finished porous structures. For 2nd and 3rd generation specimens this powder was separated by water washing to remove the coarse levels. This elutriated powder still produced structures (submitted to NASA) which required further improvement. Fifty pounds of similarly prepared powder was obtained from Monsanto Corporation and sent to Sharples Co., Philadelphia, Pa., for particle sizing on a Sharples K 8 classifier. The resulting particle size distribution is shown on Table 4-2 and Figure 4-1. About one-third of the material was classified as 1 F or with a 5 micron mean particle size. The average particle size of the original non-classified material was considerably above that originally claimed by the supplier. The compacts prepared using the classified copper powder were categorized as 4th (or higher) generation structures (Table 3-1).

4.1.3 Nickel Powder

The nickel powder was supplied as International Nickel's carbonyl grade MNP-377 which was -2 microns average particle size and 99.9% pure.

GENERAL ELECTRIC COMPANY

21800 TUNGSTEN ROAD, CLEVELAND, OHIO 44117 . . . Area Code 216 . 266-2700

LAMP METALS AND COMPONENTS DEPARTMENT

CLEVELAND WIRE PLANT

September 1, 1964

Astro Met Associates, Inc.
500 Glendale Milford Rd. (Woodlawn)
Cincinnati 15, Ohio

Attention: J. W. Graham

Below are listed the analyses of the tungsten powder lot no. U 0.88-4597
This material was shipped on 8/31/64 , Order no. 1745
Qty. shipped: 20 lbs.

SPECTROGRAPHIC ANALYSIS			
Element	ppm	Element	ppm
Al	<6	Mg	5
Ca	24	Sn	7
Si	<7		
Mo	23		
Fe	22		
Cr	5		
Ni	16		
Cu	<3		
Mn	<6		

FLAME PHOTOMETERY ANALYSIS			
	ppm		ppm
Sodium	22	Potassium	25

LECO ANALYSIS			
	ppm		ppm
Oxygen	3200	Carbon	11

AVERAGE PARTICLE DIAMETER BY FISHER SUB-SIEVE SIZER (ASTM B-330-58T)		
	as supplied	Lab milled
Number (microns)	.84	.86
Porosity	.785	.662

APPARENT DENSITY BY SCOTT-SCHAEFFER-WHITE VOLUMETER (ASTM B 329-58)
30.2 gms. per cu. in.

WT. % PARTICLE SIZE DISTRIBUTION BY PHOTELOMETER	
Micron Range	Lab Milled
0 - 1	66.8
1 - 2	15.3
2 - 3	6.2
3 - 4	7.5
4 - 5	3.8
5 - 6	
6 - 7	
7 - 8	
8 - 9	
9 - 10	
10 - 11	
11 - 12	
12 - 13	
13 - 14	
14 - 15	
15 - 20	
20 - 25	

Signed F. C. Chapman
F. Chapman
Powder & Rod Quality Control

FC/evp

TABLE 4-2 Copper Powder Size Classification Report

Sharples K-8 Test Report No. 1436

Company: Astro Met Associates, Inc.
500 Glendale Milford Road (Woodlawn)
Cincinnati 15, Ohio

Run No.	1	2	3	4	Balance(+20 μ)
Feed Material	Copper	Coarse Run 1	Coarse Run 2	Coarse Run 3	
Vane Setting	AA	CC	D-E	E(.591)	
Rotor Speed	7800	4250	3550	3050	
Feed Wt.	51.5 lbs.	35.0	26.6	19.1	
Coarse Wt.	35.0	26.6	19.1	14.2 4C	
Fine Wt.	13.6 1F	8.0 2F	7.7 3F	5.2 4F	14.2

1F Minus 5 microns

2F 5-10 microns

3F 10-15 microns

4F 15-20 microns

4C plus 20 microns

Test and Report by

(signature) M. J. Maggio

MICHAEL J. MAGGIO
Classifier Technical Sales

NOTE: Portion inside block is a copy of Sharples Report

FIGURE 4-1 Particle Size Distribution Curves of Separated Copper Powder

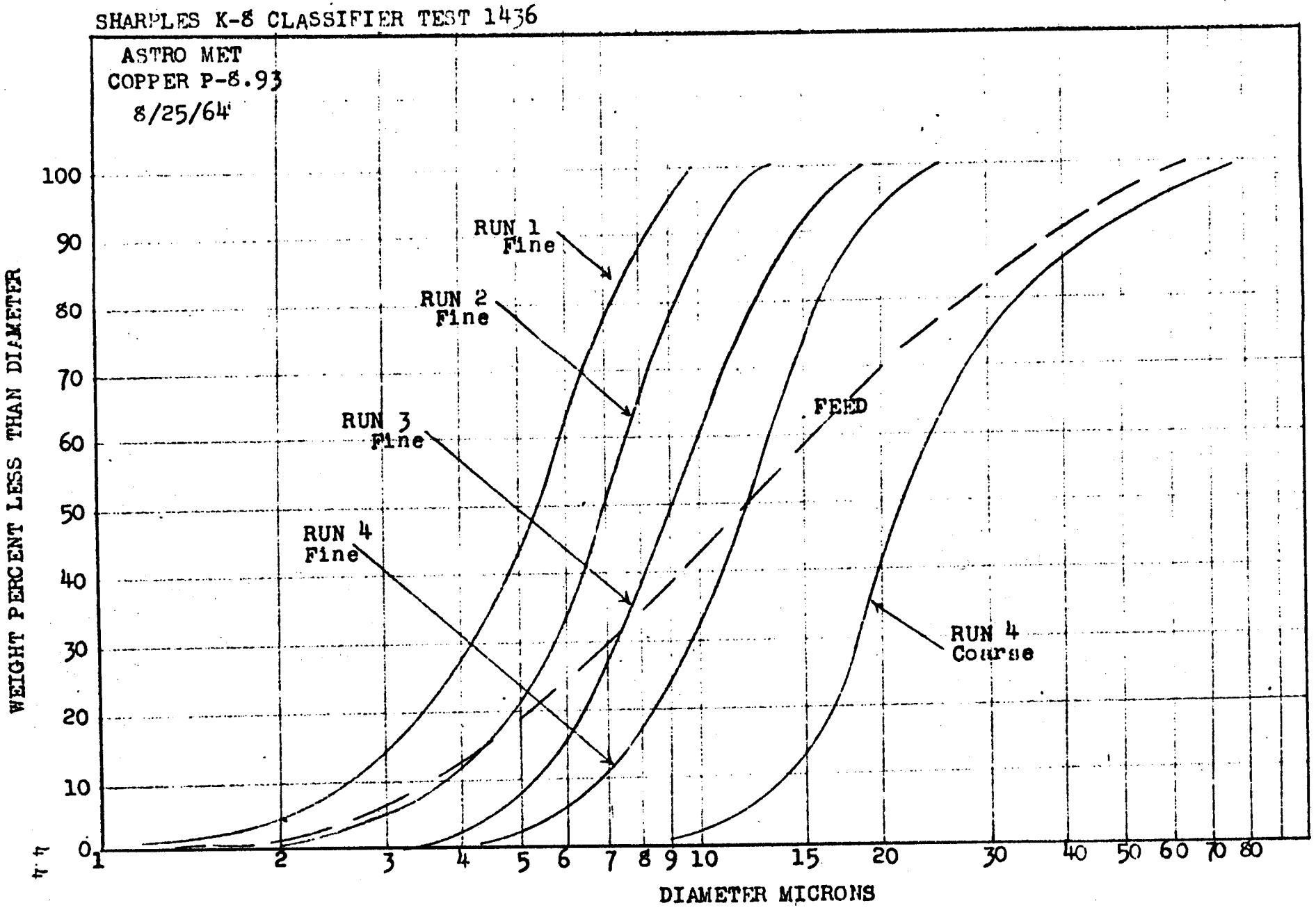

4.2 Compositions

As a result of the previous year's feasibility project, the composition Area 4 in the W-Cu-Ni ternary field Figure 4-2 was explored in greater detail. This area had a range from 8 - 14% copper in 2% levels, and 0.8 to 2.0% Ni in 0.2% levels, the balance being tungsten. This provided 28 initial composition variations.

Later large 200 gm slugs of compositions 8-1, 10-1, 12-1 and 12-0.5 copper-nickel respectively (balance tungsten) were prepared and used for most of the scale-up studies. Final emitter specimens were prepared from the W-8Cu-1Ni and W-10Cu-1Ni compositions.

4.3 Processing

4.3.1 Milling

Since previous work had shown that grain size control was most dependent upon composition and processing temperature, the first and second generation studies pursued the refinements of these variables without milling.

It was observed that though grain size was uniform, the pore diameter range was greater than desired due to non-uniform structures. Milling was conducted as described in Section 3.1 in 3rd and higher generation mixes in order to achieve improved grain and pore size uniformity by eliminating copper agglomerates.

4.3.2 Pressing

The powders which were dry blended without additives (1st and 2nd generation) or vibratory milled (3rd and higher generations) were hydrostatically pressed at 20,000 psi within rubber balloons.

FIGURE 4-2

COMPOSITION WORK SHEET
W-Cu-Ni Ternary System for
Ion Emitter Structures

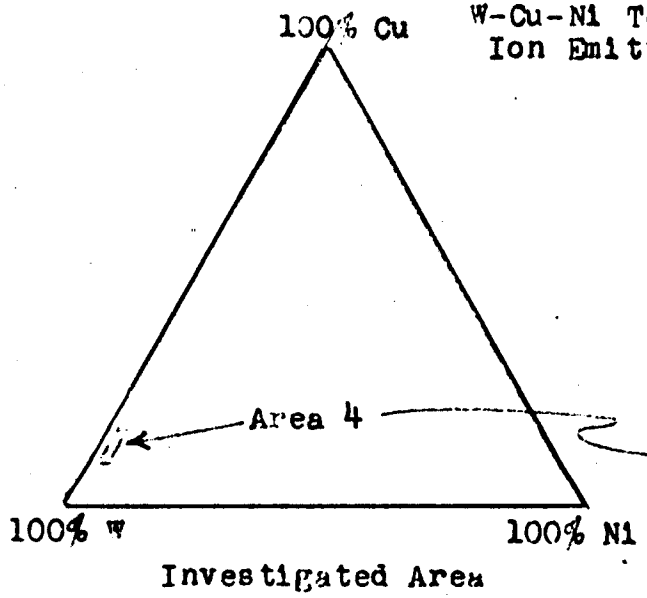

Investigated Area

4.3.3 Sintering

Composition and sintering variables were studied on small 1st generation specimens cut from 200 gram hydrostatically pressed slugs.

The small pressed (green) slugs were cut into 0.040 inch discs, which were then cut into 1/2 cm^2 pieces for sintering and grain growth studies. Prior to sintering, the specimens were scribed for identification and placed in a book type 99.5% pure alumina holder where each specimen was separated from adjacent specimens. Four hundred and forty-eight composition and sintering variations were processed by sintering the twenty-eight composition variations at 2050, 2100, 2150 and 2250°F for periods of 1, 5, 25 and 50 hours, as is described in Section 3.4. The grain size analyses of these variables is discussed in the Evaluation Section 4.4.3.1 and are plotted as Figures 4-4 and 4-4a.

NASA evaluation specimens were also made during the second quarter from 2nd generation slugs of the 8-1, 10-1, 12-1 and 12-0.5 copper-nickel (balance tungsten) compositions. These and a 3rd generation (ball milled) 12-1 slug were prepared and sintered at 2150°F for 5 hours to produce grain sizes of about 5 microns. These were also used for aging studies in a hydrogen atmosphere furnace at 2500°F.

A flow chart describing the applied process steps is shown as Figure 4-3. The main distinctions between these process steps by generation has been shown previously as Table 3-1.

4.3.4 Specimen Surface Finishing - Mechanical

During this second project quarter, extensive efforts were given to surface finishing prior to the development of etching techniques since surface pore closure was believed responsible for low permeabilities in NASA test specimens.

Initially, flat 0.157" diameter 2nd generation S.T.L. specimens were polished in a quartz crystal lapping machine which simultaneously lapped the top and bottom surfaces. It was determined that the non-uniform distribution of tungsten-copper and nickel in these 2nd generation specimens resulted in the wear of the softer phase, thereby producing surface pits. As it was later determined, such precise lapping was found to be unnecessary since anodic etching was found to more easily remove the worked tungsten structure from ground surfaces.

FIGURE 4-3 PROCESS FLOW SHEET FOR PREPARING N.A.S.A. EVALUATION EMITTER SPECIMENS

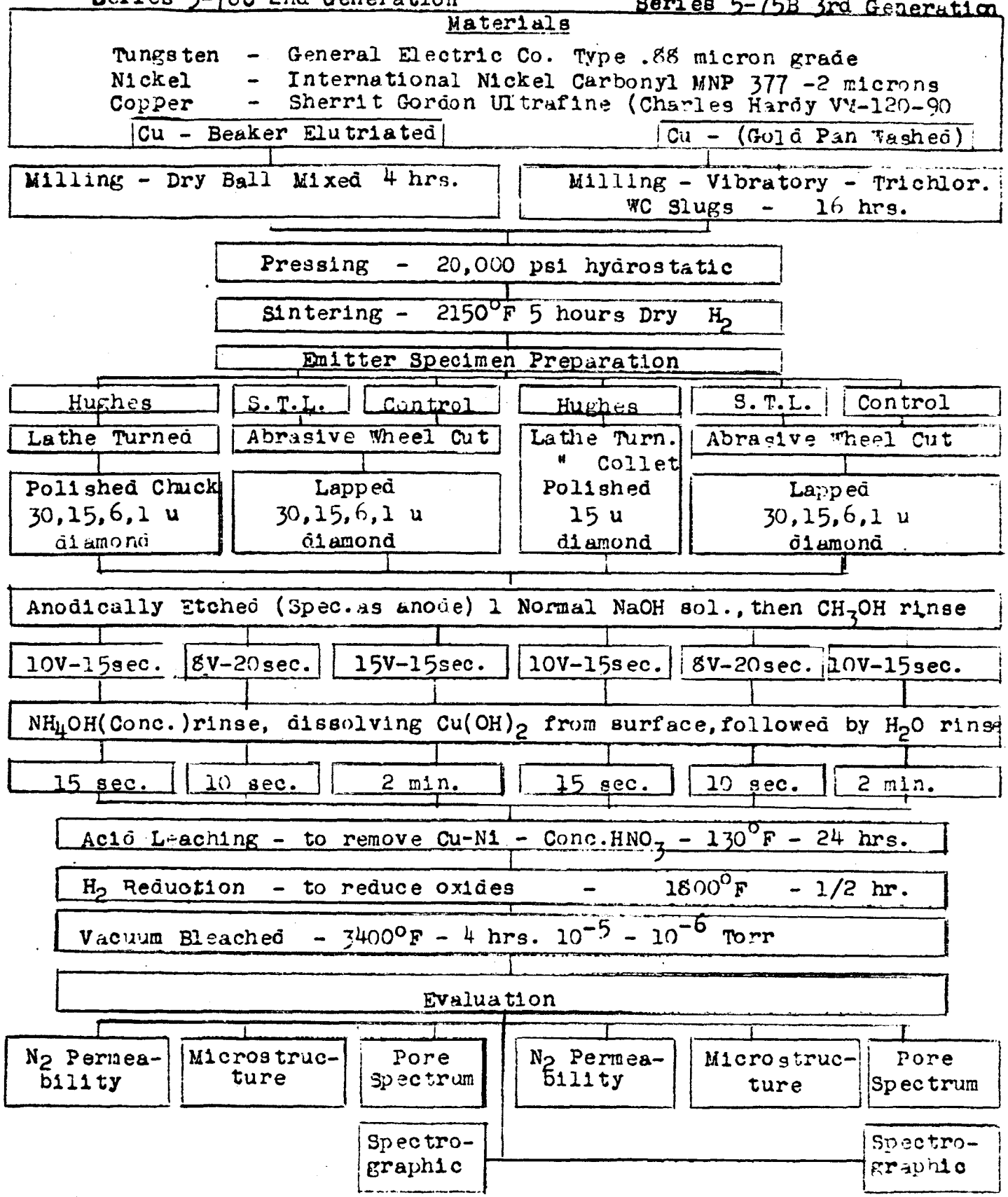

For sixth generation specimens these discs were cut off of lathe turned W-Cu-Ni sintered rods, with the Dremel Moto Tool and alumdum abrasive discs. A small collet was made during the last project phases to precisely hold the small cut off disc specimens for finish grinding the surfaces to close tolerances. These ground surfaces were then etched prior to acid leaching as is discussed in the next Section which is Section 4.3.5.

Larger diameter domed (Hughes) specimens for NASA evaluation were lathe turned by an external machine shop using a precision lathe and ground tool steel. Microscopic examination of machined discs disclosed that this operation produced serious surface smearing. Polishing procedures were then developed for these specimens at Astro Met. The domes were clamped in a three jaw chuck which was rotated at about 3200 RPM. Diamond polishing compound of decreasing particle size was alternately applied between cleansing with methanol and polishing. Polishing felts were used. However, the worked tungsten alloy surfaces could not be completely removed by these procedures. Metallographic analyses of such surfaces showed extensive smearing. High temperature bleaching studies caused these worked surfaces to close up very rapidly, decreasing permeability. Then anodic etching was developed as is discussed in Section 4.3.5 below.

The use of the three jaw chuck was later found to have been the cause of specimen cracking at clamping points, which would come about in acid leaching or in vacuum bleaching.

Though original surface finish concepts considered that ion emitter surface emittance could be extensively influenced by various machining, grinding, or polishing techniques, such effects are now believed to be relatively minor provided etching is used.

4.3.5 Specimen Etching

As mentioned above, grinding and machining produced seriously worked tungsten surfaces. Metallographic analyses indicated that the outer 10 micron layer would close at bleaching temperatures. Since anodic etching was known to improve the surface polish of tungsten emitters, a thorough study was made in order to determine if all of the worked surface could be removed.

The tungsten-copper-nickel sintered specimens were readily etched by a normal NaOH solution, where the specimen is anodic (connected to the + side of a D.C. voltage supply). Voltages from 2 to 20 volts can be used, depending on specimen size and anode-to cathode distance. One-eighth square inch specimen areas can be etched with 20 volts for a period of 15 seconds when the specimen is set on a tungsten screen and a tungsten or platinum cathode-to specimen anode distance is about one-quarter of an inch. If the specimen is horizontal with the cathode directly above, etching will be mostly confined to the upper surface with some minor peripheral etching on the under side. This localized etching is due to gases collecting on the under side, as well as due to an increased electrical path.

One inch diameter specimens of leached and bleached (porous) tungsten which were horizontally supported on tungsten screen have been uniformily etched on the upper surface using a tungsten screen anode somewhat larger than the disc (specimen)and spaced at about 1/2 inch with a 2 volts D.C. voltage for a period of 25 minutes.

This orientation effect requires that the specimen should be turned over after one face is etched and etched again on the opposite (now upper) surface.

Another technique worked out to etch both sides of relatively thin specimens simultaneously is that of orienting the specimen so that the larger flat surfaces are both in a vertical plane. By using a double cathode formed of tungsten wire, etching on both surfaces was done at one time. A sketch of the two specimen orientation procedures is shown below:

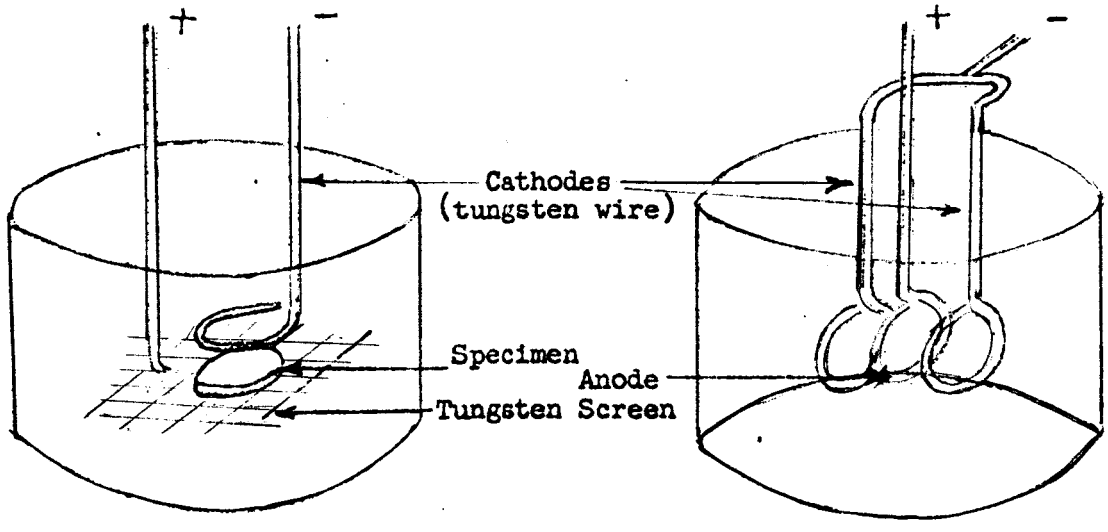

Alkaline etching of the smeared tungsten phase appears to be sufficient when the W-Cu-Ni specimen attains a uniform copper color over the entire surface. Following etching, the specimens were rinsed with distilled water, with alcohol, or placed directly in the leaching acids. No significant rinsing advantages were determined.

Metallographic studies of machined, ground or polished, then etched surfaces, at about 1000X magnification (with an oil immersion objective lens), verify that the entire outer surface of smeared tungsten can be readily removed, exposing the Cu-Ni phase which normally fills the tungsten grain interstices. The copper-nickel phase that becomes apparent by alkaline etching also exhibits the surface worked condition to some extent. This is removed almost instantly when placed in concentrated nitric acid at 130°F, or in concentrated HCl at room temperature.

4.3.6 Nitric Acid Leaching & H_2 Reduction

4.3.6.1 Composition Studies

The twenty-eight 1st generation compositions sintered at 2050, 2100, 2150 & 2250°F for 1, 5, 25 and 50 hours as described earlier were all acid leached in concentrated HNO_3 @ 130°F for 24 hours. The acid leached specimens were rinsed with distilled water and were then vacuum dried (to prevent internal freezing of ∱ .060" thick specimens which were often otherwise shattered by internal ice formation). Specimen weight losses from acid leaching were accurately determined. The specimens were generally oxidized and were very brittle and fragile. After acid leaching, rinsing and drying, they were heated at 1800°F for 1/2 hour in a dry hydrogen atmosphere - in order to chemically reduce the trace of oxide formed by the leaching process.

Later leaching studies evaluated the significance of oxide formation by HNO_3 leaching on specimen growth and cracking. A discussion of this study is given in Section 5.2.2.1.

4.3.6.2 Large Slug Acid Leaching

Previous work has shown that when section thicknesses exceed about 60-70 mils on 1/2" or so diameter specimens, acid leaching causes serious cracking. Believing that the problem was related to internal stress conditions, it was

further considered that stress relieving subsequent to sintering would minimize this problem. A W-12Cu-0.5Ni slug sintered at 2150°F for 5 hours was cooled in 50°F increments from 2150°F, holding at each level for 1 hour, until 1800°F was reached, when the specimen was withdrawn from the furnace. This procedure produces a greater resistance to leach cracking, though it still occurred in specimens of about this size.

In addition to basic stress relieving to 1800°F, the tungsten-nickel phase diagram indicates a phase transformation at 1778°F, though only a small volume change is expected since thd α and β phases are nearly the same crystallographic dimensions. In addition, the total amount of such transformation should be relatively low since the included nickel content in these compositions is so low. A study was made of the possible influence of such stress on leach cracking. A W-10Cu-1Ni slug sintered at 2150°F for 5 hours was machined to about 0.5 inch diameter. This slug was the annealled by slowly cooling, as described above, from 2140°F to 1800°F, and then further cooled to about 1600°F at a rate of 30°F/hour. This procedure considerably reduced the cracking tendency when acid leached. After partial leaching had been accomplished, this slug was reheated to 1850°F to exfiltrate and redistribute the Cu-Ni phase to allow further acid leaching, as well as to hydrogen reduce any chemically formed oxides. The specimen was cooled quickly from this temperature. When resaturated with concentrated HNO_3 the slug immediately exploded.

Later leaching studies showed that leaching was done with less cracking when the leached specimens are in the as sintered condition (ie) not machined or ground after sintering. 10-1 composition discs about one inch in diameter were cut in four thickness levels prior to sintering. The as sintered (2150°F - 5 hours) thicknesses were 0.56, 0.67, 0.83 and .110 inch. The single 2200°F - 5 hour disc was .112 inch thick. The thinnest specimen was free of cracks after 24 hours at 130°F in concentrated nitric acid. As thickness increased, cracking increased. However, cracking appeared to be dependent upon an edge stress phenomenon, which resulted in an uncracked area of about .75 inch diameter in the .110 inch thick disc. This suggested two approaches which were studied in order to attempt to minimize this effect. One approach was that of rounding off the disc edges to reduce the edge stress effect; the second approach was that of coating the cylindrical periphery with an acid

further considered that stress relieving subsequent to sintering would minimize this problem. A W-12Cu-0.5Ni slug sintered at 2150°F for 5 hours was cooled in 50°F increments from 2150°F, holding at each level for 1 hour, until 1800°F was reached, when the specimen was withdrawn from the furnace. This procedure produces a greater resistance to leach cracking, though it still occurred in specimens of about this size.

In addition to basic stress relieving to 1800°F, the tungsten-nickel phase diagram indicates a phase transformation at 1778°F, though only a small volume change is expected since thd α and β phases are nearly the same crystallographic dimensions. In addition, the total amount of such transformation should be relatively low since the included nickel content in these compositions is so low. A study was made of the possible influence of such stress on leach cracking. A W-10Cu-1Ni slug sintered at 2150°F for 5 hours was machined to about 0.5 inch diameter. This slug was the annealled by slowly cooling, as described above, from 2140°F to 1800°F, and then further cooled to about 1600°F at a rate of 30°F/hour. This procedure considerably reduced the cracking tendency when acid leached. After partial leaching had been accomplished, this slug was reheated to 1850°F to exfiltrate and redistribute the Cu-Ni phase to allow further acid leaching, as well as to hydrogen reduce any chemically formed oxides. The specimen was cooled quickly from this temperature. When resaturated with concentrated HNO_3 the slug immediately exploded.

Later leaching studies showed that leaching was done with less cracking when the leached specimens are in the as sintered condition (ie) not machined or ground after sintering. 10-1 composition discs about one inch in diameter were cut in four thickness levels prior to sintering. The as sintered (2150°F - 5 hours) thicknesses were 0.56, 0.67, 0.83 and .110 inch. The single 2200°F - 5 hour disc was .112 inch thick. The thinnest specimen was free of cracks after 24 hours at 130°F in concentrated nitric acid. As thickness increased, cracking increased. However, cracking appeared to be dependent upon an edge stress phenomenon, which resulted in an uncracked area of about .75 inch diameter in the .110 inch thick disc. This suggested two approaches which were studied in order to attempt to minimize this effect. One approach was that of rounding off the disc edges to reduce the edge stress effect; the second approach was that of coating the cylindrical periphery with an acid

resistant coating. This was expected to limit nitric acid attack to the two flat faces and eliminate the third dimensional leaching from the periphery, which in turn was expected to eliminate the edge stress effect.

The results of scale-up acid leaching studies definitely indicated that cracking was an edge effect and became proportionally less severe as specimen area was increased.

The specimens in several thicknesses were edge coated with several materials such as epoxy plastic, two glass enamel coatings, electroplated chromium and gold. These were then leached with HNO_3 at 130°F for periods up to 48 hours with the following results.

The glass coatings were highly successful in eliminating edge cracking. Though grit blasting readily removed the glass coating, after leaching, such procedures should be done only with a non-contaminating system.

The epoxy coating was attacked by the HNO_3 in a few minutes. Other organic coating systems were expected to be similarly limited.

The chromium plated specimens appeared to be only partially protective due to the fact that the coating was thin. Chromium plating generally is also highly cracked.

Gold plating was tried because of its resistance to HNO_3, its plating capability and characteristics, as well as its high vapor pressure at bleaching temperatures. It offered considerable potential - at a cost for such experimental quantities no higher than chromium plating. Gold plating was effective when burnished between two plating cycles - to smear over minute pits. When so processed, thick (.140-200") W-Cu-Ni specimens were readily acid leached with no edge fracture. No serious problem exists for leaching scale-up specimens since even with no edge protection, only the specimen edges are damaged and this effect was molified by using over-size specimens, as described in Sec. 5.2.

4.3.7 Vacuum Evaporation (Bleaching)

The specific objective of bleaching was to further remove copper and nickel to below 50 parts per million. It is currently believed that this level is

too high and that spectrographically pure emitters would be optimum. A second purpose was to increase strength while producing open porosity levels of about 20%. The second and third generation acid leached specimens were bleached at 3000°, 3400° and 3600°F for 1, 4 and 10 hours in Astro Met's vacuum furnace (described in Section 3.8) to select best bleaching temperature and time. Efficiency of bleaching variations was judged by (1) weight loss, Section 4.4.1, (2) spectrographic analyses, Section 4.4.2, (3) metallographic analyses, Section 4.4.3 and (4) pore spectrum analyses, Section 4.4.4.

The results of these tests are discussed in the above indicated sections.

In addition, some unsuccessful trials were made to determine if the copper nickel phase could be removed only by the vacuum bleaching process - by eliminating the acid leaching step. The evaluation of structures prepared in this manner are discussed in Section 4.4.3.3.

4.4 Evaluation

As described in Section 2.0, evaluation of various process variations was done by relative weight loss, chemical, spectrographic, metallographic, pore spectrum, nitrogen permeability and X-ray back reflection analyses. The results of these tests are described in the following sections.

4.4.1 Relative Weight Loss

The 28 composition 1st generation series previously described as being sintered at 3 temperatures and for 4 time periods, and being acid leached, were vacuum bleached at 3400°F for 4 hours. The total weight loss of each of these specimens, resulting from nitric acid leaching, hydrogen reduction and vacuum bleaching are given in Table 4-3. This data shows that most of the compositions lose nearly 100% and often slightly more than the available Cu-Ni content. In the latter case, some tungsten has obviously also been removed, presumably as a contained solute in the Cu-Ni phase during acid leaching. Another observation is that the weight loss decreases as original sintering temperature and time increases. When sintered at 2250°F for 50 hours, the Cu-Ni removal appears to be incomplete, with as much as 10% of that available Cu-Ni weight still remaining with the tungsten specimen. These low weight losses correlate directly with those produced initially by acid leaching of the 2250°F - 40 hour sintered specimens. The higher sintering temperature and longer sintering periods apparently produce the greatest acid resistance.

TABLE 4-3 Relative Total Weight Loss of Ternary W-Cu-Ni 1st Generation Specimens[a] Due to Acid Leaching and to Vacuum Bleaching Sintered at 2050, 2150 & 2250°F for 1, 5, 25 & 50 hrs.

Proportion of Copper-Nickel Phase Removed[c]

Sintering Temp.→		2050°F				2150°F				2250°F			
Period (hours)→		1	5	25	50	1	5	25	50	1	5	25	50
Spec.	Composi.[b]												
1	8-0.8	98.2	98.5	101.0	92.5	99.3	100.6	95.7	93.6	96.4	99.3	90.2	88.2
2	-1.0	98.0	99.3	99.3	99.9	96.9	95.0	99.4	95.4	99.7	97.6	92.4	91.9
3	-1.2	96.8	98.8	96.2	100.3	96.1	98.0	99.6	94.9	99.1	100.2	92.8	87.5
4	-1.4	100.8	97.5	94.7	94.5	98.4	96.4	99.2	95.8	99.8	99.7	92.8	90.8
5	-1.6	96.7	96.9	97.1	95.1	99.9	100.8	99.7	97.7	96.7	99.6	95.1	91.0
6	-1.8	98.2	96.5	95.2	97.8	100.2	98.3	99.8	97.8	99.5	99.6	91.6	94.1
7	-2.0	100.0	97.2	97.3	99.1	98.5	99.2	99.0	96.2	99.6	98.9	95.4	95.3
8	10-0.8	101.3	98.4	100.0	99.2	98.4	98.7	98.5	97.6	100.7	97.5	91.1	90.8
9	-1.0	101.7	99.3	98.5	97.7	101.3	100.6	99.0	98.2	102.5	100.3	95.9	94.2
10	-1.2	101.3	99.5	97.9	98.5	100.5	98.7	98.8	96.4	99.6	100.4	95.8	89.9
11	-1.4	100.9	97.0	97.8	96.8	99.3	101.4	98.9	99.5	97.8	100.6	95.0	91.9
12	-1.6	101.1	98.4	97.3	99.1	100.0	100.7	99.7	98.5	101.5	101.4	98.0	95.7
13	-1.8	102.3	99.5	95.2	100.3	99.7	102.0	101.4	97.8	101.2	100.7	99.2	94.8
14	-2.0	102.0	100.5	99.5	99.4	99.5	100.2	98.9	93.1	100.5	100.3	95.3	95.2
15	12-0.8	99.7	98.3	99.2	98.8	101.8	100.4	99.8	95.1	98.8	98.7	93.3	88.0
16	-1.0	102.0	98.0	98.1	99.8	99.5	100.3	99.6	95.5	100.9	99.0	97.1	94.6
17	-1.2	100.3	100.3	97.6	100.5	99.8	101.3	97.9	96.5	100.3	97.2	96.8	93.0
18	-1.4	100.6	100.9	99.7	96.7	97.5	100.3	98.7	95.1	100.3	100.4	97.8	97.3
19	-1.6	100.0	101.4	98.9	97.5	99.1	100.9	100.5	97.5	99.5	100.4	94.7	93.3
20	-1.8	102.3	98.8	97.2	100.6	100.8	100.2	99.2	95.9	99.5	99.8	98.9	94.4
21	-2.0	100.6	98.9	99.0	96.7	100.9	101.2	96.8	98.2	101.2	100.7	98.2	95.3
22	14-0.8	98.9	98.5	97.9	97.8	101.0	-	99.8	95.0	102.3	98.7	97.7	91.7
23	-1.0	97.9	99.2	99.1	100.7	101.2	98.5	98.9	96.0	99.8	99.7	97.7	93.2
24	-1.2	99.4	99.8	97.2	97.9	100.0	101.5	100.5	98.3	101.3	99.8	95.8	94.9
25	-1.4	99.4	99.7	95.3	99.6	100.8	100.3	100.3	99.0	100.8	101.7	97.1	96.2
26	-1.6	101.5	97.9	96.6	98.2	100.4	101.7	100.2	97.7	99.8	101.7	99.7	95.9
27	-1.8	103.2	97.8	99.7	100.2	99.8	100.4	100.9	99.0	101.2	100.7	99.2	97.8
28	-2.0	102.2	97.9	97.9	100.2	100.3	99.8	100.2	97.3	99.1	99.1	99.7	96.4

(a) Specimens averaged about 1 gram; were acid leached in Conc.HNO_3 @ 130°F for 24 hrs. H_2 reduced @ 1800°F - 1/2 hr.; Vacuum bleached @ 3400°F - 4 hrs.

(b) Composition % by weight of copper and Nickel respectively, balance being tungsten.

(c) % based on available Cu-Ni content, which was removed by leaching and bleaching.

4.4.2 Spectrographic Analyses

The spectrographic analyses of 2nd generation acid leached and Abar vacuum bleached specimens were conducted by LeDoux and Company, Teaneck, New Jersey, and were reported as their laboratory number 831572. Table 4-4 lists the analyses on the 5-76 series specimens.

The maximum contamination level of 43 elements is given. The Table indicates that no detectable impurities existed in any specimen except nickel, iron, aluminum and silicon. For reviewing simplicity, therefore, the first column indicates the lowest detectable level for those non-detected elements.

The nickel, iron and silicon levels are reported not to exceed 10 ppm in all specimens. The aluminum level in the 12-1 specimen indicates 20 ppm, but 10 ppm or less for all other specimens.

This aluminum level could have been due to two possible sources (1) all specimens were sintered in alumina boats and (2) the spectrographic samples were cut from sintered discs with an alundum cut-off wheel.

The overall purity level of nickel and iron were less than the initial levels in the starting powders; the aluminum and silicon levels were at about the same magnitude as originally existed in the starting material.

Most importantly, these analyses proved that the good vacuum bleaching procedures do remove extensive levels of added copper and nickel which are required in this liquid phase sintering process.

4.4.2.1 Spectrographic Cross-Check Analysis

Three separate spectrographic analyses were conducted on each of two leached and bleached porous tungsten specimens. The results are given in Table 4-5 as reported by LeDoux and Materials Testing Laboratory. These cross-check analyses show several inconsistencies which indicate the probable accuracy of such analyses made within one laboratory and between two laboratories on identical specimens. Two important inconsistencies should be noted. M.T. Labs reported that the 12-1 specimen contained no detectable Ni while one LeDoux analysis indicated a high of 150 ppm vs 70 ppm for their first analysis. The M.T. Labs reported 400 ppm silicon while the LeDoux reported none detectable at a 10 ppm

TABLE 4-4 SPECTROGRAPHIC ANALYSES

Series 5-76B - 2nd Generation Tungsten Emitter Control Specimens
LeDoux Analyses #831572 June 26, 1964. Astro Met P.O. No. 1648 &
#832438 July 17, 1964 for 12-1 5-75 B

Composition (Cu-Ni) →			8-1	10-1	12-1	12-0.5	1-1
Code →			5-64	5-65	5-64	5-64	5-75B
Heat →			9-33	9-37	9-35	9-36	5-110
Element	All Spec*						
Tellurium	ND	1000					
Thallium	ND	100					
Titanium	ND	10					
Vanadium	ND	10					
Zinc	ND	300					
Zirconium	ND	10					
Lithium	ND	500					
Magnesium	ND	10					
Manganese	ND	10					
Molybdenum	ND	10					30
Sodium	ND	500					
Columbium	ND	50					
Nickel			10	10	10	ND<10	70
Osmium	ND	500					
Lead	ND	30					
Palladium	ND	10					
Platinum	ND	50					
Rhodium	ND	50					
Ruthenium	ND	500					
Antimony	ND	500					
Silicon			10	10	10	ND<10	ND 10
Tin	ND	10					
Strontium	ND	10					
Tantalum	ND	500					
Silver	ND	10					
Aluminum			10	10	20	ND<10	ND 10
Arsenic	ND	500					
Gold	ND	500					
Boron	ND	50					
Barium	ND	10					
Beryllium	ND	10					
Bismuth	ND	10					
Calcium	ND	50					
Cadmium	ND	500					
Cobalt	ND	10					
Chromium	ND	10					
Copper	ND	10					
Iron			10	10	10	10	50
Gallium	ND	10					
Germanium	ND	50					
Hafnium	ND	500					
Indium	ND	10					
Iridium	ND	500					

NOTE: *As determined on all four compositions unless otherwise indicated - Not Detectable - less than in ppm (values in parts per million)

TABLE 4-5 SPECTROGRAPHIC ANALYSES (Parts per Million)
TUNGSTEN EMITTER CONTROL SPECIMENS
W-CU-NI ACID LEACHED AND VACUUM BLEACHED SPECIMENS

Composition (Cu-Ni) →	8-1 Series 4-178 1st Gen.			12-1 Series 5-75B 3rd Gen.		
Condition →	After 500 hrs. aging @ 2500°F			Prior to Aging		
(a)Spectro.Lab	Ledoux	Ledoux	M.T.	Ledoux	Ledoux	M.T.
Lab. Report No.	832438	832965	26865-4-1	832438	832965	26865-4-2
Date of Report	7/17/64	8/13/64	9/4/64	7/17/64	8/13/64	9/4/64
Element						
Tellurium	1000*	-	-	1000*	-	-
Thallium	100*	50*	-	100*	50*	-
Titanium	10*	10*	10*	10*	10*	10*
Vanadium	10*	10*	-	10*	10*	-
Zinc	300*	400*	-	300*	400*	-
Zirconium	10*	10*	-	10*	10*	-
Lithium	500*	-	-	500*	-	-
Magnesium	10*	10*	10*	10*	10*	10*
Manganese	10*	10*	10*	10*	10*	10*
Molybdenum	30	50	100	20	20	100*
Sodium	500*	-	-	500*	-	-
Columbium	50*	30*	-	50*	30*	-
Nickel	20	40	40	70	150	10*
Osmium	500*	300*	-	500*	300*	-
Lead	30*	30*	-	30*	30*	-
Palladium	10*	10*	-	10*	10*	-
Platinum	50*	50*	-	50*	50*	-
Rhodium	50*	50*	-	50*	50*	-
Ruthenium	500*	200*	-	500*	200*	-
Antimony	500*	300*	-	500*	300*	-
Silicon	10*	10*	400	10*	10*	400
Tin	10*	10*	-	10*	10*	-
Strontium	10*	10*	-	10*	10*	-
Tantalum	500*	500*	-	500*	500*	-
Silver	10*	10	-	10*	10	-
Aluminum	10*	20	100*	10*	10*	100
Arsenic	500*	500*	-	500*	500*	-
Gold	500*	200*	-	500*	200*	-
Boron	50*	30*	-	50*	30*	-
Barium	10*	10*	-	10*	10*	-
Beryllium	10*	10*	-	10*	10*	-
Bismuth	10*	10*	-	10*	10*	-
Calcium	50*	50*	10*	50*	50*	10*
Cadmium	500*	300*	-	500*	300*	-
Cobalt	10*	10*	-	10*	10*	-
Chromium	10*	10*	10*	10*	10*	10*
Copper	10*	10*	10*	10*	10*	10*
Iron	100	150	300	50	20	100*
Gallium	10*	10*	-	10*	10*	-
Germanium	50*	30*	-	50*	30*	-
Hafnium	500*	300)	-	500*	300*	-
Indium	10*	10*	-	10*	10*	-
Iridium	500*	300*	-	500*	300*	-

NOTE: (a) Ledoux & Co., Teaneck, N.J.; Materials Testing Lab., Los Angeles, Ca.
* Not detectable less than the indicated amounts
\- Not analyzed

level. These and the other minor inconsistencies are probably the result of technique and are similar to spectrographic analyses inconsistencies reported from like tests conducted on Contract NAS 3-2513 and also as has been observed by other ion emitter development contractors.

These laboratories have indicated an ability to determine contamination levels in the 1-10 parts per million range by using standardized control specimens. Such analyses are more involved and as a result are more expensive. It is recommended that such standardized control checks should be established by the cognizant sponsor in order that reliable and meaningful data will be consistently obtained.

4.4.3 Metallographic Analysis

4.4.3.1 Grain Size Analysis - 1st Generation Specimens

Figures 4-4 and 4-4a show the plots of grain size relationships resulting from the evaluation of twenty-eight compositions of the W-Cu-Ni 1st generation ternary system. These compositions range from .8 to 2.0% nickel in .2% increments, and from 8 to 14% copper in 2.0% increments. The following are several observations of grain growth relationships.

At 2050°F, sintering for 1 hour produces little tungsten grain growth from the original particles averaging .88 microns. Practically every specimen contains large macro pore areas larger than 30 microns due to lack of tungsten rearrangement which occurs at slightly higher temperatures.

When sintered for 5 hours at 2050°F, the high-nickel low-copper area results in increased tungsten grain growth where a greater randomness of tungsten grain size occurs. At longer periods at 2050°F this randomness in tungsten grain size makes it difficult to estimate average grain size. Further, there appears to be inconsistent grain growth trends which would reduce the predictability of sintering to some finite grain growth level of about 4 to 5 microns. This level has been shown, by previous pore spectrum studies, to produce the best average pore size near the one micron level. It can therefore be concluded that 2050°F is probably too low for sintering this ternary area in order to obtain good emitter structures.

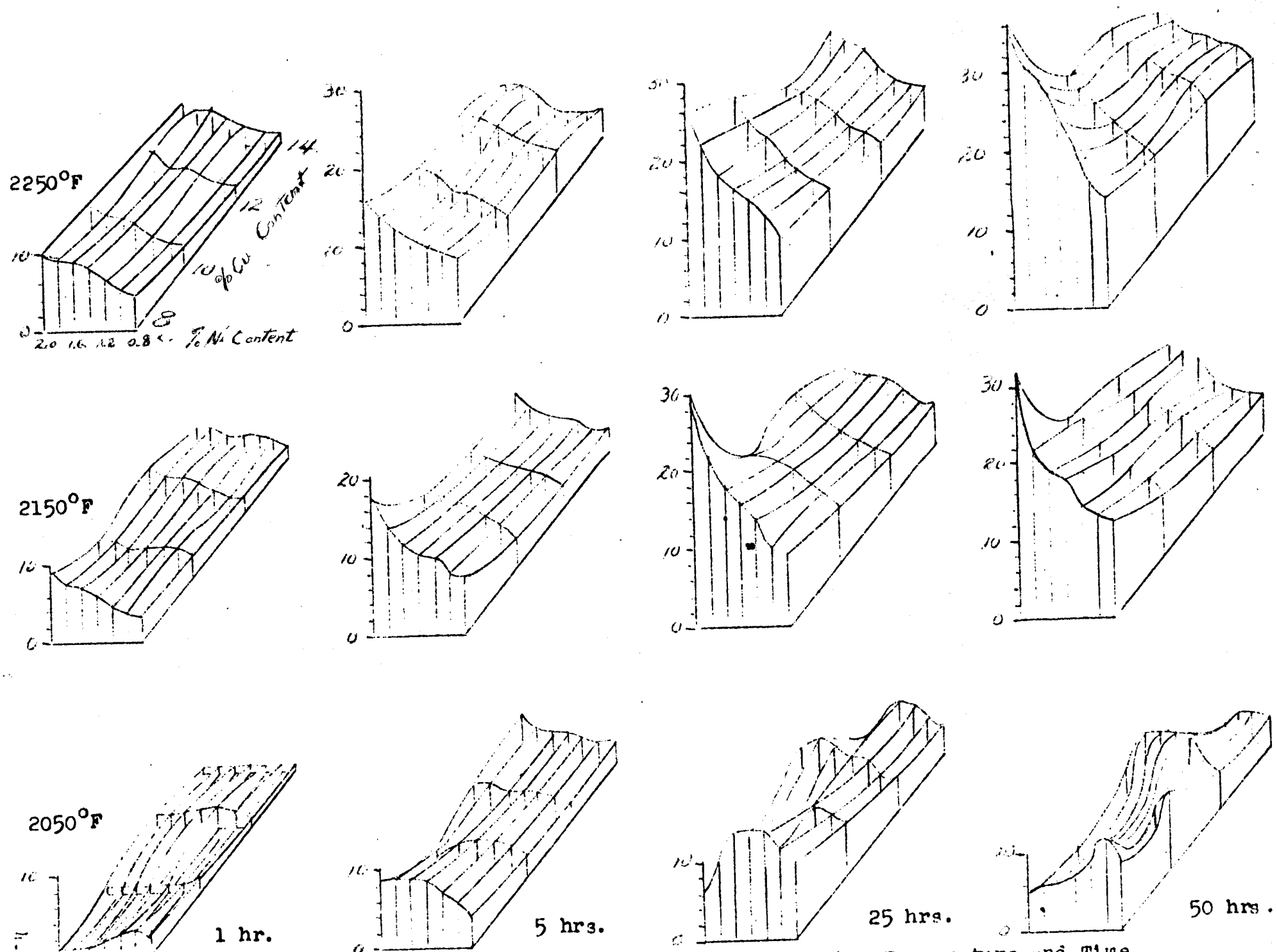

FIG. 4 4 W-Cu-Ni Ternary Area Grain Size vs Composition, Sintering Temperature and Time
Composition in weight %, Grain Size on verticle scale in microns (1st generation)

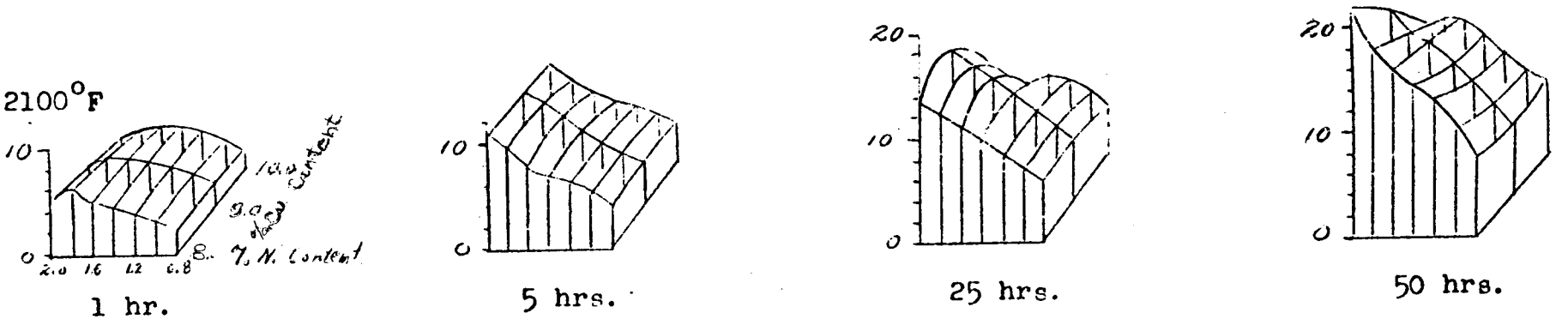

FIGURE 4-4a W-Cu-Ni Ternary Area Grain Size vs Composition, Sintering Temperature and Time
Composition in weight %, Grain Size on verticle scale in microns (1st generation)

The sintering program had initially exposed the 28 specimen groups to temperatures of 2050, 2150 and 2250°F. The above analyses and those of the higher sintering temperature suggested that another, but more limited, composition series should be sintered at the intermediate temperature of 2100°F for the four time periods. The results of this intermediate sintering temperature are plotted in Figure 4-4a and indicate that good grain size control existed at 2100°F between 1 and 50 hour sintering time periods. Grain diameters from 5 to 20 microns were developed during this time range, at 2100°F.

Sintering studies at 2150°F will be discussed later since they are conclusively more important.

Sintering the W-Cu-Ni ternary area at 2250°F for periods of 1 and 5 hours produces tungsten grain sizes in the desirable emitter level. 2-10 microns over a good part of the composition area. As is very evident when evaluating the entire Figure 4-4, grain growth in the lower copper levels is more responsive to nickel content. As nickel ratios increase, grain growth rates increase almost parabolically. This is particularly apparent when the system is sintered for 25 and 50 hours, where it appears on first observation that desirable grain size levels might result in high copper areas when sintered at 2250°F for 25 hours.

However, extensive microstructural analyses of the complete ternary area indicate that those compositions prepared with 12 and 14% copper have large Cu-Ni lake areas proportional to the quantity of the Cu-Ni phase. These areas are devoid of tungsten grains. These large tungsten depleted areas were later determined to be due to the presence of large copper particles and agglomerates which were later minimized by copper classification and milling procedures - as is discussed in Section 4.2 and Section 4.3.1. Such structures would not exhibit optimum pore count levels desirable for ion emitters. The 8 and 10% copper area structures exhibit a good distribution of spherical tungsten grains, and when grain diameters average 4-6 microns, the pore count levels are expected to meet ion emitter objectives. Reiterating, the microstructural analyses of the ternary group sintered at 2250°F for 1 hour show that possible useful emitter structures (which exhibit grain sizes below 5 microns) occur over a great part of the ternary area. When sintered at 5 hours, the useful grain size area appears to be eliminated by large grain size or large tungsten devoid lakes produced in high Cu-Ni weight levels.

The best grain size control appears to occur at 2150°F temperature levels, when sintered for 1 and 5 hours. One hour sintering periods at this temperature produce a grain size range from 2 to 9 microns, the latter occurring at the 8Cu-2Ni corner. Again the high Cu contents (ie) 12 and 14%, produce significant tungsten free Cu-Ni areas. The 5 hour sintering period converts most of the 8 and 10% copper compositions to grain size levels above 6 microns.

In summary, and based only on grain size analyses of 2nd generation specimens, the most desirable structures were produced at 8 and 10% copper levels, from 0.8 to 2% nickel levels, the balance being tungsten. These structures should be sintered no higher than 2150°F and above 2050°F to produce structures having pore diameters near 1 micron. For this pore size, sintering periods in this temperature range should not exceed 5 hours.

4.4.3.2 Grain Size Analyses of Leached and Bleached Emitters

As described in Section 3.10, leached and bleached specimens were copper infiltrated for metallographic analyses. The 2nd generation emitter structures contained significant levels of large 5-50 microns diameter pores. (Such pores were randomly spaced and were believed to be interconnected only by small pores averaging the mean pore diameter. Mercury intrusion pore spectrum analyses will always indicate that such isolated large pores will appear as a volume of pores in a size equal to the largest diameter of the constricting openings to the surface.)

It is believed that such large pores are detrimental to ion emission. The third generation milled 12-1 emitter structures were completely free from such void areas. An unusual observation was made on a single 20 mil thick emitter specimen processed for metallographic observation. One surface still retained the original 2-3 micron grain size, though the balance of the specimen had a grain growth to about 5 microns.

A related specimen had shrunk 8.5% during bleaching, and the resulting open porosity was 16.4%; the mean pore diameter was 1.0 micron. The relative low open porosity apparently was due to low grain size and apparent lower activation energy levels.

4.4.3.3 Furnace Leached Specimens

In an attempt to determine if the acid leaching step could be by-passed, an exploratory trial was made to remove the Cu-Ni solely by vacuum bleaching. Six specimens, including two acid leached specimens, were processed at 3400°F for four hours at pressures of 10^{-4} - 10^{-6} Torr. The 10-1 specimens (.040 in. thick) showed that grain size was more uniform in those specimens that were not acid leached. The average grain size in both cases were in the 7-8 micron diameter range.

The .040 inch thick 12-1 specimens had very similar structures where the average grain size of the acid leached specimen was 10 microns and that of the non-acid leached specimen was 8-9 microns.

In both compositions, no density or grain size gradient existed through the .040" thick specimens.

A .38" long x .38" diameter 10-1 slug was also vacuum bleached without prior acid leaching.

It appeared that some liquid phase had exuded from the bottom as a droplet with a good wetting angle on the tungsten slug.

The grain structure showed a considerable change from this droplet, to what was believed to have been the top. The top of the specimen had a very uniform grain size of about 8 microns. The grain size increased uniformily to about 35 microns near the droplet area bottom. The droplet was porous though all the pores were closed and ranged from 5 to 10 microns.

The wide grain size range in thick specimens suggested that control would be difficult and results would be widely scattered.

Large scale emitter plates were initially attempted during the latter part of the 3rd project quarter. An attempt was made to vacuum bleach some large 1/8" thick W-10Cu-1Ni emitter plates containing about 20% of the added copper nickel phase. This residual bow melting phase content remained after 92 hours of nitric acid (at 130°F) leaching which had resulted in extensive specimen

oxidation, and caused the specimen leaching to be interrupted before the balance of the added Cu-Ni was removed. With the possibility that this lower Cu-Ni content could be eliminated without causing densification, these specimen plates were bleached at 3400°F for 4 hours. The copper nickel vaporized extensively, coating the temperature viewing window and causing erroneous reading and power supply adjustment. The specimens were believed heated to about 3600°F during the furnace heat. This increased temperature and the high original nickel content caused pore closure with a resultant 8% open porosity.

4.4.4 Porosity Analyses

4.4.4.1 Porosity vs Bleaching Temperature and Time

The 8-1, 10-1, 12-1 and 12-0.5 Cu-Ni, balance tungsten, 2nd generation specimens as acid leached and hydrogen reduced were bleached at 3000, 3400 and 3600°F for 1, 4 and 10 hours in Astro Met's vacuum furnace (10^{-3} Torr). The open porosity data as measured by water absorption method are given in Table 4-6 and Figure 4-5.

This data indicates that the lower bleaching temperature produces earlier stability than higher bleaching temperatures; that vacuum bleaching of an 8-1 composition at 3000°F for 4 hours establishes an equilibrium condition at about 22% porosity which changed very little in an additional 6 hours. Such structures may be stable at 2500°F in emitter operating conditions. It is probable that pore diameters are larger and obviously would be more resistant to aging (ie) pore closure. This substantiates, somewhat, the proposition that structures with pore diameter of 1.5 to 2.0 microns may be significantly more stable than those of 1 micron and justifies the approach to prepare comparative structures with both pore diameters for such evaluation.

4.4.4.2 Emitter Pore Spectrum Analyses - 1st, 2nd and 3rd Generation Structures

Pore spectrum analyses of composition and processing variations were made on 2-4 gram control specimens. These specimens had been cut from the same composition slugs or plates and processed through the various sintering, leaching and bleaching steps used for the emitter specimens (these steps are described in the flow chart as Figure 4-3 in Section 4.3.3)

TABLE 4-6 POROSITY DATA FOR W-Cu-Ni SINTERED COMPACTS FOR DIFFERENT BLEACHING TEMPERATURE AND TIME IN VACUUM (2nd Generation Structures)

Temp. oF	Time (hrs.)	Specimen Open Porosity (%)			
		8-1	10-1	12-1	12-0.5
3000	1	26.3	25.5	27.4	28.1
	4	22.0	20.1	19.1	17.9
	10	21.6	18.5	19.1	19.1
3400	1	22.9	23.4	23.6	21.8
	4	18.5	16.0	17	17.4
	10	16.7	12.8	15.6	17.0
3600	1	22.5	19.7	21.1	20.0
	4	16.6	13.1	15.7	16.6
	10	13.95	12.4	13.9	15.4

All Specimens - Code (5-23) (5-48) (5-105)

FIGURE 4-5 PLOT OF OPEN POROSITY (%) vs BLEACHING TIME AT 3000, 3400, 3600°F IN VACUUM FOR W-Cu-Ni SINTERED, LEACHED AND H_2 REDUCED COMPACTS

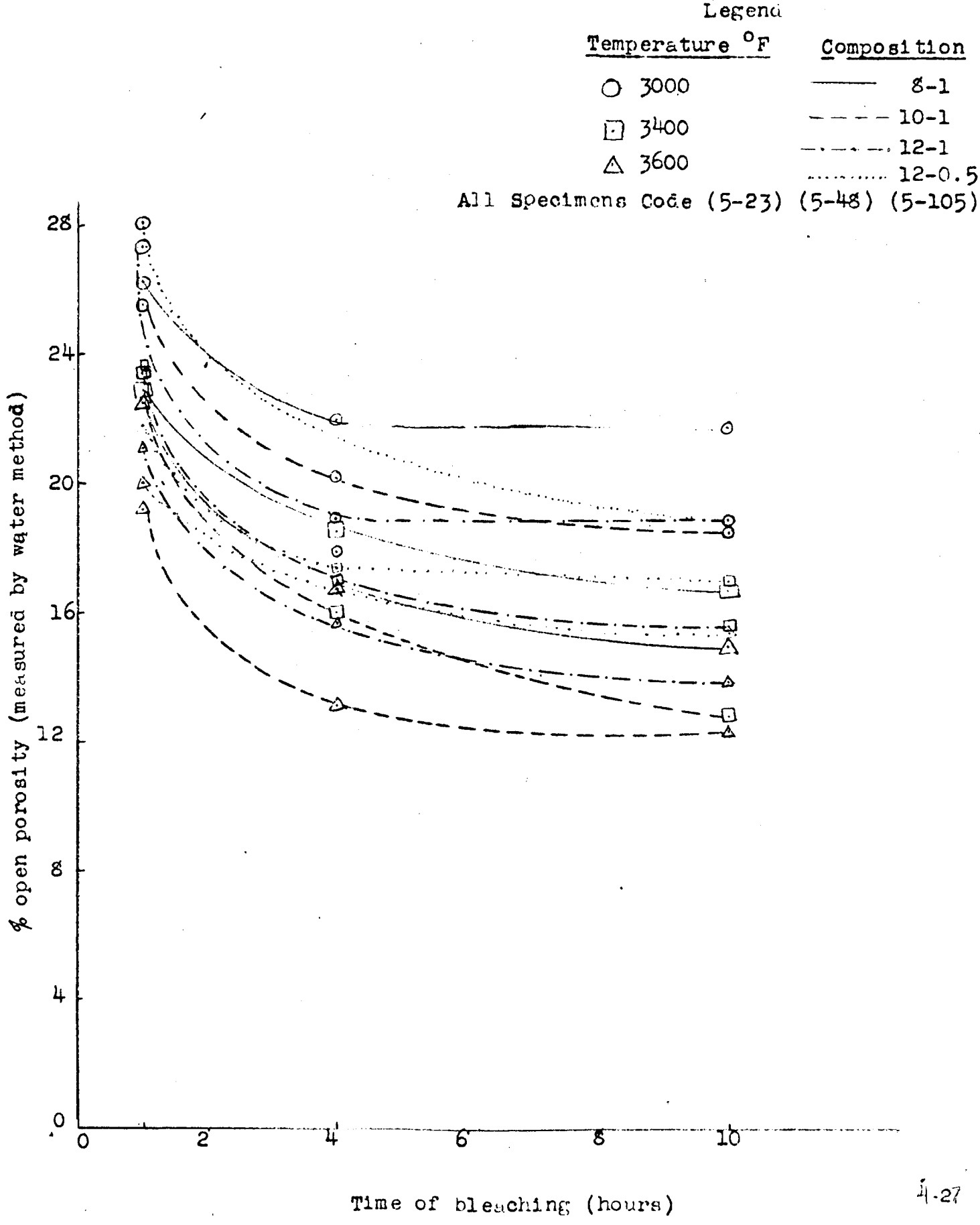

After bleaching, the specimens were cut with a small high speed alundum cut-off wheel into pieces which would fit the mercury penetrometer capsule. One small piece was used for spectrographic analyses, as is discussed later.

The % bulk density, % total, open and closed porosity, range of maximum porosity and mean pore size are listed in Table 4-7 as were measured by the Porosimeter.

The pore spectrum curves are plotted in Figure 4-6. The pore levels above the knee in the otherwise sharp curve, show macroporosity due to non-milling, therefore, the range of maximum porosity data was arbitrarily limited to the values below the "90% finer than" level. Similarly, for tabulating purposes, the cut-off point at the lower pore diameters was arbitrarily set at 10%. This was because the finer pore diameters, (ie) below .5 micron or so, are expected to contribute proportionally little to cesium flow when the mean pore diameters are double that diameter and five times the volume. In turn, these two cut-off points which establish the maximum and minimum pore diameters at the center 80% pore volume, in a sense identify the slope of the relatively straight line portion of the pore spectrum curve.

The Porosity Evaluation Table 4-7 also includes data obtained on the 1st generation specimens prepared in October, 1963, as reported in the final report of the NAS 3-2513 contract. These first generation specimens were also made with the fine pan-washed copper powder, but were hand mixed. The 2nd generation specimens were dry ball mixed for a four hour period. As was later determined by microscopic examination of mixed powder specimen smears on glass slides, serious copper agglomeration existed. This agglomeration caused large Cu-Ni lake areas in the sintered specimens which subsequently resulted in large macro 5-50 micron non-interconnected voids in completed leached and bleached emitters. The 3rd generation specimens were made by using more highly selected fine Cu powders and wet vibration milling for 16 hours. The mean pore diameters of all 2nd and 3rd generation specimens of four composition levels 8-1, 10-1, 12-1 and 12-0.5 (Cu-Ni) fell within a very narrow range between 0.9 to 1.2 microns, which shows that the selected composition range and process parameters produce a relatively narrow range of mean pore diameters. In general, it can be concluded that as process refinements have been incorporated, the pore spectrum range becomes more narrow. This narrow range is desirable for emitter application.

TABLE 4-7. Porosity Evaluation Data 1st & 2nd Generation Tungsten Emitter Structures Processed by Liquid Phase Sintering of W-Cu-Ni Ternary System Sintered @ 2150°F - 5 hrs, Acid Leached. & Vacuum Bleached.

Specimen				HNO_3 Leached and Bleached Porosity Characteristics (d)					
	Composition (a)		Genera- (c)	Bulk Dens.	Porosity in % (b)			Range of Max. Porosity in u	Mean
No.	Cu	Ni	Code	tion	% Theoret.	Total	Open	Closed	Center 80%	Size (μ)
1.	12	0.5	4-166	1st	77.2	22.8	19.7	3.1	1.1 -2.05	1.7
2.	12	0.5	9-97,5-76C	2nd	76.2	23.8	18.1	5.7	.53-2.2	1.2
3.	8	1	4-166	1st	79.5	20.5	19.6	0.9	.45- .7	.60
4.	8	1	9-96,5-76C	2nd	76.7	23.3	22.3	1.0	.65-1.9	1.2
5.	10	1	4-166	1st	78.3	21.7	20.1	1.6	.8 -2.1	1.5
6.	10	1	9-97,5-76C	2nd	79.8	20.2	18.7	1.5	.6 -1.2	0.9
7.	12	1	4-166	1st	77.7	20.3	19.7	2.6	1.0 -2.15	1.7
8.	12	1	9-97,5-76C	2nd	77.7	22.3	20.2	2.1	.55-1.3	1.2
9.	12	1	9-86,5-75B	3rd	82.1	17.9	16.4	1.5	.68-1.3	1.0

NOTES: (a) In weight %, balance tungsten - all materials below ≃ 5 micron average diameter.

(b) Porosity by mercury intrusion - Aminco Porosimeter as % of specimen bulk volume.

(c) Generation - 1st as reported from NAS 3-2513 Final Report Table 8, hand-mixed powders.
2nd specimens delivered to NASA June, 1964. - dry ball milled 4 hrs.
3rd specimens delivered to NASA July, 1964. - powders vibration milled 16 hrs.

(d) Bleached at 3400°F - 4 hours.

FIGURE 4-6 PORE SPECTRUM ANALYSES of TUNGSTEN EMITTERS by AMINCO-WINSLOW POROSIMETER
W-Cu-Ni Ternary Leached and Bleached. 2nd & 3rd Generation

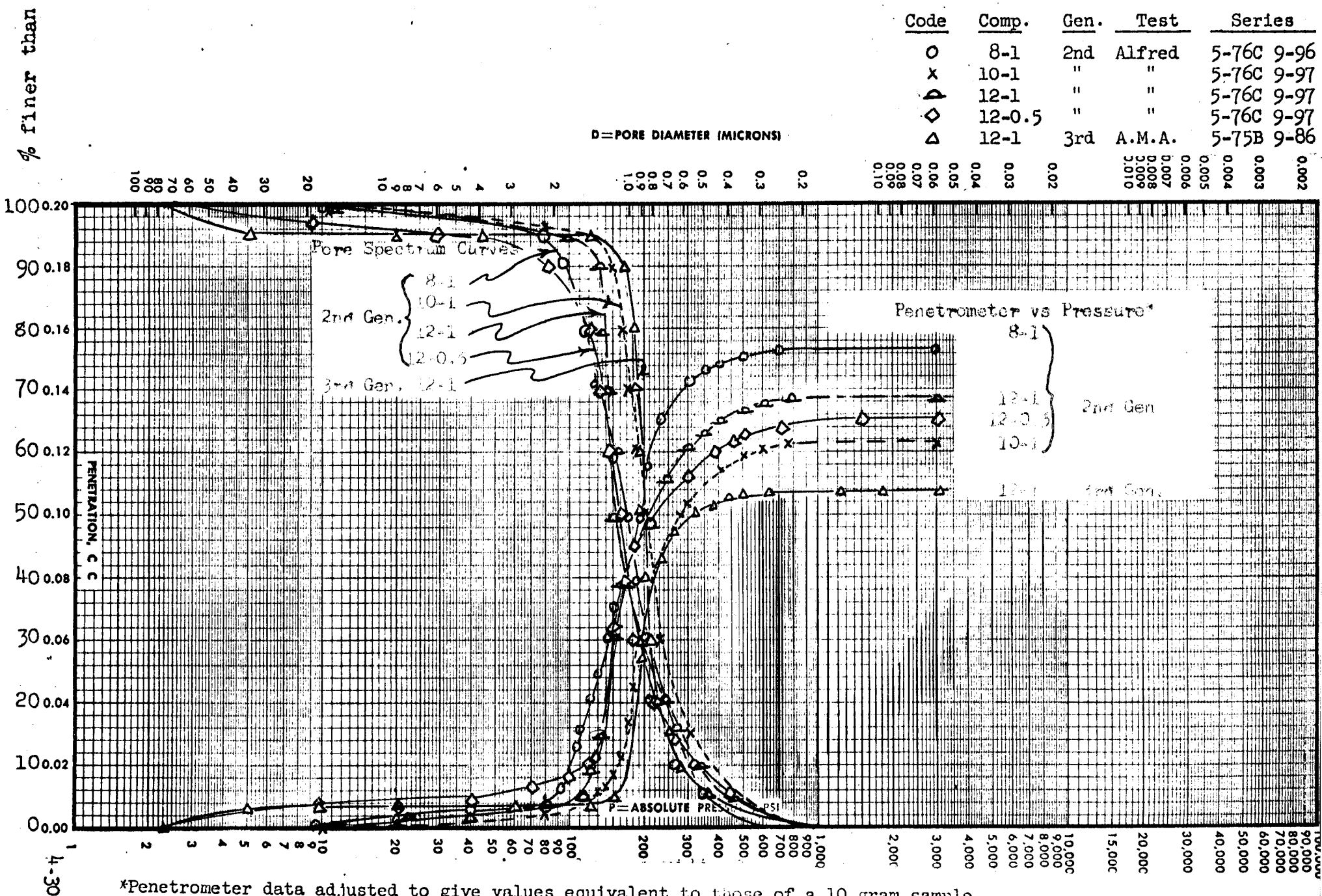

*Penetrometer data adjusted to give values equivalent to those of a 10 gram sample

The overall bulk density of the various second generation emitters is lower, (ie) higher total porosity, than the 1st generation emitters. This was probably due to the greater amount of macro porosity due to copper agglomeration during initial dry ball milling. The 3rd generation composition, however, had a higher bulk density, (ie) a lower porosity. This is probably due to the initially lower sintered grain size and greater shrinkage.

Pore spectrum analyses of 6th generation specimens is discussed in the Improvement Studies Section, part 5.3.3.

4.4.5 Aging

The porous tungsten metallurgical thermal stability was evaluated by aging the various 2nd and 3rd generation compositions 12-0.5, 8-1, 10-1 and 12-1 at 2500°F in a dry hydrogen atmosphere. The specimens were those control discs prepared with delivered evaluation emitter test specimens, and which had been used for initial pore spectrum analyses. The specimens were placed on fine decarburized tungsten wool within a 99% pure alumina crucible (prepared in this laboratory). The alumina boat and samples were placed in a small molybdenum wire wound hydrogen atmosphere tube furnace and brought to temperature in about 2 hours.

Temperature control is manual, with a L & N optical pyrometer used for measurement. Line voltage, amperage and temperature are measured periodically and adjusted if necessary, though temperature was observed to remain within $\pm$ 15°F at 2500°F.

The relative stability of these 2nd and 3rd generation emitters was judged by conducting both pore spectrum and permeability as well as X-ray back reflection tests after 50, 150 and 500 hours of aging at 2500°F in dry hydrogen.

4.4.5.1 Porosity and Transmission Coefficient Testing

Mercury porosimeter pore spectrum and transmission coefficient (C) analyses were also conducted on the aged porous tungsten specimens after 50, 150 and 500 hours at 2500°F in hydrogen.

The data from these tests are given in Table 4-8. Values were determined for density; total, open and closed pore volume; mean pore diameter; and 80% median pore diameter range. The rate of open pore closure was calculated and plotted in Figure 4-7 with a similar plot of rate of transmission coefficient change. A further discussion of this comparison is given in the next section.

The porosimeter data show that the 8-1 and 12-0.5 2nd generation specimens retained the greatest open pore volume with time. The 8-1 mix exhibited the highest original transmission coefficient with time.

The pore size analyses curves generally indicate that the fine pores are closing. As a result, the pore spectrum curves shift to higher mean pore diameters with time. Though the coarse pores are not changing significantly, their ratio increases as the small pores close.

Nitrogen permeability tests on the 2nd and 3rd generation specimens were conducted with equipment and techniques described in Section 3.12. Tests were made on .157 inch diameter discs .020 inch thick after the 50, 150 and 500 hour exposures at 2500°F in dry hydrogen. The "Transmission Coefficient X Length" data were calculated and are given in Table 4-8 and plotted on Figure 4-8. The rate of permeability change due to aging at 2500°F was calculated and plotted in the lower section of Figure 4-7.

The rate of pore closure "k" was calculated from transmission coefficient and porosity data as follows:

$$\frac{\Delta C}{C_o} = k_c t$$

$$\sqrt[3]{\frac{\Delta P}{P_o}} = k_p t$$

where

$\Delta C = C_o - C_t$ = change in transmission coefficient with aging time (t)

C_o = transmission coefficient x L = before aging

$\Delta P = P_o - P_t$ = change in open pore volume percent with aging time (t)

P_o = open pore volume percent before aging.

Since open porosity is an indication of the open pore volume, it was necessary to take cube root of $\frac{\Delta P}{P_o}$ to correlate open porosity data with transmission coefficient data.

"k_c" and "k_p" were calculated as the slopes of the graphs $\frac{\Delta C}{C_o}$ vs t and $\sqrt[3]{\frac{\Delta P}{P_o}}$ vs t.

The values of pore closure rate for 0 to 50 hours (k_{p1} and k_{c1}) and for 50 to 150 hours (k_{p2} and k_{c2}) and for 150 to 500 hours (k_{p3} and k_{c3}) are given in Table 4-9. From analysis of this data, the following conclusions are evident:

(1) As the aging time increases, the rate of closure of pores decreases. The average rate of closure of pores decreases by a factor of about 10 after 50 hours of aging (ie) $k_1 - = \frac{k_2}{F_1}$ where $F_1 \cong 10$.

Also $k_3 = \frac{k_2}{F_2}$ where $F_2 \cong 10$, $k_3 = \frac{k_1}{F_3}$ where $F_3 = 100$

(2) the values of k_1, k_2 and k_3 are of the same order of magnitude for the different samples.

(3) The values of k_1, k_2 and k_3 as determined from open porosity data are somewhat lower than those determined from transmission coefficient data.

The apparent rapid pore closure rate was believed much higher than that theoretically expected. This could have been due to either or both of two possible contributing factors. Activation energy levels are lowered by nickel and are believed lowered by hydrogen atmospheres vs vacuum. Hydrogen atmospheres are used to sinter commercial powder metallurgy tungsten because sintering rates are higher than in vacuum.

Because most of these specimens contain 10 parts per million or less nickel as shown in Table 4-4, its contribution is believed nil. One exception is that of the 12-1 3rd generation specimen which had about 70 ppm nickel as well as a fine grain size. It had the highest pore closure rate However, it is very important to determine if such low nickel levels as 10 ppm could be so influential in causing densification of porous tungsten emitters at 2500°F.

TABLE 4-8 Porosity Characteristics of Porous Tungsten Ion Emitter Structures (2nd & 3rd Generation vs Aging Time at 2500°F in dry hydrogen.

Specimen No.	Composition(a) Cu	Ni	Code	Generation(c)	Aged Time (hrs.)	Bulk Dens. % Theoret.	Porosity in %(b) Total	Open	Closed	Range of Max. Mean Porosity in μ Center 80%	Size (μ)	Trans Cf. x L x 10
1-a	12	0.5	9-97, 5-76C	2nd	0	76.2	23.8	18.1	5.7	.53-2.2	1.2	.151
b					50	77.7	22.3	16.1	6.2	.9 -2.6	1.75	.13
c					150	78.8	21.2	15.0	6.2	1.2 -3.5	1.75	.1
d					500	78.8	21.2	13.4	7.8	1.3-50.0	1.9	.047
2-a	8	1	9-96, 5-76C	2nd	0	76.7	23.3	22.3	1.0	.65-1.9	1.2	1.16
b					50	77.8	22.2*	20.1*	2.1	.9 -2.3	1.65	.55
c					150	79.2	20.8	16.1	4.7	.95-2.6	1.65	.22
d					500	80.1	19.7	13.0	6.7	.9-12.0	1.8	.056
3-a	10	1	9-97, 5-76C	2nd	0	79.8	20.2	18.7	1.5	.6 -1.2	0.9	.30
b					50	81.9	18.1	12.4	5.7	.9 -2.3	1.65	.55
c					150	81.3	18.7	9.9	8.8	.95-2.3	1.6	.016
d					500	81.8	18.2	9.4	8.8	.7 -5.0	1.5	.005
4-a	12	1	9-97, 5-76C	2nd	0	77.7	22.3	20.2	2.1	.55-1.3	1.2	.32
b					50	80.2	19.8	17.7	2.1	1.0 -3.0	1.8	.14
c					150	80.8	19.2	13.5	5.7	1.0 -3.0	1.8	.06
d					500	81.8	18.2	11.0	7.2	.9 -6.0	1.7	.026
5-a	12	1	9-86, 5-75B	3rd	0	82.1	17.9	16.4	1.5	.68-1.3	1.0	.13
b					50	81.8	18.2	9.4	8.8	.6 -1.5	.9	.013
c					150	87.0	13.0	4.7	8.3	.5 -1.5	.7	.009
d					500	100.0.	0.0	1.5	98.5	Not measurable		.004

NOTES: (a) In weight %, balance being tungsten; all materials below ~5 micron average diameter.
(b) Porosity by mercury intrusion - Aminco Porosimeter as % of specimen bulk volume.
(c) Generation - 2nd specimens delivered to NASA June, 1964 - dry ball milled 4 hrs.
3rd specimens delivered to NASA July, 1964 - powders vibration milled 16 hrs.
* changed since Monthly Report 9-1, dated August 10, 1964.
(Spectrographic Analyses are in Table 4-4)

FIGURE 4-7 RATE OF OPEN PORE CLOSURE - POROUS TUNGSTEN ION EMITTERS
2nd and 3rd Generation
Resulting from Aging @ 2500°F for 500 hrs. in Dry H_2
Series 5-76 - 5-75

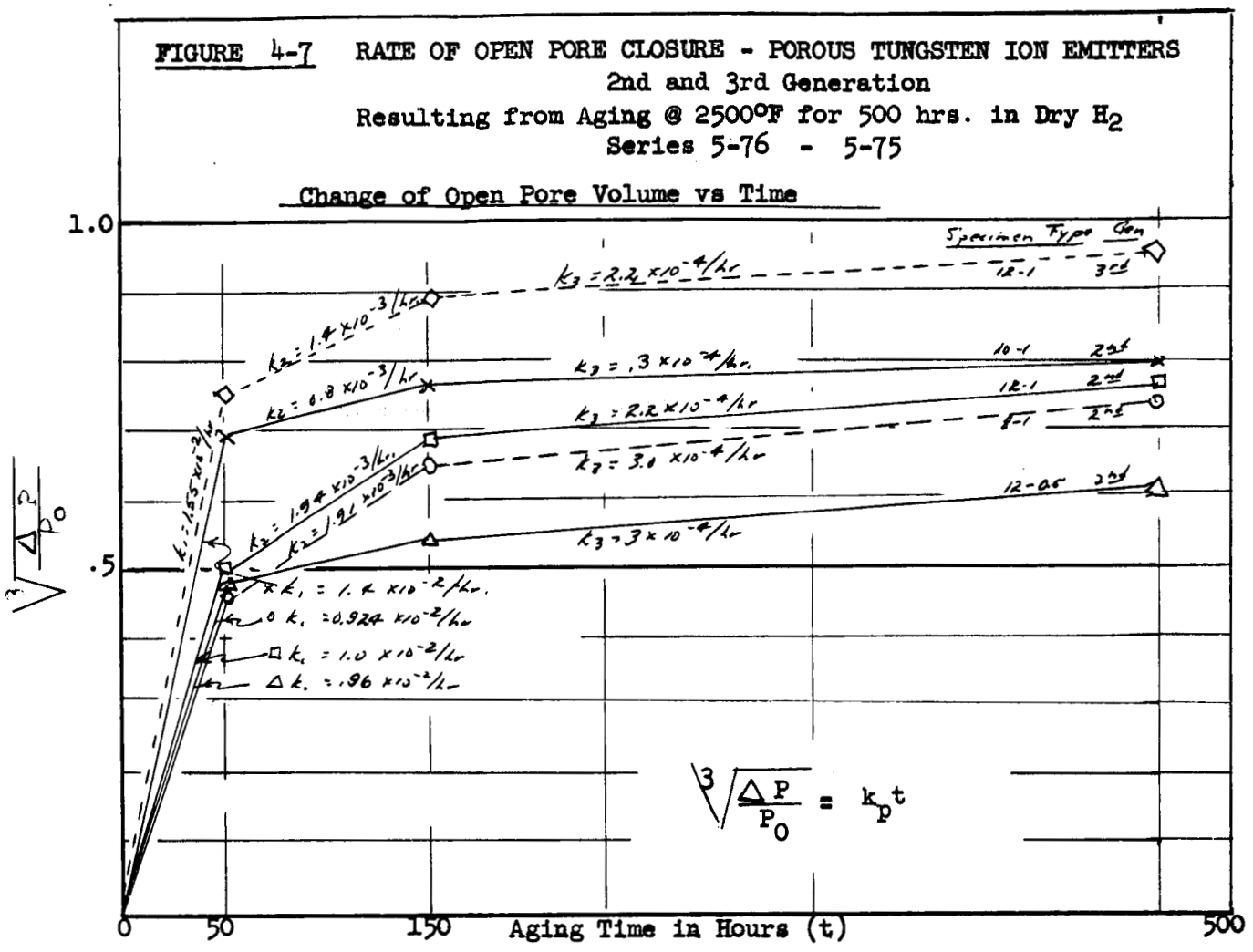

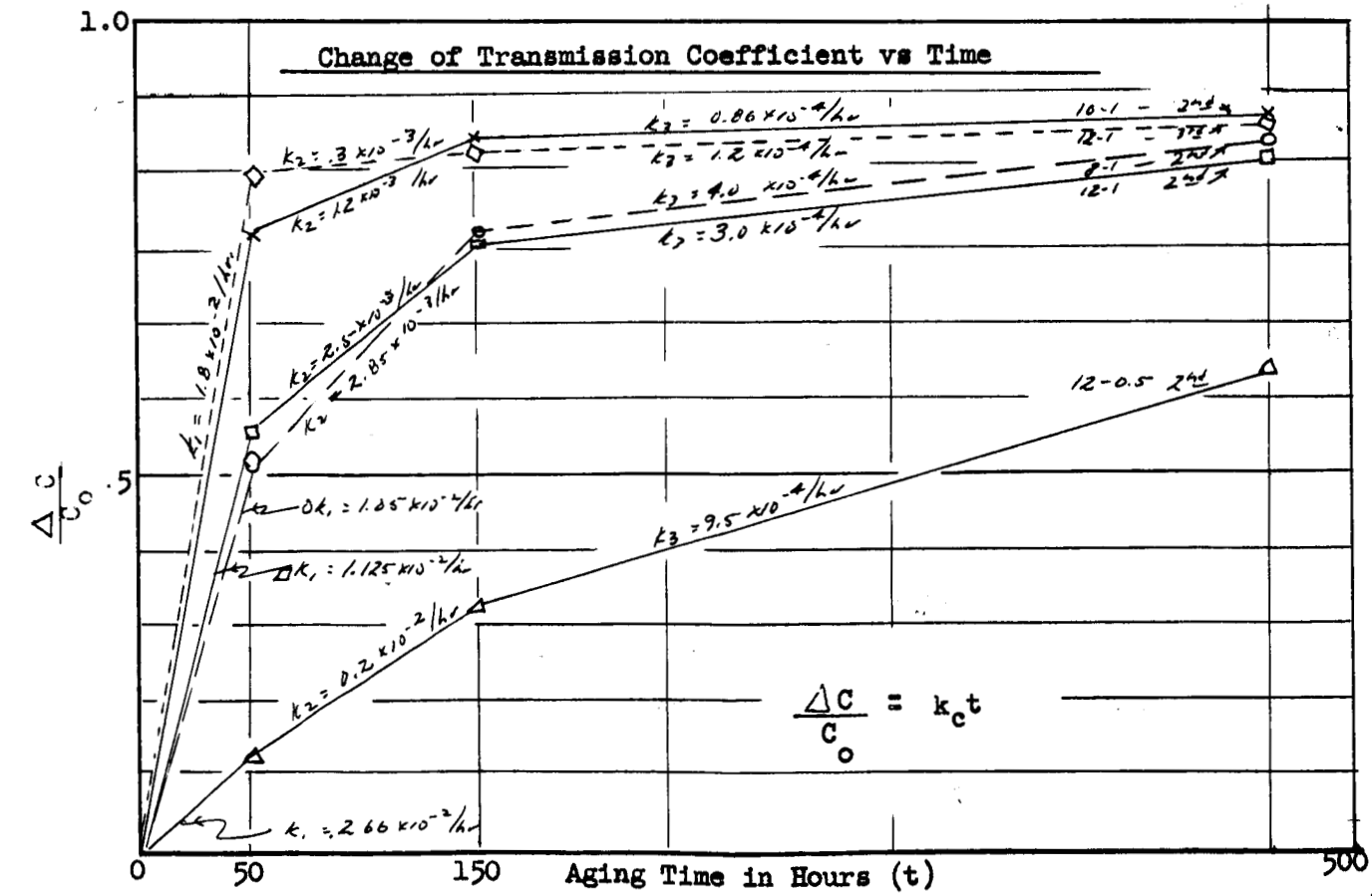

TABLE 4-9 PORE CLOSURE RATE DUE TO AGING AT 2500°F IN DRY HYDROGEN

Series 5-76 & 5-75 Specimen (a)	Generation (b)	Aged 50 hours k_{c1} $\frac{\Delta C}{C_o} \times 10^2$	Aged 50 hours k_{p1} $\sqrt[3]{\frac{\Delta P}{P_o}} \times 10^2$	Aged 150 hours k_{c2} $\Delta C/C_o\ 10^3$	Aged 150 hours k_{p2} $\sqrt[3]{\frac{\Delta P}{P_o}}\ 10^3$	Aged 500 hours k_{c3} $\Delta C/C_o\ 10^4$	Aged 500 hours k_{p3} $\sqrt[3]{\frac{\Delta P}{P_o}}\ 10^4$
8-1	2nd	1.052	.924	2.85	1.91	4.	3
10-1	2nd	1.666	1.40	1.2	.8	.86	.3
12-0.5	2nd	.266	.96	2.0	.7	9.5	3
12-1	2nd	1.125	1.0	2.5	1.94	3	2.2
12-1	3rd	1.8	1.55	.3	1.41	1.2	2.2
Average k		1.41	1.17	2.14	1.15	3	2.2

k_{c1} = Transmission Coefficient Rate of Change with Aging Time

k_{p1} = Open Porosity

NOTE: (a) = Original weight % of Cu-Ni levels, balance being W.

(b) = Process generation number. 2nd not milled; 3rd fine grain size, milled.

FIG. 4-8 TRANSMISSION COEFFICIENT vs DENSITY
For DIFFERENT AGING TIMES (0, 50, 150, 500 Hrs.)
Astro Met Porous Tungsten Ion Emitter Structures

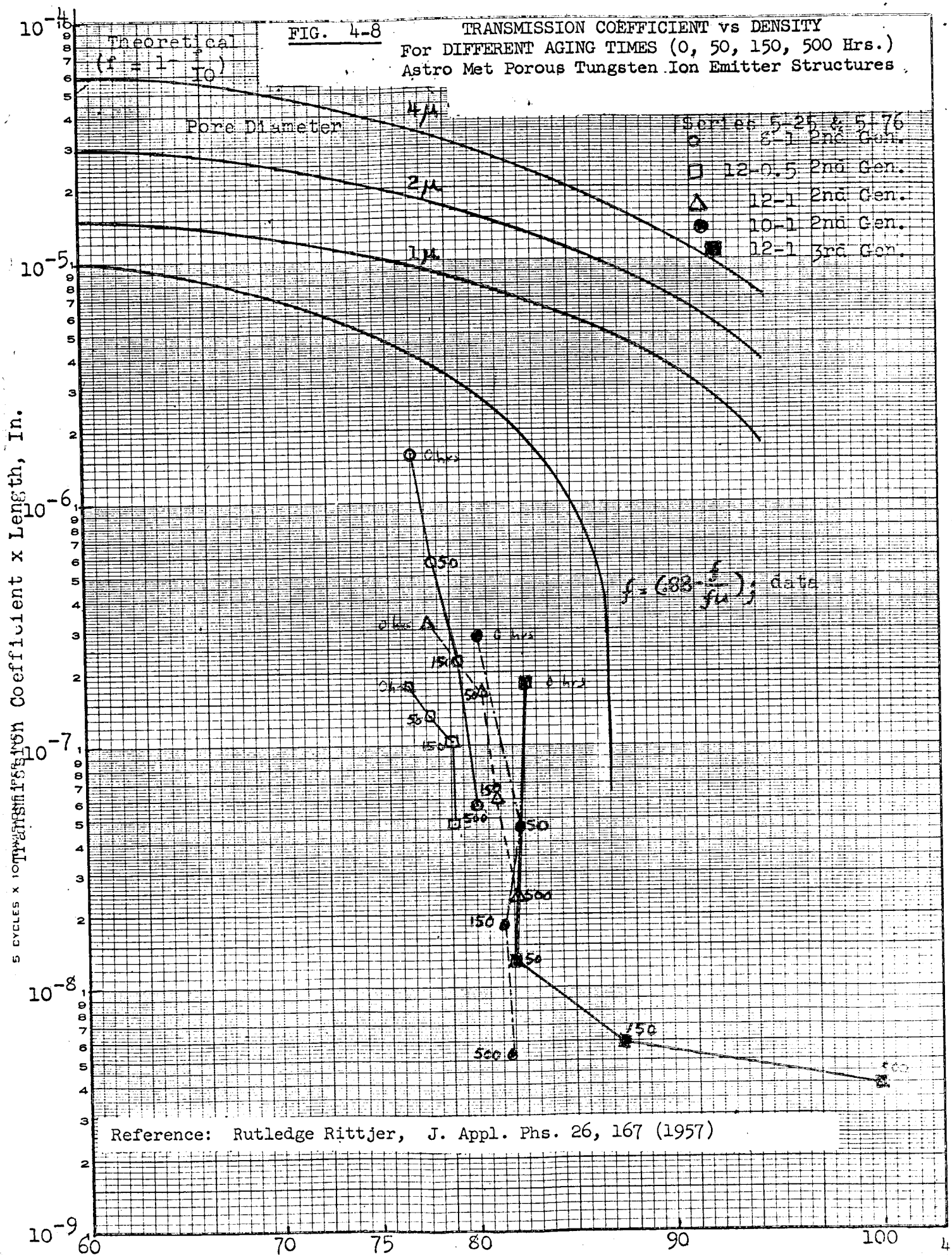

Reference: Rutledge Rittjer, J. Appl. Phs. 26, 167 (1957)

The hydrogen atmosphere is believed to be more responsible for such high aging rates in this group of 2nd and 3rd generation specimens. This is because other pore closure rate tests on vacuum (10^{-3} Torr) (as described in Section 4.4.4.1, Table 4-6 and Figure 4-5) indicate a higher degree of stability is attained by some similar specimens following the initial bleaching period of four hours. Such stability appeared at even higher temperatures than those used for these hydrogen aged specimens. Both of these discussed tests were made on different specimen series, for widely different time periods, for different purposes. An exact comparison of aging characteristics would be questionable. Since hydrogen aging atmospheres were suspect, all further tests were done in vacuum. Fine pore size tungsten emitter plates were prepared, as is discussed later in Section 5.3.4, which exhibit little or no change in porosity and pore diameters in 6 hours at 2750°F. These structures were delivered to NASA for ion emission evaluation.

4.4.5.2 X-Ray Back Reflection Analyses

Diffraction patterns were made of the porous tungsten structures as processed and after hydrogen aging at 2500°F for 50 and 150 hours. The small S.T.L. discs .157" diam. x .020" thick were used from the same sintered, acid leached, alkaline etched and vacuum bleached group supplied to NASA as the 5-75, 5-76 series. The pore spectrum pore volume and aging relationships of these specimens were discussed just above.

Definite crystal growth trends were observable as shown by a reproduction of the X-ray patterns as Figure 4-9. These X-ray analyses were initially limited to these feasibility trials due to funding levels. It is believed that correlative relationships could be established by these non-destructive analyses, with more extensive studies.

4.4.6 Ion Emission Tests

Initial ion emission tests were conducted by S.T.L. on those specimens previously described and furnished to NASA in June, 1964. The specimens were rhodium brazed into refractory feed tubes by S.T.L. This resulted in almost vacuum tight emitters, which had to be etched in order to open up the porosity prior to emitter testing. Several disadvantages of these brazing procedures

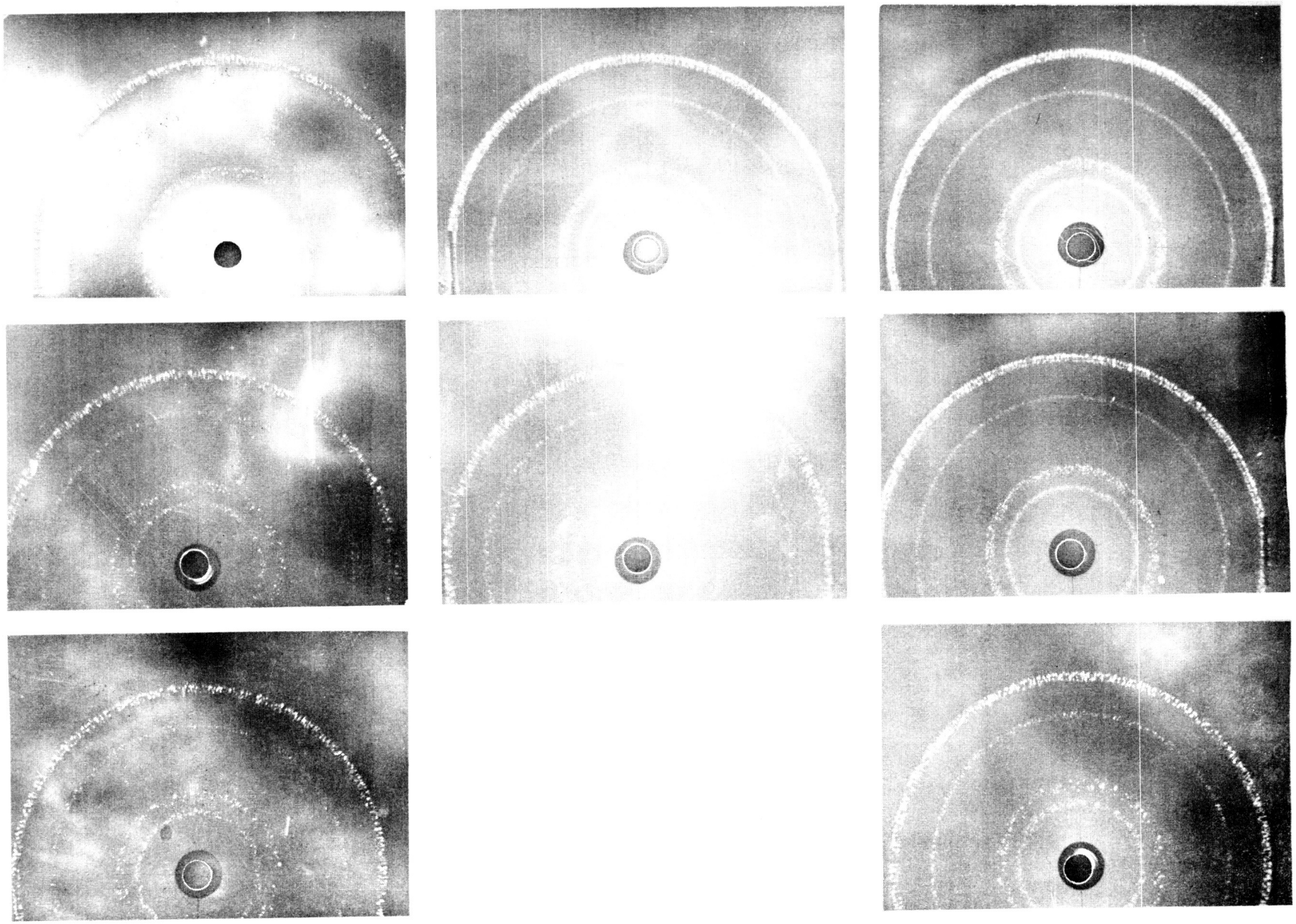

FIGURE 4-9 X-RAY BACK REFLECTION PATTERNS. LEACHED, ETCHED and BLEACHED W-Cu-Ni COMPOSITIONS. SHOWING GRAIN (PATTERN) COARSENING DUE TO AGING AT ION EMITTER OPERATING TEMPERATURES. RADIATION COPPER k - DISTANCE 2cm

suggest that only electron beam welding should be used for joining the porous emitters. An analysis of potential problems brought about by rhodium as well as other brazing techniques follows.

The furnished emitter structures were originally open as evidenced by Astro Met's permeability tests on retained 10-1 2nd generation and 12-1 3rd generation discs from the same processed lots as listed in Table 4-7 and 4-8. Previous brazing trials on Astro Met's liquid phase sintered, leached and bleached, porous tungsten emitters, by another ion propulsion systems laboratory about a year ago demonstrated that Astro Met's structures were more easily wetted by brazing. This resulted in pore closure by braze saturation at that time, as was expected to have occurred in these current braze operations.

If such brazed porous tungsten structures are anodically etched subsequent to brazing, selective removal of tungsten will occur in areas where rhodium content is low, thusly large pores would tend to be further enlarged due to both low rhodium content in these areas, and due to the greater access of etchant into large pore areas.

These specimens were obtained for metallographic analyses. Examination of both the W-10Cu-1Ni 2nd generation (non- ball-milled compacts) and the W-12Cu-1Ni 3rd generation (ball-milled compacts) indicated that rhodium brazing had caused serious pore occlusion in several ways. This was determined by etching the mounted and polished specimens by three methods.

Initially, Murakami's etch was used. Metallographic examination showed that excessive rhodium had created a solid meniscus between the porous tungsten disc and the molybdenum housing. This meniscus appeared to cover about 50% of the specimen diameter or 75% of the specimen inner face area. Electrolytic etching with NaOH solution removed the smeared tungsten and revealed that considerable open porosity still remained, though some pore closure had occurred from the high brazing temperature. Etching with concentrated nitric acid then allowed the tungsten and rhodium phases to be more readily distinguished. As a result, the rhodium appeared to have flowed in a thin coating over most of the observable porous tungsten inner surface. Rhodium had penetrated this surface of the porous tungsten to a depth of 60 to 80 microns. Tungsten densification had occurred in this infiltrated rhodium area, presumably due to the lowered activation energy level of this alloy system, as is further discussed below.

The significance of rhodium on reducing tungsten activation energy is shown in Figure 4-10 and Table 4-10 where activation energy relationships are shown for various alloy additives to tungsten, including rhodium. This data was reported by Brophy[21] who suggested that rhodium would be effective as an activator when present in monomolecular layers. Brophy stated that 0.25 weight % rhodium is sufficient to activate .56 micron tungsten powder. The surface area of a five micron average grain diameter emitter structure would be at least one-hundredth that of the fine powder used by Brpphy. The rhodium quantity required for coating internal emitter surface area would suggest that .025%, or 250 parts per million, would be effective in increasing aging rates by a factor of about 35 or so over that of pure tungsten, at emitter operating temperatures.

This suggests that rhodium is a probable serious metallurgical contaminant on ion emitters which must operate for long periods. Considering its effect on contact ionization work function, rhodium would probably not be detrimental, though other group VIII elements have considerably lower work functions and may reduce ionization efficiencies.

As a result of this analysis, it is recommended that rhodium brazing should not be done on small porous tungsten emitters, particularly when their mean pore diameters are near the 1 micron level and estimated pore counts are in the 10^7 pore/cm^2 range due to expected high wicking characteristics.

This analysis of activation energy relationship further suggested that iridium would be a useful additive to increase stability of tungsten in emitters. An analysis of this possibility is later made in Section 6.0 where exploratory trials were made using iridium additives. Some physical property characteristics are listed in Table 4-10 for comparison with rhodium and its effect on tungsten.

An Arrhenius plot of densification rates vx temperature for tungsten and tungsten plus iridium is shown in Figure 6-1.

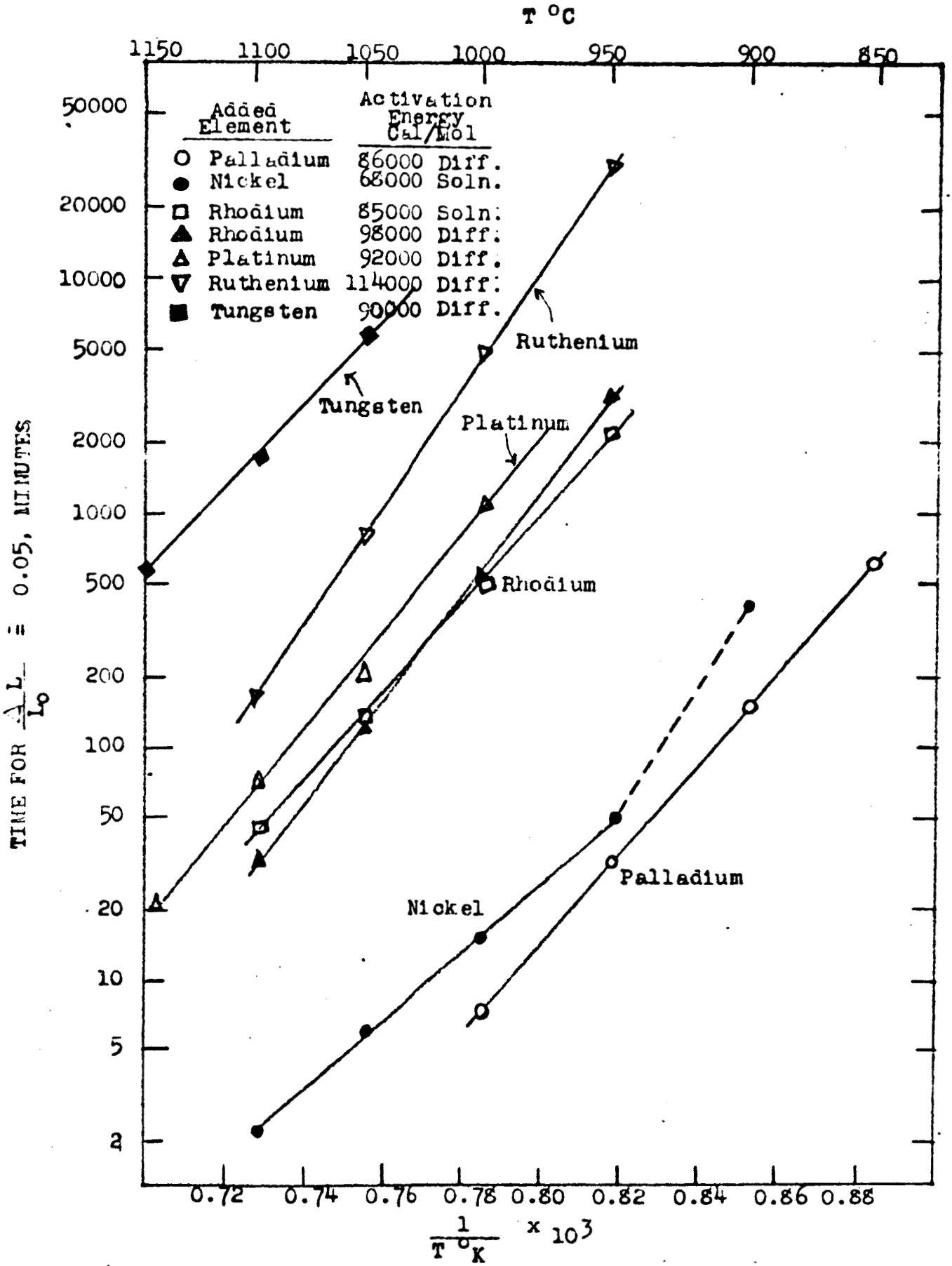

FIGURE 4-10 Arrhenius Plots of Data from Sintering of Tungsten with Additions of Palladium, Nickel, Rhodium, Platinum and Ruthenium.(21)

TABLE 4-10 Comparison of Physical Properties and Sintering Characteristics of W, Ir and Rh.

No.	PROPERTY	W	Ir	Rh
(1)	Melting Point	3370°C	2454°C	1966°C
(2)	Boiling Point	5900°C	5300°C	4500°C
(3)	Work Function	4.25-5.1 ev.	5.3 ev	4.58-4.90 ev
(4)	Vapour-Pressure (mm Hg)	$2554^{\circ}C=4600^{\circ}F=10^{-5}$ $2767^{\circ}C=5000^{\circ}F=10^{-4}$ $3016^{\circ}C=5450^{\circ}F=10^{-3}$ $3309^{\circ}C=6000^{\circ}F=10^{-2}$	$1427^{\circ}C=2500^{\circ}F=2.9\times10^{-10}$ $1827^{\circ}C=3300^{\circ}F=1.9\times10^{-6}$ $1993^{\circ}C=3500^{\circ}F=10^{-5}$ $2154^{\circ}C=3800^{\circ}F=10^{-4}$ $2340^{\circ}C=4250^{\circ}F=10^{-3}$ $2556^{\circ}C=4600^{\circ}F=10^{-2}$	$1472=2700^{\circ}F=10^{-6}$ $1582=2900^{\circ}F=10^{-5}$ $1707=3100^{\circ}F=10^{-4}$ $1857=3400^{\circ}F=10^{-3}$ $2037=3600^{\circ}F=10^{-2}$
(5)	Density (gm/c.c.)	19.3	22.42	12.44

(6) RELATIVE Ddensification RATES OF TUNGSTEN, W-Ir, and Rh ALLOYS[21]

Temperature °C	Temperature °F	Time for 5% Shrinkage (in Minutes) W	W + 4 w% Ir	W + >0.25 w% Rh
1000	1830	-	-	550
1050	1920	6000	230,000	150
1100	2015	1,700	40,000	45
1150	2105	600	7,000	-
1200	2195	180	1,300	-

(7)	Activation energy (K cal/mole)	Grain Boundary = 90-100 Volume self-diffusion = 135	W + 4w% Ir Volume self-diffusion = 133	W + >0.25 w% Rh solution = 85 Grain Boundary diffusion = 98

5.0 Improvement Studies

From the Preliminary Studies it became more evident that a uniform porous tungsten ionizer with about 1 μ pore diameter, 4-5 μ grain size, 20% open porosity and 10^6 to 10^7 pores/cm^2 pore count could be made. Also, the process of liquid phase sintering allows precise control of pore size and grain size. However, the combination of these characteristics with thermal stability at 2500°F in vacuum remained to be demonstrated in the improvement task.

As a result, improvement studies were undertaken to achieve even greater uniformity and thermal stability of porous tungsten ionizers, and to prepare emitter plates 1/8" thick, 1.35" wide and 2.25" long. The studies were directed towards -

(1) exploring different leaching solvents which could remove the major amount of Cu-Ni phase without causing oxidation, reaction or contamination;

(2) investigating bleaching temperatures lower than 3400°F so that residual Ni could be removed to spectrographic levels and yet not cause excessive pore closure by nickel diffusion in tungsten or specimen shrinkage during the bleaching operation.

5.1 Material and Compositions

Eight pound slugs were prepared of both W-8Cu-1Ni and W-10Cu-1Ni by vibrational milling and by hydrostatic pressing to 20,000 psi. These green slugs were cut into large .150" x 2" x 4" slabs and .325" x .325" x 2" long bars by abrasive wheel sawing for both slab and disc type specimens.

5.2 Processing

5.2.1 Sintering

The above specimens were divided into several sets which were sintered to both 2150°F for 5 hours and to 2250°F for 5 and 25 hours which was expected to give a grain size ranging from 5 to 10 microns respectively. Microstructural analyses of the 8-1 control specimens indicate that mean grain size is about 4 microns for the lower and 10 microns for the upper sintering temperature and time periods.

The W-10Cu-1Ni composition grain sizes averaged between 4 and 5 microns for both temperatures for 5 hour sintering and to about 10 microns for 2250°F -

25 hour sintering conditions. It appears that the vibration milling produces slightly lower grain diameters than were previously produced in hand-mixed specimens The grain size uniformity and grain distribution are much improved by milling. This provides an advantage by increasing the pore count per cm^2 to more desirable levels. As reported in Table 5-10 later, the pore spectrum analyses on the resulting structures indicate that they have narrow pore size ranges from 1 to 1.7 microns, giving an estimated pore count of about 10^7 pores per square centimeter.

5.2.2 Leaching Studies

A review of solvent systems, which could possibly remove efficiently the Cu-Ni phase without oxidizing or contaminating the tungsten sample, was made from Uhlig's "Corrosion Handbook"(26). Several different solvents were tried at temperatures varying from room temperature to 130°F. Also, direct current electrolytic leaching was explored.

Leaching studies were made on thin and thick specimens representing the range of discs and plates desired in emitter structures. Following leaching, the specimens were rinsed in distilled water and vacuum dried four times, then oven dried prior to weighing.

The specimen details, leaching media, conditions and results are shown on Table 5-1 and Figure 5-1 with the measured weight loss and calculated leaching efficiency data. The results are as described below.

Ammonium hydroxide generally exhibits low leaching efficiency on most of the W-Cu-Ni alloy systems studied. In addition, it appeared to produce a hydroxide coating.

Both concentrated sulfuric acid, and sulfuric acid / ferric sulphate exhibit low leaching efficiencies plus oxidize the tungsten.

Chromic acid at 60°C is slow acting in removing the Cu-Ni phase, but boiling chromic acid is very effective. Chromic acid (hot or boiling) does not appear to oxidize the tungsten sample but leaves CrO_3 layer on it. Some of the CrO_3 film could be subsequently dissolved in ammonium hydroxide.

Hydrochloric acid at 60°C can remove the Cu-Ni phase completely and efficiently, but oxidizes the tungsten. Its leaching action is very similar to that of hot nitric acid.

Hydrochloric acid at room temperature, however, can remove the Cu-Ni phase completely, but the leaching action is slow. It has the advantage that it does not oxidize the tungsten at all.

Since dissolved oxygen in hydrochloric acid at room temperature can accelerate the corrosion rate of copper at least by a factor of five, it was decided to also study the leaching action of concentrated HCl through which oxygen was being bubbled.

In order to increase the leaching rate of HCl on several W-10Cu-1Ni specimens, two approaches were used where oxygen was incorporated in the HCl solutions.

Oxygen was added to the HCl by bubbling through the solution during the leaching period. Though leaching rates increased significantly, a deposit (probably cupric chloride or copper oxychloride) coated the specimen. Though this deposit could be readily removed by NH_4OH, the specimen appeared to be slightly oxidized as evidence by its resulting dull appearance.

The second oxygen-HCl approach consisted of pre-saturating the solution by oxygen bubbling for 20 hours only before, and not during, the leaching cycle. The leaching rate appeared to be the same as that produced by straight HCl.

Electrolytic leaching was studied with HCl and with NH_4Cl solutions. The results of these tests are summarized in Table 5-2. The acid electrolytic leaching was very rapid and caused excessive specimen chipping plus what was believed to be slight specimen oxidation. The NH_4Cl electrolytic trials gave similar results.

Straight HCl (at 70°F) leaching studies showed that, though leaching was slower, the specimens appeared to be non-oxidized, as was apparent by the resulting bright surface. Because specimen oxidation is believed to be highly detrimental, HCl leaching at room temperature was the procedure used for all

TABLE 5-1a RESULTS OF LEACHING W-Cu-Ni SPECIMENS SINTERED AT 2150°F for 5 hrs. in VARIOUS AQUEOUS MEDIA

Leaching Media	Temp. °C	Time (hrs.)	Sample Cu-Ni & Code	Sample Features before leaching	Condition of sample after leaching	Leaching Media Color		Total % wt. loss	Efficiency %
						Before leaching	After leaching		
I(a) Chromic Acid (60% CrO_3)	57-60	24	12-1 (9-35)B (5-141)	Wt.. = 6.7913 gm. Thick. = .040" Dia. = .972"	One side of sample covered with a greenish yellow film probably of CrO_3.	Dark Orange	Dark Orange	0.365	2.81
"	108	8	"	Same sample as above	Whole of the sample covered with a yellowish layer probably of CrO_3	"	"	11.84*	91.1*
NH_4OH	35	45	"	Same sample as above	Covered with a greenish layer at few spots	Colorless	Light green	14.01*	107.7*
H_2 red.	980	1/2	" (9-182)	Same sample as above	Covered with a black layer at few spots	-	-	14.6*	108.1*
I(b) Chromic Acid	57-60	24	10-1 (5-136) (9-162) (5-141)	Wt.. = 8.1108 gm. Thick. = .237"	One side of sample covered with a v.v.thin yellow film probably of CrO_3	Dark Orange	Dark Orange	0.48	4.37
"	108	8	"	Same sample as above	Whole of the sample covered with a greenish yellow film probably of CrO_3	"	"	3.6*	33.33*
NH_4OH	35	45	"	Same sample as above	Sample covered with a greenish layer at some spots	Colorless	Light green	4.13*	37.55*

(contd.)

TABLE 5-1b (continued)

Leaching Media	Temp. °C	Time (hrs.)	Sample Cu-Ni & Code	Sample Features before leaching	Condition of sample after leaching	Leaching Media Color: Before leaching	Leaching Media Color: After leaching	Total % wt. loss	Efficiency %
Chromic Acid	106	18½	same as I(b)	same as I(b)	Sample covered with a yellowish layer probably CrO_3	Dark Orange	Dark Orange	9.98*	90.73*
NH_4OH	35	55	"	"	Sample covered with a green layer at some regions & yellow layer at others	Color-less	Light Green	10.70*	97.27*
H_2 red.	980	1/2	" (9-182)	"	Light dark spots on the sample	-	-	10.75*	97.73*
II NH_4OH	35	50	(8-1) (9-33) (5-145)	Wt. = 7.2433 gm. Thick. = .048"	Surface dull and covered with bluish $Cu(OH)_2$ at two spots	Color-less	Blue	.45	5
III Conc. H_2SO_4	56	27	(8-1) (9-33)A (5-146)	Wt. =11.5321 gm. Thick. = .073"	Sample covered with black & brown layer at considerable region. This is Tungsten Oxide probably.	Color-less	Color-less	0.35	4.4
IV Conc. H_2SO_4 - Ferric Sulphate	54 85	18½ 16	(10-1) (9-37)B (5-147)	Wt. = 5.697 gm. Thick. = .036"	" "	White	White	1.48	13.5 (contd.)

TABLE 5-1c (continued)

Leaching Media	Temp. °C	Time (hrs.)	Sample Cu-Ni & Code	Sample Features before leaching	Condition of sample after leaching	Leaching Media Color		Total % wt. loss	Efficiency %
						Before leaching	After leaching		
V(a) Conc. HCl	52	46	12-0.5 (9-36) (5-148)	Wt. = 11.0948 gm. Thickness = .080"	Covered with greenish layer probably tungsten oxide	Colorless	Brown-yellow	12.18	97.44
H_2 red.	1800°F	1/2	" (9-182)	" "	Covered with a black film and is not shiny		-	13.71*	109.7*
V(b) Conc. HCl	52	46	12-1 (9-35)A (5-148)	Wt. = 5.4331 gm. Thickness = .036"	Covered with greenish layer probably tungsten oxide	Colorless	Brown-yellow	14.54	111.8
H_2 red.	980	1/2	" (9-182)	" "	Covered with a black film & is not shiny	-	-	16.58*	127.6*
VI(a) Conc. HCl	Room Temp. 25°C	5½ 2	10-1 (9-37)A (5-65) (5-150)	Wt. - 8.0577 gm. Thickness - .055" - .066"	Sample shiny & no evidence at all of any oxidation	Colorless	Brown-yellow	10.87	98.83
H_2 red.	980	1/2	"	" "	Sample shiny	-	-	10.92*	99.3*

*Accumulative data.

TABLE 5-1d

Leaching Media	Temp. °C	Time (hrs.)	Sample Cu-Ni & Code	Sample Features before leaching	Conditions of sample after leaching	Leaching Media Color		Total % wt. loss	Efficiency %
						Before leaching	After leaching		
VI(b) Conc.HCl	Room Temp. 25°C	76	10-1 (5-124) (9-159)	Wt. = 8.0577 gm. Thickness = .101" to .139"	Sample shiny & no evidence at all of any oxidation	Colorless	Brown yellow	4.4	40
"	"	167	"	" "	" "	"	"	7.7*	70*
VII Conc.HCl with oxygen bubbling at 1 bubble /sec.	"	88	10-1 TCN (5-136) (9-162)	Wt. =12.4817 gm. Thickness = .25"	Sample covered with a yellowish green layer (of copper oxy chloride or cupric chloride) & covered with black layer at the edges	"	yellowish green	11.14	101.3
NH_4OH	"	5	"	" "	The yellowish green layer dissolved but the sample is not shiny. Some chips came off.	"	Faint blue	16.90*	154*
VII Conc.HCl with dissolved oxygen (No bubbling when sample is in HCl)	"	122	10-1 TCN (5-136) (9-187) "G"	Wt. =14.0365 gm. Thickness ≈.17"	Sample edge chipped off.	"	Brown yellow	6.3	57.3
"	"	433	"	" "	Sample chipped off & dull on one side	"	"	13.83*	126*

*Accumulative data

FIGURE 5-1 LEACHING EFFICIENCY vs TIME FOR ACID and ALKALINE SOLUTIONS IN LEACHING THE Cu-Ni PHASE FROM W-Cu-Ni SINTERED COMPACTS.

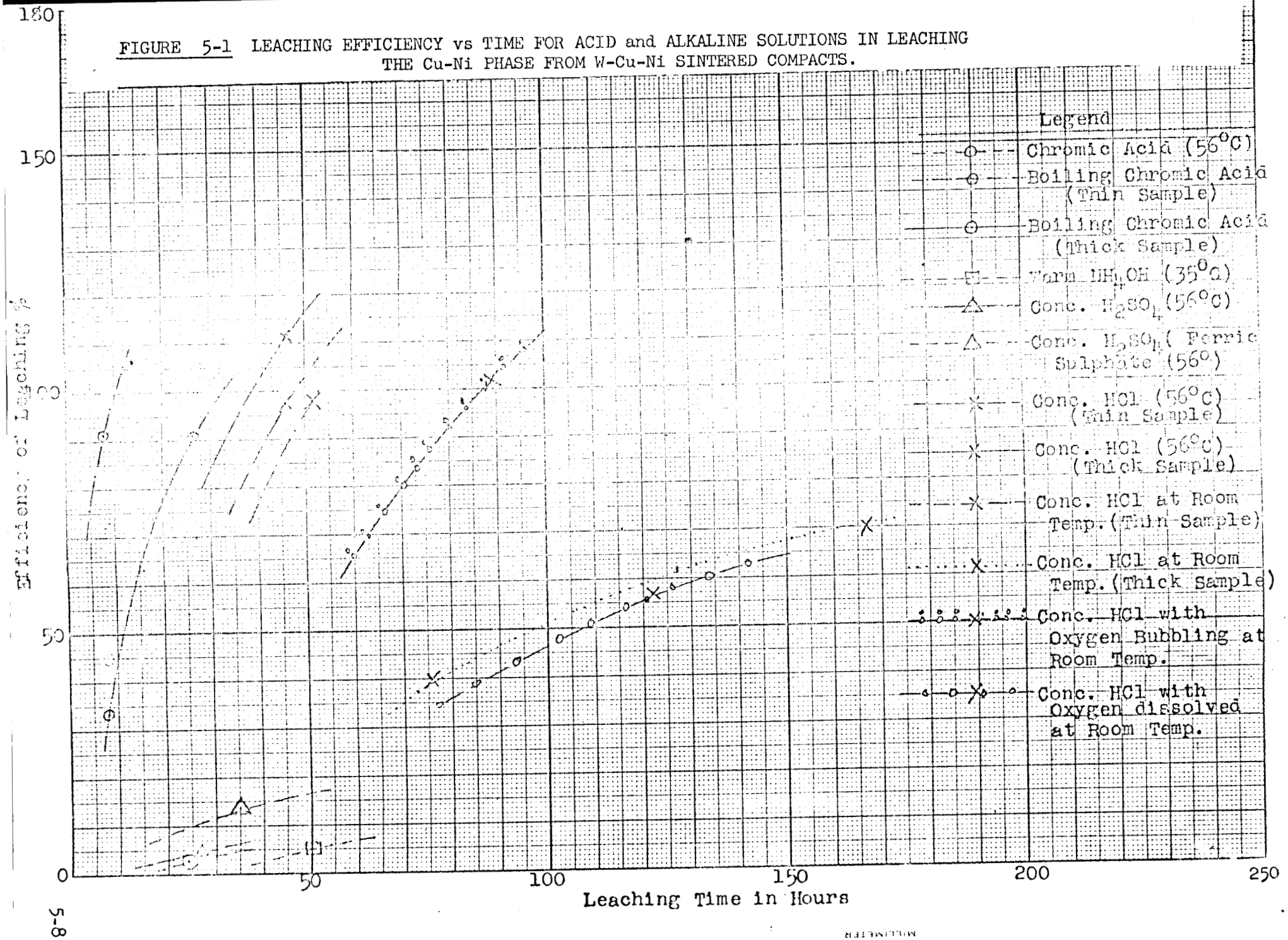

TABLE 5-2 RESULTS OF ELECTROLYTIC LEACHING AT ROOM TEMPERATURE OF W-10Cu-1Ni SAMPLES
Sintered at 2150°F - 5 hrs.

Electrolytic Leaching Media	Time	Voltage	Sample Code	Sample Features Before Leaching	% Wt. Loss	Efficiency %	Remarks
I(a) Conc.HCl	12 hrs.	5-6 volts	(5-124) (9-159) No. 2	Wt. = 16.3225 gm. Thickness = .154"	10	90.9	Sample covered with yellow spots (probably of copper oxy chloride) at few places. Some chips & tungsten particles could be seen in the acid.
I(b) Conc.HCl	24 hrs.	3	"	Wt. = 8.4970 Thickness t_1 = .146" t_2 = .176 to .223"	24.24	220	Sample chipped off at one edge & covered with a yellow layer (probably of copper oxy chloride). During electrolytic leaching, the tungsten particles were seen falling from the sample & also flakes came off.
NH_4OH	5 minutes	-	"	" "	26.51*	241*	The yellow layer dissolved in NH_4OH but the sample is not shiny & bright.
II 29.7% NH_4Cl in cold water	19½ hrs.	4-5	"	Wt. = 8.8220 Thickness = .145"	14.10	128	Sample is not shnny & bright Some flakes could be seen in the solution. The color of NH_4Cl solution after leaching was blue at top & green at the bottom.

*Accumulative data

specimens in this latter group which with this step shall be identified as fifth generation specimens. The leaching end point was determined when a daily acid change subsequently results in no solution color change. This saves specimen drying, weighing etc. Quantitative chemical analyses of two leached 0.150" thick W-10Cu-1Ni control specimens indicated that 99.9% of the Cu-Ni phase had been removed in about 10 days.

The W-8Cu-1Ni was more resistant to HCl leaching than the W-10Cu-1Ni; further, leaching resistance increased on specimens sintered to the higher temperatures as well as longer periods.

As mentioned in Section 4.3.6.2, thick specimens tended to incur edge spalling during HCl acid leaching. The W-8Cu-1Ni spalled the least of the two compositions, and then only after being sintered at the lower temperature and time levels (2150°F - 5 hours). The W-10Cu-1Ni spalled less after having been sintered to the higher temperature and time level.

5.2.2.1 Leaching Stresses

The open pore volume of nitric acid leached specimens was always higher than that believed to be due to the removed volume of the copper and nickel phase. This was believed due to specimen expansion due to internal (pore) oxidation caused by the hot nitric acid.

In order to determine if this premise were valid, a .040" x 1/2" x 2" long W-10Cu-1Ni sintered (2150°F - 5 hours) specimen was cut into two 1/4" strips. Each half was measured, then leached, one in HNO_3 at 130°F and the other in HCl at 70°F, for 24 hours. Subsequent length changes were measured. Hydrochloric acid leached specimens did not change length while those leached in nitric acd grew 1.5% in length. This linear change, when converted to a specimen volume change is equivalent to a total volume increase of 4.5% over the original average volume levels of about 22%. This dimensional change could create a linear shear stress of 750,000 psi between the leached and non-leached zones of a W-Cu-Ni specimen - and is no doubt highly responsible for edge shearing during acid leaching. This, however, would suggest that if HCl leaching causes no expansion, it should not have edge shear failure. This is contrary to what is observed since HCl does cause some edge shearing, though it is less than that caused by HNO_3 leaching. As is discussed in the following section, it is likely

that a tungsten-chlorine compound is formed which can cause biaxial shear stresses at specimen corner, sufficient to cause spalling. This problem was solved simply by making the large emitter plates about 3/8" over size in the flat dimensions to provide for edge loss by spalling. Figure 5-6 shows four such completed plate blanks prior to trimming where some edge cracking is evident.

5.2.2.2 Problems in Hydrochloric Acid Leaching

5th Generation emitter plate and control specimens resulted in a high shrinking and pore closure rate during furnace bleaching. Data analysis suggested that the cause was related to the new acid leaching procedure or a subsequent dependent step. Several factors which were thought to be responsible were: specimen oxygen or chlorine residues; the residual Ni and the further removal of this retained nickel by mercury. A review of the HCl procedures were made with the following discussed observations.

The finalized acid leaching procedures had consistently indicated that 99.9% of the Cu-Ni phase could be removed from the sintered plates with concentrated hydrochloric acid at 70°F, though as much as 14 days leaching was required for thick specimens. The acid leached specimens were dried by heating in a vacuum of about -28 in. within a glass flask. The dried HCl acid leached specimens were invariably of a bright metallic appearance, whereas previous nitric acid leached specimens were a dull grey-green color, indicative of an oxide film. A significant weight loss, up to .75%, always resulted when small HNO_3 leached specimens were hydrogen reduced - a standard procedure. However, small HCl leached specimens usually lost less than half as much (from .1 to .2%) This is shown in Table 5-3 which lists the weight changes of sixteen small specimens following HCl acid leaching and vacuum drying. The weight values generally resulted from measurements made for pore spectrum analysis where infiltrated mercury was subsequently removed by heating to 1800°F for 1/2 hour in dry hydrogen. The weight losses due to this heating in hydrogen ranged from about 1000 to 2000 parts per million. This weight loss could be from the reduction of oxygen by the hydrogen, the dissociation of chemically absorbed or combined chlorine, or the further leaching of surface bonded nickel by mercury exudation. In general, it appears that most of the control specimens which had been impregnated with mercury and then heated in hydrogen for mercury vaporization were readily stabilized at 2750°F when subsequently vacuum bleached. This hydrogen furnace step was only incidental in removing

TABLE 5-3 TUNGSTEN EMITTER STRUCTURES - WEIGHT CHANGES RESULTING FROM VARIOUS FURNACE PROCESSING FOLLOWING LEACHING BY HCl COMPOSITIONS W-Cu-Ni

No.	Heat Treatment After Leaching: H_2 Furnace (Hg)	H_2 Furnace Tot. Time (hrs.)	H_2 Furnace Temp. (°F)	Vacuum Furnace Tot. Time (hrs.)	Vacuum Furnace Temp. (°F)	Vacuum Furnace Press. (Torr)	W-8Cu-1Ni 2150°F (z) 5 hrs. Weight (grams)		W-8Cu-1Ni 2250°F (z) 5 hrs. Weight (grams)	W-10Cu-1Ni 2150°F (z) 5 hrs. Weight (grams)	W-10Cu-1Ni 2250°F (z) 5 hrs. Weight (grams)
1	-	-	-	-	-	-	(a) 2.8450	(b) 3.3771	-	(c) 4.0213	(d) 4.4834
2	*	1/2	1800	-	-	-	2.8414	-	-	4.0183	4.4763
3	*	1/2	1800	-	-	-	2.8420	-	-	-	-
4	-	-	-	1	3000	10^{-3}	-	-	-	4.0180	4.4753
5	*	1/2	1800	4	3000	10^{-3}	2.8403	-	-	4.0193	4.4757
6	-	-	-	4	3000	10^{-3}	-	3.3694	-	-	-
7	-	-	-	-	-	-	(e) 2.6705	-	(f) 5.8213	(g) 4.8246	(h) 6.4386
8	-	-	-	4	2750	10^{-3}	-	-	-	4.8168	6.4246
9	*	1/2	1800	4	2750	10^{-3}	2.6649	-	5.8183	4.8163	6.4248
10	*	1/2	1800	10	2750	10^{-3}	2.6632	-	5.8189	4.8158	6.4252
11	-	-	-	-	-	-	(i) 3.2178	(j) 2.6450	(k) 4.2351	-	-
12	*	1/2	1800	-	-	-	-	2.6420	-	-	-
13	-	-	-	4	2600	10^{-3}	3.2122	-	-	-	-
14	*	1/2	1800	4	2600	10^{-3}	-	-	4.2321	-	-
15	*	1/2	1800	10	2600	10^{-3}	3.2125	-	4.2315	-	-
16	-	-	-	4	3000	10^{-5}	(l) 5.1599	-	(m) 3.7818	(n) 3.1517	(o) 2.8429
17	*	1/2	1800	-	-	-	5.1579	-	3.7806	3.1501	2.8387
18	*	1/2	1800	-	-	-	5.1569	-	-	3.1500	-
19	-	-	-	4	2750	10^{-5}	-	-	(p) 4.1294	-	(q) 4.2452
20	*	1	1800	-	-	-	-	-	4.1284	-	4.2441

(z) Original sintering temperature prior to leaching.
Alphabetical index identified 16 separate specimens & their original wt. begore further furnace processing

mercury from the pore spectrum analysis. It was not known at that time that pore structure instability would occur if this step were not followed.

Several factors had previously suggested that hydrogen reduction of HCl leached specimens could or should be eliminated from the process: (1) the HCl specimens visually appeared to be non-oxidized, (2) WO_3 has a high vapor pressure and was expected to be readily removed by vacuum bleaching, (3) this was preferred since it was also believed that this would eliminate the possibility of a large content of polycrystalline tungsten coating on the surface of the tungsten grains in the porous network if the WO_3 had been hydrogen reduced prior to bleaching, and (4) such polycrystalline W grains were expected to contribute to rapid aging, as had earlier been determined to have occurred in nitric acid leached, vacuum bleached specimens when subsequently aged in hydrogen at 2500°F.

As a result of these considered factors, the first group of the large emitter plates and their related control and S.T.L. specimens were not hydrogen reduced prior to vacuum bleaching in an Abar furnace at pressures of 10^{-5} Torr. This resulted in extensive densification rates as is shown by data in Tables 5-4 through 5-7.

The possibility that chloride formation could have contributed to the rapid densification rates of the HCl leached tungsten specimens was reinforced by several factors - (1) a chlorine analysis was made on one W-8Cu-1Ni sintered specimen after HCl acid leaching where .027% chlorine was determined in the /99% pure porous tungsten specimen, (2) McIntyre[27] had reported that HCl gas added to a hydrogen atmosphere to as low as 1% levels lowered the activation energy of tungsten to 52,000 cal/mol from a level of 72,000 cal/mol in pure hydrogen, (3) McIntyre reported that the maximum effect of HCl gas on tungsten densification rates occurred at 2750°F which corresponds closely to the temperature where tungsten and chlorine are in equilibrium as various tungsten chlorides, and (4) pore closure rate in these HCl leached tungsten emitters was higher at 2750° than at 3000°F.

This is observable on Table 5-5 lines 1, 2 and 6 and on Table 5-7 lines 1, 4 and 9 for W-8Cu-1Ni and W-10Cu-1Ni respectively. The interrelationships were examined of various process steps, compositions and vacuum furnace pressures by analyzing data given in Tables 5-4 through 5-7. These interrelationships

were compounded by the fact that the exact nickel contents prior to bleaching were expected to be low as a result of weight loss measurements. Chemical analyses indicated that as much as .074% residual nickel remained in such HCl leached specimens. This nickel level could in combination with the chlorine content activate tungsten sintering to more rapid densification levels.

5.2.2.3 Double Leaching and Hydrogen Reduction (6th Generation)

The analyses of the data in Tables 5-4 through 5-7 led to the conclusion that an intermediate process treatment could be effective in eliminating thermal instability of the porous tungsten emitters made by this basic process including HCl leaching. Though hydrogen treatment at 1800°F for 1/2 hour was often effective, the best intermediate step was that of releaching in HNO_3 at 130°F for 48 hours This step was expected to serve a double purpose, (ie) convert chlorides to oxychlorides and further reduce the residual nickel level This step was adopted and was followed by warm vacuum drying with intermediate distilled water rinsing. In order to further reduce possible oxychlorides or carbon which was believed responsible for some specimen darkening, wet hydrogen reduction at 1800°F for 45 minutes plus 1/2 hour in dry hydrogen was used prior to vacuum bleaching.

These steps were the distinctive ones which established the 6th generation process used for the emitter plates and S.T.L. test discs supplied to NASA for evaluation. This is shown on the flow sheet given in Figure 5-2.

5.2.3 Vacuum Bleaching Studies

As reviewed in Section 5.0, bleaching studies were conducted to determine the possibility of bleaching at temperatures lower than 3400°F. Bleaching studies were made on 5th generation control samples in Astro Met's vacuum furnace described in Section 3.8, and analysis was made by porosimeter before and after bleaching on the same sample. Three bleaching temperatures were used, viz. 3000, 2750 and 2600°F, for periods of 1, 4 and 10 hours. The temperature was reached in about 20 minutes. The resulting porosity data on samples W-8Cu-1Ni and W-10Cu-1Ni sintered at 2150 and 2250°F for 5 hours are given in Tables 4-5 through 4-7, as mentioned previously.

The results of the vacuum bleaching at 3000, 2750 and 2000°F for 1, 4 and 10 hours indicated that good stability resulted from 2750°F and 3000°F vacuum bleaching for 4 hours. The lower temperature resulted in higher open porosity.

Therefore, as previously described, slab specimens were sent to Abar for vacuum bleaching at these two conditions. After bleaching, these specimens had only about 15% porosity and, as discussed in Section 5.2.2.2, this rapid pore closure was believed to be due to residual chloride and nickel formation following HCl leaching, and was eliminated by the added nitric acid treatment (6th Gen.).

From above studies, it was decided to conduct bleaching on 6th generation specimens only at 2750°F for 4 hours as this was expected to result in higher porosity and less volume shrinkage than bleaching at 3000°F for 4 hours. Porosity data for samples W-8Cu-1Ni and W-10Cu-1Ni, both sintered at 2150°F for 5 hours and at 2250°F for 25 hours, are given in Table 5-8. There was no significant drop in open porosity after bleaching at 2750°F for 4 hours at 10^{-4} Torr at Astro Met, and hence the 6th generation specimens were sent to Abar for vacuum (at 10^{-5} Torr) bleaching at 2750°F for 4 hours. The resulting porosity data is also included in Table 5-8. Practically no pore volume change occurred, with the result that several emitter test plates were produced with over 20% open porosity, a narrow pore spectrum range and mean pore diameters between 1.1 and 1.7 microns. The final 6th generation process is shown as a flow sheet as Figure 5-2.

TABLE 5-4 TUNGSTEN EMITTER STRUCTURES - POROSITY CHARACTERISTICS RESULTING FROM VARIOUS FURNACE PROCESSING FOLLOWING LEACHING BY HCl
COMPOSITION W-8Cu-1Ni: CODE 5-140, 5-167, 9-205 5th Generation

Data	Spec. No.	Slab	Heat Treatment After Leaching: H_2 Furnace Time (hrs.)	H_2 Furnace Temp. (°F)	H_2 Furnace Hg	Vacuum Furnace Time (hrs.)	Vacuum Furnace Temp. (°F)	Vacuum Furnace Press. (Torr)	Originally Sintered 2150°F - 5 hrs. Grain Size 6 μ: Volume (cc) Spec.	Volume (cc) Open Pore	Porosity % Open	Porosity % Closed	Porosity % Tot.	Mean Pore Diam.
1	1a	I_1	-	-		-	-	-	.189	.039	20.2	1.5	21.7	1.1
2	1a	"	1/2	1800	"	4	3000	10^{-3}	.176	.028	15.4	0.9	16.3	1.0
3	1b	"	-	-		4	3000	10^{-3}	.209	.032	15.0	1.6	16.6	0.95
4	2	F	-	-		4	3000	10^{-5}	.324	.055	16.9	0.6	17.5	1.0
5	2	E	1/2	1800	"	-	-	-	.324	.056	17.3	0.3	17.6	1.1
6	3a	I_1	-	-		-	-	-	.177	.038	21.6	0.4	22.0	1.1
7	3a	"	1/2	1800	"	4	2750	10^{-3}	.175	.036	20.4	0.7	21.1	1.1
8	3a	"	1/2	1800	"	10	2750	10^{-3}	.173	.035	20.4	0.0	20.4	1.1
9	3b	E	-	-		-	-	-	-	-	21.6	0.4	22.0	-
10	3b	"	-	-		4	2600	10^{-3}	.205	.038	18.4	0.4	18.7	0.95
11	3b	"	1/2	1800	"	10	2600	10^{-3}	.205	.038	18.4	0.4	18.7	1.0

Slab = Specimen Zone in Original Slug - 1/8" Layers in Alphabetical order from top.

Vacuum - 10^{-3} Astro Met Furnace, 10^{-5} Abar Furnace

TABLE 5-5 TUNGSTEN EMITTER STRUCTURES - POROSITY CHARACTERISTICS RESULTING FROM VARIOUS FURNACE PROCESSING FOLLOWING LEACHING BY HCl
COMPOSITION W-8Cu-1Ni: CODE 5-140, 5-167, 9-203, 9-208 5th Generation

Data	Spec. No.	Slab	Heat Treatment After Leaching: H_2 Furnace Time (hrs.)	H_2 Furnace Temp. (°F)	H_2 Furnace Hg	Vacuum Furnace Time (hrs.)	Vacuum Furnace Temp. (°F)	Vacuum Furnace Press. (Torr)	Originally Sintered 2250°F - 5 hrs. Grain Size 8 μ: Volume (cc) Spec.	Volume (cc) Open Pore	Porosity % Open	Porosity % Closed	Porosity % Tot.	Mean Pore Diam.
1	1	I_2	-	-		-	-	-	-	-	20.8	1.0	21.8	1.1
2	2	I_2	-	-		4	3000	10^{-5}	.236	.038	16.2	0.7	16.9	1.0
3	3	I_2	-	-		-	-	-	.385	.080	20.8	1.0	21.8	1.1
4	3	I_2	1/2	1800	*	4	2750	10^{-3}	.381	.078	20.6	0.4	21.0	1.15
5	3	I_2	1/2	1800	*	10	2750	10^{-3}	.380	.076	19.9	0.8	20.7	1.2
6	4	I_2	-	-		4	2750	10^{-5}	.251	.036	14.9	0.5	15.4	0.9
7	5	I_2	-	-		-	-	-	.279	.056	19.7	1.6	21.3	1.05
8	5	I_2	1/2	1800	*	4	2600	10^{-3}	.267	.047	17.5	0.4	17.9	1.1
9	5	I_2	1/2	1800	*	10	2600	10^{-3}	.267	.047	17.5	0.4	17.9	1.1

Slab = Specimen Zone in Original Slug - 1/8" Layers in Alphabetical order from top.

Vacuum - 10^{-3} Astro Met Furnace, 10^{-5} Abar Furnace

TABLE 5-6 TUNGSTEN EMITTER STRUCTURES - VACUUM BLEACHING vs POROSITY
FOLLOWING HCl LEACHING OF W-Cu-Ni TERNARY ALLOYS
WITH AND WITHOUT HYDROGEN REDUCTION
COMPOSITION W-10Cu-1Ni - CODE 5-136, 5-165 5th Generation

Data No.	Spec. No.	Heat Treatment After Leaching: H_2 Furnace Time (hrs.)	H_2 Furnace Temp. (°F)	H_2 Furnace Hg	Vacuum Furnace Time (hrs.)	Vacuum Furnace Temp. (°F)	Vacuum Furnace Press. (Torr)	Originally Sintered 2150°F - 5 hrs. Code 9-187 Slab G Grain Size 4 μ: Volume (cc) Spec.	Volume (cc) Open Pore	Porosity % Open	Porosity % Closed	Porosity % Tot.	Mean Pore Diam.
1	1	-	-		-	-	-	.278	.066	23.3	1.7	25.0	0.8
2	1	1/2	1800	*	1	3000	10^{-3}	.270	.060	22.3	0.5	22.8	0.9
3	1	1/2	1800	*	4	3000	10^{-3}	.266	.056	20.8	1.0	21.8	0.95
4	1	1/2	1800	*	10	3000	10^{-3}	.255	.046	17.7	0.5	18.2	0.95
5	2	-	-		4	3000	10^{-5}	-	-	17.2	1.0	18.2	1.05
6	3	-	-		-	-	-	-	-	23.3	1.7	25.0	0.8
7	3	-	-		4	2750	10^{-3}	.330	.078	22.9	1.5	24.4	0.98
8	3	1/2	1800	*	10	2750	10^{-3}	.326	.076	23.3	0.0	23.3	0.98
9	4	-	-		4	2750	10^{-5}	-	-	-	-	-	-

Slab - Specimen Zone in Original Slug - 1/8" Layers in Alphabetical Order from Top.

Vacuum - 10^{-3} Astro Met Furnace, 10^{-5} Abar Furnace

TABLE 5-7 TUNGSTEN EMITTER STRUCTURES - VACUUM BLEACHING vs POROSITY
FOLLOWING HCl LEACHING OF W-Cu-Ni TERNARY ALLOYS
WITH AND WITHOUT HYDROGEN REDUCTION
COMPOSITION W-10Cu-1Ni - CODE 5-136, 5-165 5th Generation

Data No.	Spec. No.	Heat Treatment After Leaching: H_2 Furnace Time (hrs.)	H_2 Furnace Temp. (°F)	H_2 Furnace Hg	Vacuum Furnace Time (hrs.)	Vacuum Furnace Temp. (°F)	Vacuum Furnace Press. (Torr)	Originally Sintered 2250°F - 5 hrs. Code 9-185, 9-195 Slab D Grain Size 5: Volume (cc) Spec.	Volume (cc) Open Pore	Porosity % Open	Porosity % Closed	Porosity % Tot.	Mean Pore Diam.
1	5	-	-		-	-	-	.306	.071	22.9	1.2	24.1	1.0
2	5	1/2	1800	*	1	3000	10^{-3}	.294	.060	20.3	0.9	21.2	1.0
3	5	1/2	1800	*	4	3000	10^{-3}	.292	.058	19.7	1.0	20.7	1.0
4	5	1/2	1800	*	10	3000	10^{-3}	.286	.052	18.2	0.5	18.7	0.9
5	6	-	-		4	3000	10^{-5}	-	-	16.8	1.1	17.9	1.1
6	7	-	-		-	-	-	-	-	22.9	1.2	24.1	1.0
7	7	-	-		4	2750	10^{-3}	.402	.068	16.8	0.3	17.1	1.0
8	7	1/2	1800	*	10	2750	10^{-3}	.404	.068	16.6	1.0	17.6	0.9
9	8	-	-		4	2750	10^{-5}	-	-	15.2	0.5	15.7	0.9

Slab = Specimen Zone in Original Slug - 1/8" Layers in Alphabetical Order from Top.

Vacuum - 10^{-3} Astro Met Furnace, 10^{-5} Abar Furnace

TABLE 5-8 PORE CHANGES DUE TO LEACHING and BLEACHING PROCEDURES
6th GENERATION SPECIMENS

Post Sintering Process	10-1 "B" 5-187A 2150°F - 5 hrs.			8-1 "G" 5-185A 2150°F - 5 hrs.			10-1 "A" 5-188A 2250°F - 25 hrs.			8-1 "D" 5-186A 2250°F - 25 hrs.		
	Porosity		Av.Pore Dia.	Porosity		Av.Pore Dia.	Porosity		Av.Pore Dia.	Porosity		Av.Pore Dia.
	Open	Closed		Open	Closed		Open	Closed		Open	Closed	
HCl leached	23.3	1.7	1.0	20.2	1.5	1.0	21.5	2.0	1.5	18.3	0.9	1.5
HNO_3 leached & H_2 reduced	24.2	1.0	-*	21.3	0.4	- *	22.5	0.4	1.6	18.0	1.4	- *
Vac. bleached 2750°F - 4 hrs. (10^{-3} Torr)	23.7	0.5	-*	21.2	0.6	- *	22.1	0.7	1.7	18.8	0.6	- *
Vac. bleached 2750°F - 4 hrs. (10^{-5} Torr)	24.1	0.5	1.1	21.1	0.8	1.3	22.2	0.7	1.7	18.4	0.8	1.6
No. of pores per cm^2 as in #4 above as calculated from porosimeter anal.	4.02×10^7			1.61×10^7			9.80×10^6			9.16×10^6		
As measured on photo micrographs (approximate)	5×10^6			3×10^6			2×10^6			1.5×10^6		

* Not Determined

FIG. 5-2 PROCESS FLOW SHEET FOR PREPARING POROUS TUNGSTEN IONIZER SPECIMENS FOR NASA (6th Generation)

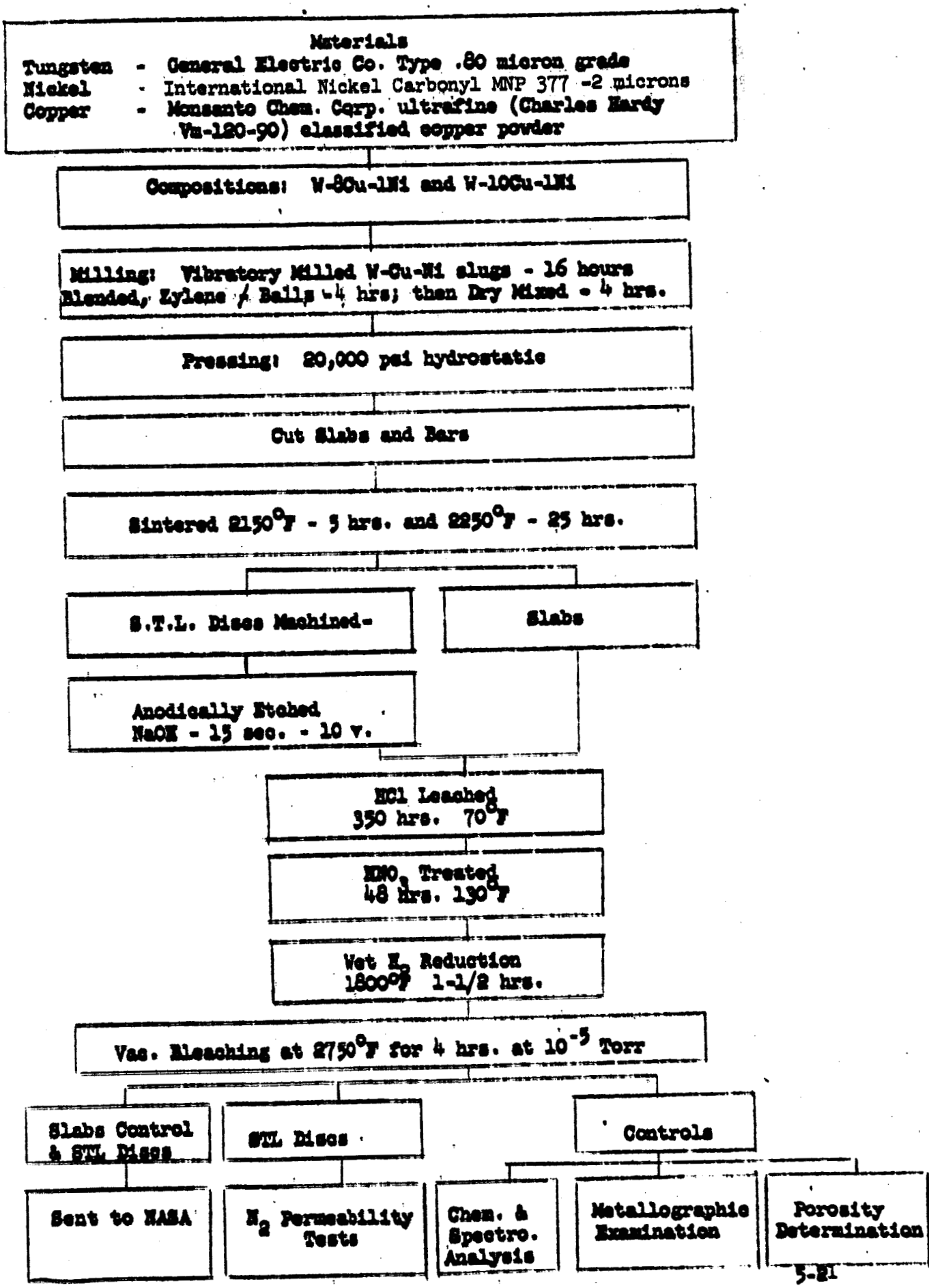

5.3 Evaluation

5.3.1 Chemical Analysis

Chemical analysis was done on 5th generation specimens for copper, nickel and chloride on, as hydrochloric acid leached samples and is described below:

Sample Cu-Ni ——→ Temp.-Time of sintering →	10-1"G" 2150°F - 5 hrs.	10-1"D" 2250°F - 5 hrs.	8-1"I" 2150°F - 5 hrs.
Copper	less than .01%	less than .01%	*
Nickel	less than .01%	less than 02%	.074%
Chloride	*	*	.027%

NOTE: * Not Analyzed

5.3.2 Metallographic Analysis

Figure 5-3 reproduces photomicrographs of the 6th generation emitter structures of the W-8Cu-1Ni and W-10Cu-1Ni, both sintered at 2150° for 5 hours and 2250°F for 25 hours. The basic objective was to produce a grain size range which would produce a pore size range between 1 and 2 microns. The photomicrographs are shown at magnifications of 400 and 1400X. The lower magnification shows the general uniformity of grain distribution. The higher magnification shows the shapes of the tungsten grains and the concomitant hole shapes now filled with infiltrated copper for polishing.

The W-8Cu-1Ni appears to be the most uniform, especially as resulting from sintering at 2250°F - 25 hours which gave a 1.6 micron mean pore diameter.

The W-10Cu-1Ni, 2150°F - 5 hours, appears to have the least micro uniformity of the series, where an estimated 1% of the surface area would have a particle void with an average width of 5 to 8 microns. These voids are believed to not be continuous as evidenced by the relative low porosimeter measurements as is discussed in the following section. This type of grain segregation is dependent upon the milling procedures and can be readily reduced by improved milling procedures. Metallographic scanning of the control specimens showed exceptional grain size and grain distribution uniformity. It is expected that the supplied large emitter 6th generation plates would be similarly uniform from one area to another. This should assure uniform cesium permeability. A further discussion of pore uniformity as determined by mercury porosimeter analyses is discusssed in the following section.

5.3.3 Porosity Measurements

The 6th generation W-8Cu-1Ni and W-10Cu-1Ni control specimens and emitter slabs for NASA were cut from the same processed slugs and within 1/2 inch of each other. In some cases, the controls were cut from the end of the slabs. Therefore, microstructural, pore spectrum, and permeability analyses should be indicative of the characteristics which would be exhibited by the emitter slabs. The pore spectrum analyses of furnace bleached specimens were conducted as discussed in Section 3.11. These 6th generation pore spectrum analyses are plotted in Figures 5-4 and 5-5. Specific open, closed and total pore volume, mean pore size and equivalent pore count data based on pore volume are listed in Table 5-8. Additional analytical data are given in Table 5-9 where ratios of open pores within narrow pore size ranges are indicated.

Mag. 175X
Mag. 700X

FIGURE 5-3 PHOTOMICROGRAPHS OF SINTERED, LEACHED, BLEACHED and COPPER REINFILTRATED 6th GENERATION TUNGSTEN EMITTER STRUCTURES

As can be seen from these pore spectrum curves and Table 5-9, all specimens exhibited high open pore volumes from 18.8 to 23.8%. All specimens had as much as 90% and up to 97% of their open pore volume in the range from 1.7 to .52 microns.

Analyses of Table 5-10 indicates the favorable stability characteristics of the entire 6th generation metallurgical group even during the original bleaching cycle where highest shrinkage rates normally occur. Pore spectrum data had been determined on the original (as HCl leached) specimens which established base line data from which bleaching effects were determined. The HNO_3 acid leach treatment (130°F - 48 hours) initially caused some specimen swelling due to chemical oxidation. A significant portion of this chemically caused volume increase remained through the subsequent hydrogen reduction and the first vacuum bleaching cycle at 2750°F for 4 hours. The thermal stability of the entire 6th generation group is shown by the fact that the open pore volume reduction due to furnace bleaching for 4 hours and an additional 6 hours was practically nil. This excellent stability contrasts with the poor stability exhibited by the 5th generation specimens which lost as much as 30% of their open porosity under the same vacuum furnace conditions. This was shown on Tables 5-4 to 5-7. Another factor is that these 6th generation specimens have unusually high open porosity volumes - and are yet so stable. Since highest pore closure rates generally occur within the first ten hours, these furnace process and stability periods were believed sufficient to demonstrate that stable ion emitter structures had been produced. Limited time prevented aging studies of the 6th generation emitters for longer periods and at higher temperature, such as had been done previously and had been planned for this work.

An additional pertinent observation of stability was made by comparing the shape of the pore spectrum curves, of the four specimen sets, which were generated from tests before and after the 6 hours vacuum thermal aging cycle following the vacuum bleaching step. This comparison showed that the open pore volume range between 1.7 and .75 microns was practically identical. The expected low contribution of fine pores below .75 microns in such small volumes, to liquid cesium flow and their closure should offer no significant permeability change due to aging.

FIGURE 5-4 PORE SPECTRUM ANALYSIS OF TUNGSTEN ION EMITTER PLATES
by MERCURY INTRUSION

6th Generation

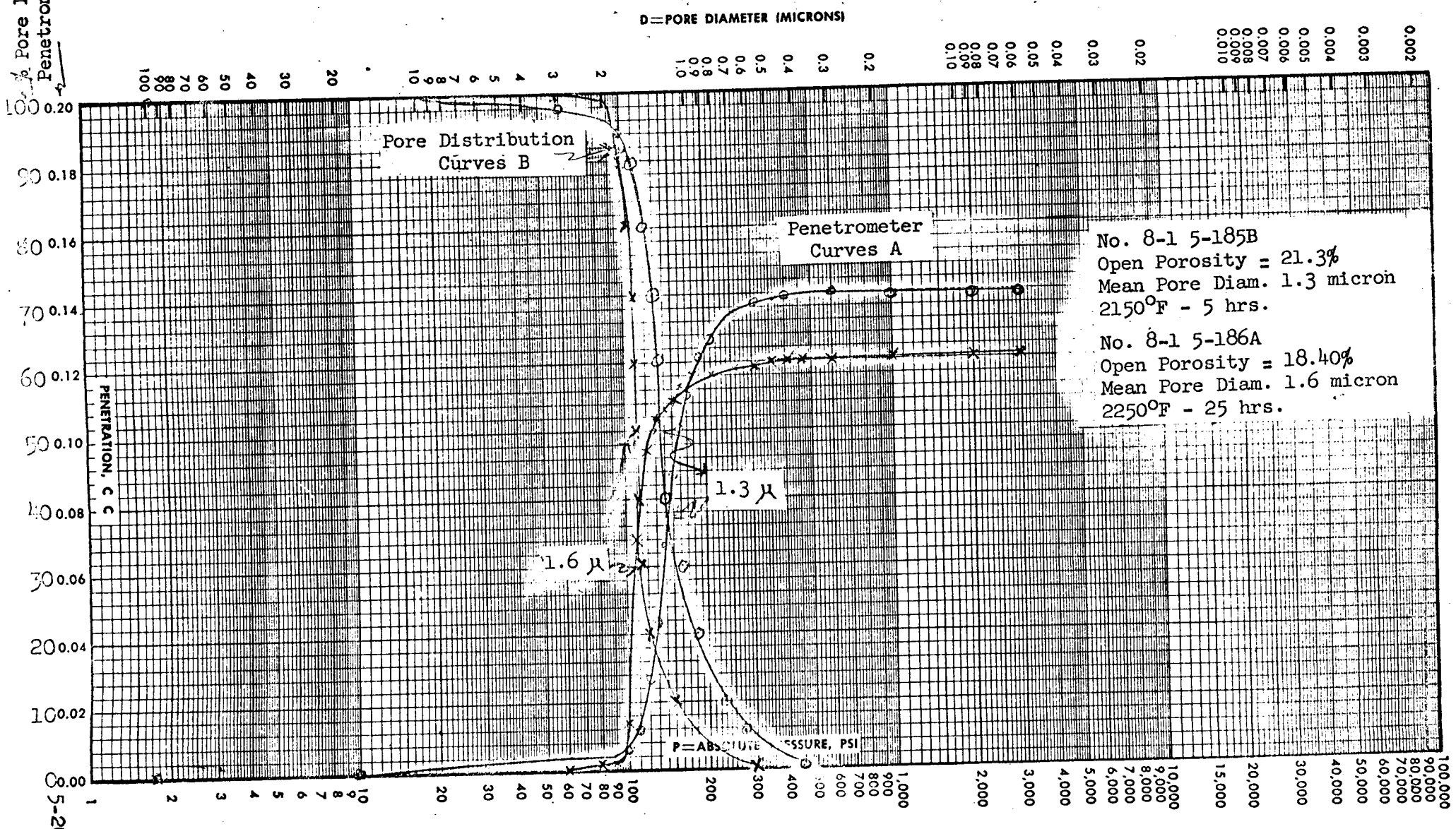

FIGURE 5-5 PORE SPECTRUM ANALYSIS OF TUNGSTEN ION EMITTER PLATES BY MERCURY INTRUSION 6th Generation

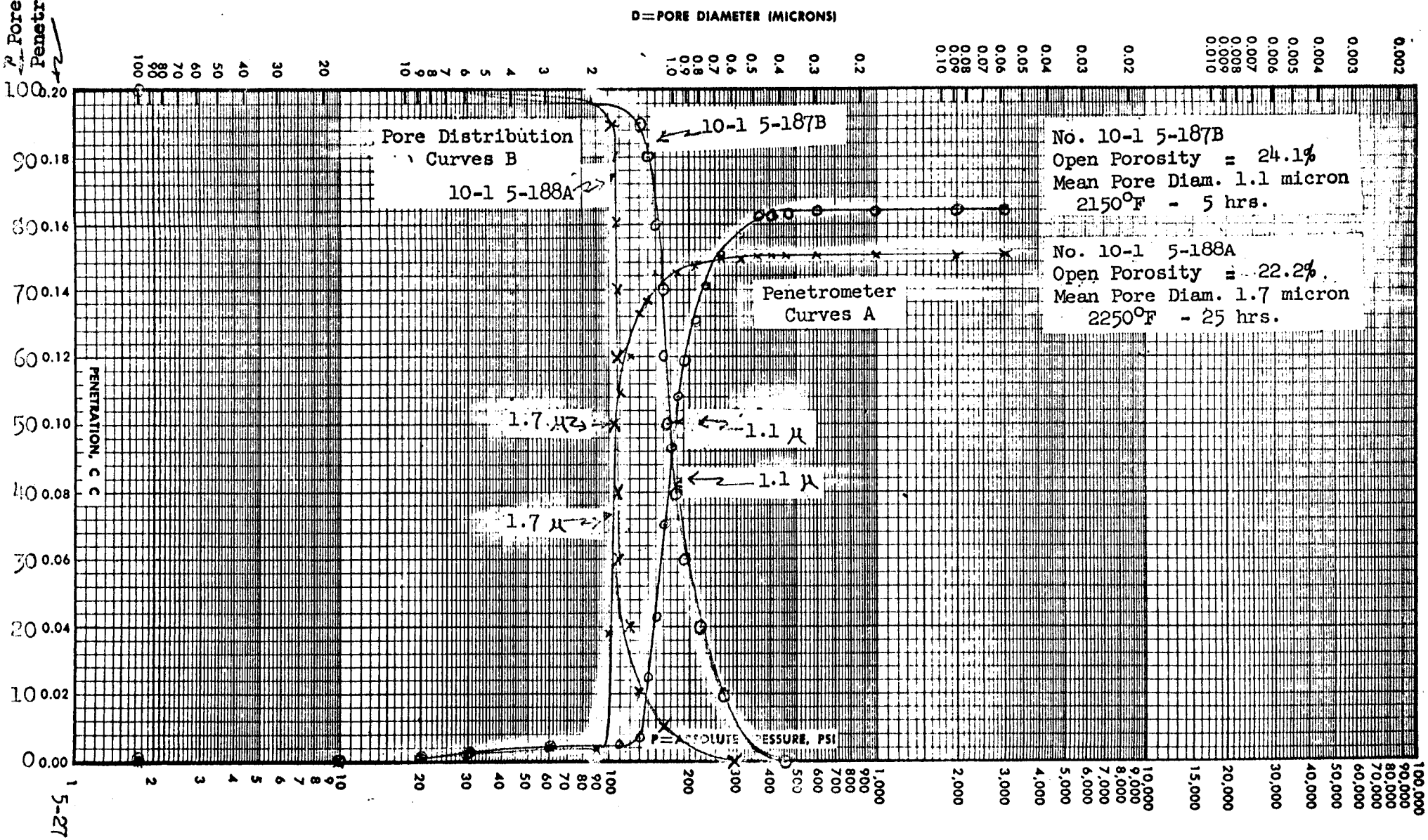

TABLE 5-9 RATIO OF OPEN PORE VOLUME IN SPECIFIC PORE DIAMETER RANGES FOR 6th GENERATION TUNGSTEN EMITTERS

Composition → / Process Temp.-Time →	W-8Cu 1Ni				W-10Cu-1Ni			
	2150°F 5 hrs.		2250°F -25 hrs.		2150°F - 5 hrs.		2250°F - 25 hrs.	
Pore Size Range (microns)	% of Volume Spec.	Pore	Spec.	Pore	Spec.	Pore	Spec.	Pore
Up - 3.2	.2	1.0		.1	.2	1.0	.2	1.0
3.2 2.5	-	0.1	.2	1.0	-	0.1	-	0.1
2.5 1.7	.6	3.0	1.7	9.0	.2	1.0	.4	2.0
1.7 1.2	9.6	45.	14.4	79.0	2.7	11.0	20.	90.
1.2 .75	8.5 - 19.8	40. - 93	1.8 - 16.4	10.0 - 90.0	16.9 - 22.7	70. - 94.	1.3 - 21.5	6. - 97
.75 .52	1.7	8.	.2	1.0	3.1	13.	.2	1.
.52 .31	.4	2.		nil	1.0	4.0		
.31 .1		-		nil	-	nil		
Summary	21.0	99.1	18.3	100.0	24.1	100.	22.1	99.0
Measured Open Pore Vol.of Spec.(%)	21.1	-	18.4	-	24.1	-	22.2	-
Mean Pore Diameter (microns)	1.3		1.6		1.1		1.7	
Transmission Coefficient x 10^{-5}	11.2		21.6		13.8		16.8	

TABLE 5-10 TUNGSTEN ION EMITTER STRUCTURES
PORE STRUCTURE ANALYSES
COMPARISON OF PORE STABILITY @ 2750°F to 10 hours - 6th Generation

No.	Cu-Ni	Sintering Temp. (°F) and Time (hrs.)	Post Sintering[a] Process Conditions Temp. (°F)	Time (hrs.)	Vac. (Torr)	Mean Pore Diameter (microns)	Spec. Vol. (cc)	Porosity (%) Open	Closed	Total	Number of pores/cm² x 10⁷	Shrinkage (c)	(d)
1	8-1"G" 5-185A	2150- 5 hrs.	As HCl leached[b]			~1.0	-	20.2	1.5	21.7	1.61		
			2750	4	10^{-5}	1.3	.2232	21.3	0.5	21.8		.09	0.73
			2750	6	10^{-4}	1.3	.2284	20.57	0.77	21.34			
2	10-1"B" 5-187A	2150- 5 hrs.	As HCl leached			~1.0	-	23.3	1.7	25.0	4.02		
			2750	4	10^{-5}	1.1	.280	24.1	0.5	24.61		.24	.51
			2750	6	10^{-4}	1.1	.278	23.78	0.46	24.24			
3	8-1"D" 5-186A	2250-25 hrs.	As HCL leached			~1.5	-	18.30	0.93	19.23	.92		
			2750	4	10^{-5}	1.6	.1880	18.40	0.77	19.17		.11	.26
			2750	6	10^{-4}	1.6	.1874	18.81	0.21	19.02			
4	10-1"A" 5-188A	2250-25 hrs.	As HCl leached			~1.5	-	21.50	1.97	23.47	.98		
			2750	4	10^{-5}	1.7	.176	22.20	0.72	22.92		0	0
			2750	6	10^{-4}	1.7	.176	22.20	0.72	22.92			
5	8-1 5-188D	2250 5 hrs.	2750	4	10^{-5}	1.2	-	20.18	1.29	21.47	-	-	-

NOTE: (a) Post Sintering After HCl Leach Plus HNO_3 Treatment
(b) After HCl leaching - prior to HNO_3 treatment and vacuum bleaching.
(c) % Linear Shrinkage due to 2750°F - 6 hrs. 10^{-4} Torr
(d) % Linear Change in Total Porosity due to 2750°F - 6 hrs. 10^{-4} Torr

5.3.4 Transmission Coefficient Measurements

The transmission coefficient measurement procedures were discussed in Section 3.1.2. Analytical data for five different 6th generation tungsten emitter specimens are given in Table 5-11. This table also lists comparative mean pore diameter and open pore volume data. The 6th generation specimens exhibit transmission coefficient values ranging from 11.2 to 21.6 x 10^5 or from 1 to 5 times those exhibited by the 2nd and 3rd generation specimens, the data for which is given in Table 4-8. This is particularly important since the sixth generation specimens had a much narrower pore size range with negligible pore volume above 1.7 microns. Small disc test specimens from the same process groups were submitted to NASA with the equivalent emitter plates for ion emission tests at the conclusion of the project.

Several attempts were made to correlate transmission coefficients with various porosity data. No good correlation was determinable with the data from but four tested specimens. It is expected that such correlation should be possible with a statistical quantity of representative specimens.

5.3.5 Emitter Test Specimens for NASA

Four large porous tungsten emitter plates (as shown in Figure 5-6) were completed and delivered to NASA with corresponding control and S.T.L. disc specimens.

Table 5-12 lists the physical characteristic goals and Astro Met's achieved results as is summarized from previous report sections.

The only major limitation to specimen size is that of any vacuum furnace capable of heating the flat slabs to a minimum of 2750°F in a vacuum of 10^{-5} Torr.

No difficulty would exist in preparing such structures with grain sizes of about 3 microns, as has been done in early generation sintering trials. The produced specimens were deliberately prepared in grain size ranges from 5 to 11 microns in order to prepare specimens of various concomitant pore diameters from 1 to 2 microns in at least two discrete levels. The metallurgical thermodynamic equilibrium characteristics allow a close control of grain and dependent pore sizes in specific levels to as close as 0.1 micron values.

TABLE 5-11 TRANSMISSION COEFFICIENT DATA - 6th GENERATION POROUS TUNGSTEN ION EMITTERS

No.	Cu-Ni & Code	Sintering Temp. (°F)	Sintering Time (hrs.)	S.T.L. Specimen Dimensions Diam. "d"	S.T.L. Specimen Dimensions Thickness	t (a)	$t^1 = t\left(\frac{d}{.157}\right)^2$ (sec.)	Transmission Coefficient (b) (10^5)	Mean Pore Diam. (μ)	Open Pore Vol. (%)
1	8-1 5-185D	2150	5 hrs.	.1665"	.0225"	19.5	21.9	11.2	1.3	20.8
2	10-1 5-187F	2150	5 hrs.	.174"	.0185"	14.5	17.8	13.8	1.1	24.1
3	8-1 5-186C	2250	25 hrs.	.159"	.024"	11.1	11.4	21.6	1.6	18.4
4	10-1 5-188B	2250	25 hrs.	.1725"	.0175"	12.1	14.6	16.8	1.7	22.2
5	8-1 5-188C	2250	5 hrs.	.165"	.020"	15.0	16.6	14.4	1.2	20.2
	"	"	"	.165"	.021"	15.9	17.6			

17.1

NOTES:

(a) δt = time in seconds required for ΔP of 50 millimeters Hg pressure

(b) Transmission Coefficient = $C^1 = \frac{245.7 \times 10^{-5}}{\delta t^1}$

Pore density levels were in the magnitudes which were desired. Finer grain and pore size systems which are possible could produce pore count levels of 10^7 to 10^8 with no difficulty. However, no clear indication of thermal stability of such fine structures can be currently projected.

The open pore volumes were generally in excess of the suggested 20% with one exception, which was that of the W-8Cu-1Ni specimen which had been processed to give a greater pore size. It is interesting to note that when sintered at 2250°F for 25 hours, the specimen open pore volumes are about identical to the copper-nickel volumes which had been originally added - then removed.

The transmission coefficient data is much higher than that specified (a desirable improvement) and ranged from 11.2 to 21.6 x 10^{-5} (dimensionless)

The thermal stability greatly exceeds original contract objectives, as based on limited tests at much higher test temperatures and for much less time periods. The validity of this conclusion is based on the fact that greatest densification rates at high temperatures occur in the first few test hours, where following densification rates are one-tenth or less. Further confirmation of this conclusion is warranted and is expected to be determined by future NASA evaluation.

Chemical purity goals had been attained in earlier generation specimens. Time and budget limitations prevented the conduction of such analyses, which are expected to be done by NASA.

Reproducibility of finished emitter structures is expected to be very high though manufacturing studies should be done. The reproducibility of grain size control was shown to be very exact for a period of over one year, using metal powders from various lots. As process improvements were made, a narrower pore size range was achieved, indicating further close reproducibility.

In conclusion, the liquid phase sintering process appears suitable for the preparation of porous tungsten ion emitters having all the identified desirable characteristics.

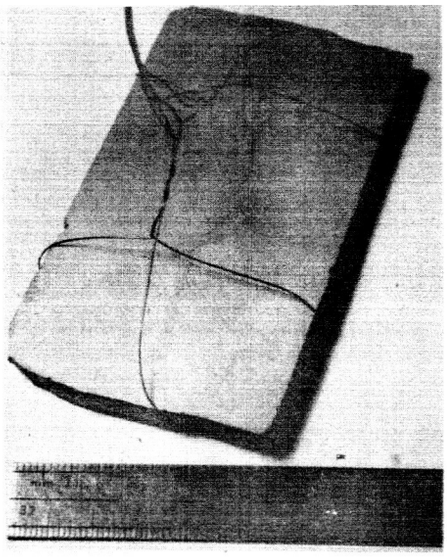

(a)

(b)

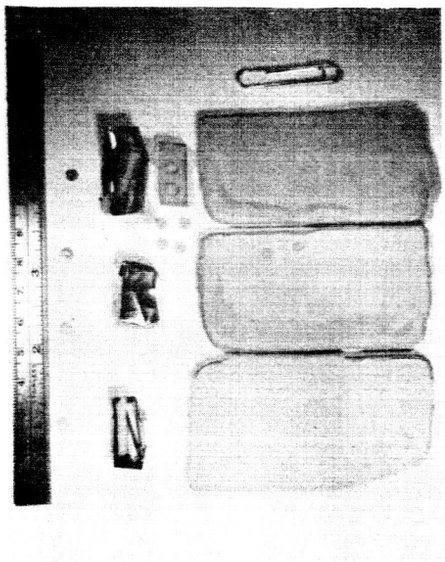

(c)

(d)

FIGURE 5-6 POROUS TUNGSTEN ION EMITTER PLATE BLANKS

(a) & (b) Prior to Leaching

(c) - After Leaching and Bleaching

(d) - Sectioned Emitter Test Mount, Astro Met Disc, S.T.L. mount showing rhodium braze meniscus.

TABLE 5-12 SUMMARY DATA - 6th GENERATION POROUS TUNGSTEN ION EMITTER SPECIMENS FOR NASA EVALUATION

NO.	Goals	General Achievable Range[a]	Achieved and Delivered (6th Generation)			
			W-8Cu-1Hi (2150°F - 5 hrs.)[b]	W-10Cu-1Hi (2150°F - 5 hrs.)	W-8Cu-1Hi (2250°F -25 hrs.)	W-10Cu-1Hi (2250°F - 25 hrs.)
1	Size (inches)		Useful Dimensions			
	0.125 thick	/ 1/2"	/ .14	/ .14	/ .14	/ .14
	1.350 wide	/ 6"	1.5	1.9	1.25	1.5
	2.250 long	/12"	3.0	3.0	2.8	3.0
2	Grain Size (microns) 3-5	3,4,5,6 to 20	7	5	11	10
3	Pore Size (micron) 1.0 to 1.5 (mean)	.7-4	1.3	1.1	1.6	1.7
4	Pore Density #/cm^2 10^7	/10^7	(c) 1.61 (d) .3	4.02 .5	.92 .15	.98 .2
5	Open Pore Vol. (%) 20%	/25%	21.1	24.1	18.4	22.2
6	Transmission Coeffi. 0.2×10^{-5}	/20×10^{-5}	11.2	13.8	21.6	16.8
6	Stability at 1200°C No Density Change / 100 hrs.	above 1500°C	Tested 6 hrs. at 1510°C (2750°F) .25	.49	.19	0
7	Purity Parts per million -50 - Hi etc.	-30	Not Determined			
9	Reproducibility	Very Good	Not Attempted			

NOTES: (a) With available or accessible equipment
(b) Temperature and time conditions used for grain spheroidization
(c) As determined by using mean pore area and total pore volume as measured by porosimeter
(d) " " " metallographic testing

6.0 Supplementary Studies

6.1 Iridium Tungsten Alloy Sintering Effects

In the search for various additives which would increase emitter stability, would exhibit desirable work function characteristics, alloy without difficulty, and exhibit low vapor pressures, iridium appears to offer the best combination of desirable properties. A summary of iridium's pertinent properties are presented in Table 4-10 and Figure 6-1 in comparison with tungsten. The densification rate data was obtained from Brophy[21].

Specifically, Brophy observed that small iridium alloy additions to tungsten inhibit tungsten grain boundary diffusion processes. This results in an activation energy level (133 K cal/mole) near that of the volume diffusion activation energy (135 K cal/mole) for pure tungsten. By analysis of Figure 6-1 it can be determined that at 1200°C the required time for 5% shrinkage of W-4% iridium compacts is about 18 times greater than that of pure tungsten. By extrapolation to 1300°C, the sintering rate factor decreases to about five. It is likely that when iridium is alloyed with tungsten in the stabilized spherical structure, this factor may be increased to a value of 10 or so, due in addition to the lower degree of tungsten polycrystallinity. Brophy indicates that no more than 1.5% of iridium in tungsten is needed for this effectiveness. Another favorable factor for using iridium is that its contact work function is significantly above that of tungsten. Therefore, potential ionization efficiencies should be high. As a result of these analyses, iridium alloy additives are expected to be superior, for both metallurgical stability as well as ionization, to other such additions as ruthenium, platinum, rhodium, palladium, osmium and tantalum.

6.2 Innoculating Tungsten with Iridium

Three methods were studied for adding iridium. One of these consisted of an infiltration approach using copper as a solvent. The second was that of adding the iridium to the initial W-Cu-Ni mix. The third approach was that of innoculating an acid leached porous tungsten specimen with iridium chloride.

Initial innoculation trials were made using a copper infiltrant in an attempt to dissolve the iridium from its position on top of and infiltrate into the porous tungsten specimen. The systems were prepared by weighing

4% iridium and 10% copper to tungsten weight ratios, and infiltrating at 2300°F. The copper was subsequently vacuum bleached. Visual examination disclosed that the iridium had either apparently been partially dissolved by and precipitated from the copper as a dense coating on top of the tungsten specimen during infiltration or that vacuum evaporation temperatures densified the layer of uninfiltrated iridium powder. The iridium distribution indicates that the first suggested process probably occurred.

Permeability tests showed that the specimens were nearly impermeable - suggesting that the coating was very dense. Whichever iridium densification method occurred, the results suggest that this technique would be useful for two emitter preparation procedures. One - iridium could be deposited in selected areas without densifying the tungsten structure and causing serious plate stresses and warpage, such as occurs by electron beam techniques. The second procedure needing improvement is that of brazing porous emitter plates to dense molybdenum or tungsten housings in a relatively stress free condition, and by a metal iridium which would not accelerate tungsten densification as rhodium is expected to do.

The second approach consisted of preparing a 50 gram specimen with the composition of W-8Cu-1Ni-4Ir. The iridium was added as the chloride in solution in water, dried and reduced at 1500°F for 1 hour. The copper and nickel powder was added and mixed, pressed at 20,000 psi and sintered at 2150°F for 5 hours.

The grain size was 2-3 microns and since an eight micron grain was desired, the same compact was sintered at 2300°F for 5 hours, giving a grain size of 8-9 microns. HCl leaching studies indicated that only 6.8% weight loss occurred after two months, indicating that corrosion resistance was high and that excessive copper and nickel remained in the specimen.

The third approach which was studied briefly was that of innoculating the acid leached porous tungsten with a solution of iridium chloride. Upon drying, a coating of iridium chloride remained only on the top surface of the tungsten specimen.

Limited time prevented further exploration of these approaches, though further work is recommended.

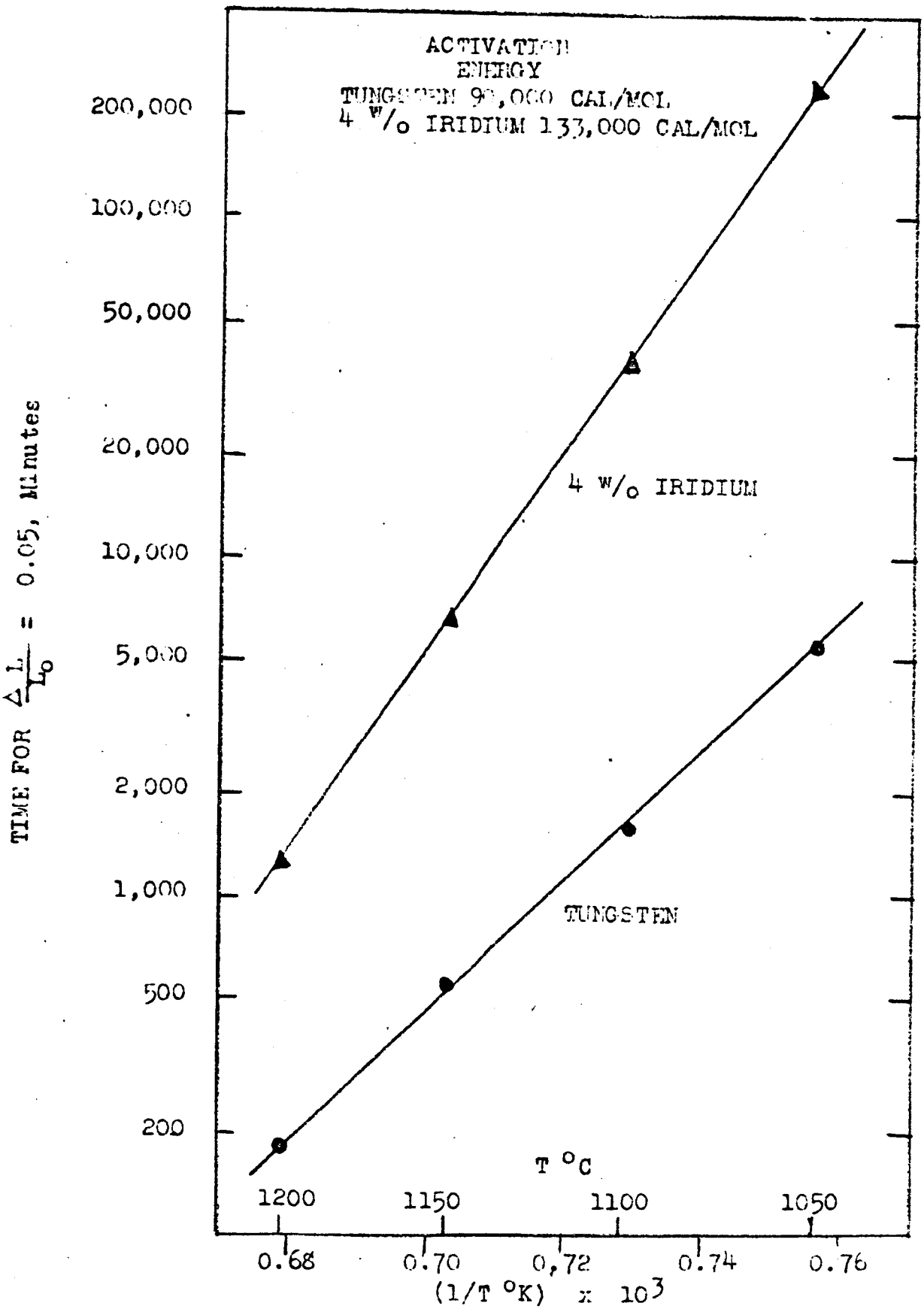

FIGURE 6-1 Arrhenius' Plots from Data from Sintering of Pure Tungsten and Iridium Tungsten.

7.0 Conclusions

7.1 Liquid phase sintering of W-Cu-Ni ternary alloy powder compacts was shown to produce a spherical tungsten structure which could be converted to useful ion emitter structures by further processing steps.

7.2 The grain size control of such structures was consistently shown to be dependent upon composition and low temperature sintering conditions which were easily controllable without highly specialized facilities.

7.3 Pore size uniformity and distribution was shown to be dependent upon fine particle copper and nickel powders, and milling procedures.

7.4 HCl acid leaching was shown to remove /99% of the initial copper-nickel content without specimen oxidation.

7.5 A hot nitric acid treatment was found to be necessary in order to eliminate finished ionizer thermal instability, which was believed to be caused by residual chlorine or nickel.

7.6 Though acid leaching caused edge spalling of thick specimens, this could be eliminated by coating specimen edges with glass or plated gold coatings.

7.7 The edge spalling problem was minimized simply by making the specimens oversize by about 3/8 of an inch.

7.8 High chemical purity and good specimen strength were attained by a vacuum vaporization and sintering cycle to a temperature of at least 2750°F for 4 hours.

7.9 Porous tungsten structures were prepared which met or exceeded porosity, density and permeability characteristic goals.

7.10 Mechanical surface finishing of sintered specimens was found to cause a serious problem due to increased densification and pore closure rates at high temperatures, such as attained during furnace bleaching and thermal aging.

7.11 Anodic etching was found to easily remove the worked tungsten surface when done prior to furnace bleaching where pore closure could occur.

7.12 The process is readily reproducible, uses relatively inexpensive materials and procedures.

8.0 Recommendations

8.1 In order to prepare even more perfect porous tungsten ion emitters by the liquid phase sintering process, studies should be conducted using copper and nickel powders below 1 micron, as well as tungsten at about 0.1 micron particle diameter.

8.2 More extensive studies should be made of various milling techniques and correlated with tungsten grain size, pore size, pore distribution, permeability and cesium ionization characteristics.

8.3 Studies should be made of other leaching procedures in order to decrease leaching periods.

8.4 The significance should be determined of residual nickel and chlorine contents (following HCl leaching) upon pore closure rates. This should be done by a systematic approach where more extensive chemical analyses are used for identifying exact contamination levels resulting from various process steps.

8.5 Sixth generation tungsten emitter specimens should be processed through higher bleaching temperatures in order to determine resulting pore characteristics and thermal stability.

8.6 The process reproducibility should be determined by producing a series of large scale-up plates at least 2" x 4" in area, and measuring grain and pore characteristics.

8.7 Structural uniformity levels should be determined by quality control measurements.

8.8 Studies should begin on advanced emitter structures with pore diameters of about 0.5 micron, and pore density of 10^8 pores/cm^2, which are feasible by this process.

8.9 Thermal stability of 6th generation, as well as advanced sub-micron pore size structures, should be established by determining activation energy and densification rate values by more extensive aging studies.

8.10 Tungsten-iridium structures should be further explored for increasing thermal stability.

8.11 Further studies should be made of the iridium deposition process, using copper as a solvent, to produce controlled closed pore zones in various emitter plate configurations.

8.12 Iridium deposition should be explored as a means of joining porous tungsten emitters to non-porous capsules, as an improvement over rhodium brazing and electron beam welding.

8.13 Improved spectrographic analysis techniques should be developed in order that consistent results may be more readily attainable.

9.0 REFERENCES

1. Husman, O. K.; Hughes Research Laboratories; "A Comparison of the Contact Ionization of Cesium on Tungsten with That of Molybdenum, Tantalum and Rhenium Surfaces"; AIAA Electric Propulsion Conference, March 11-13, 1963, AIAA Preprint No. 63019.

2. Todd, H.; "Ionizer Development and Surface Physics Studies"; NAS 8-1537, Interim Summary Report, December 21, 1962.

3. LaChance, M. and Kuskevics, G.; Electro-Optical Systems, Inc.,; "Ionizer Reservoir Development Studies"; EOS Report 2150-Final; Contract NAS 8-2547; May 30, 1963

4. Husman, O. K.; Hughes Research Laboratories; "Experimental Evaluation of Porous Materials for Surface Ionization of Cesium and Potassium"; presented American Rocket Society; March 14-16, 1962; ARS #2359-62

5. Saunders, N.T.; "Experimental Method of Producing Porous Tungsten for Ion Rocket Engines"; NASA Technical Note D864, June 1961

6. Gerken, J. M., Hiltz, R. H., and Lally, F. J.; "Development and Testing of Tungsten Emitters for Ion Propulsion Systems"; ASD-TDR-62-756, August, 1962; Thompson-Ramo-Wooldridge, Inc.

7. Taylor, L. H. and Teem, J. M.; Electro-Optical Systems Inc.; "Ionizer Development and Surface Physics Studies"; EOS Report 1660/1-IR-1; NASA Contract NAS 8-1537; December 21, 1962

8. Schwarzkopf, P.; Powder Metallurgy, Macmillan, 1947, Chapter 8, p 171 and Chapter 13

9. Smithells, C. J.; "Tungsten", 2nd Edition, Chapman & Hall, London, 1945, pp 54-59

10. Kieffer, R., and Hotop, W.; "Pulvermetallurgie and Sinterwerkstoff" Springer, Berline, 1943, p 231 ff.

11. Met. Powder Report, 2, No. 8, 119 (1948)

12. Kurtz, J., Procedures of Second Annual Spring Meeting of Metal Powder Asso., New York, June 13, 1946, p 40.

13. Goetzell, C. G., "Treatise on Powder Metallurgy", Interscience Publishers, Inc.

14. Kamm, R., Steinberg, M. A., and Wulff, J., "Trans. Am, Inst.Mining Met. Engrs., 180,694 (1949)

15. Seitz, F., Physics of Metals Chapter XII

16. Anglin, A. E., Jr.; "Problems of Porous Tungsten Ionizers for Cesium Electric Propulsion Systems", SAMPE June 3-5, 1963, Philadelphia

17. Brophy, Hayden, Kreider and Wulff; "Activated Sintering of Pressed Tungsten Powders and Plasma Jet Sprayed Tungsten Deposits", BuWeaps - No. 61-0326-c, Sept. 25, 1961

18. LaChance, M.; Electro-Optical Systems, Inc.; "Porous Ionizer Development and Testing"; 2nd Quar. Report on NASA Contract NAS 3-2519; EOS Report 3720-Q-2, August 20, 1963

19. Price, Smithells and Williams; "Sintered Alloys - Part I"; J. Inst. Metals, V62 No. 1, 1938, pp 239-254

20. Smithells, C. J.; "Method of Manufacturing of Heavy Metallic Materials; U. S. Patent No. 2,183,359, December 12, 1939

21. Brophy, Hayden, Prill and Wulff; "The Investigation of the Activated Sintering of Tungsten Powder" Bu. Weaps. No. 61-0326-d, Final Report, February 28, 1963

22. Brophy, Shepard and Wulff; "The Nickel Activated Sintering of Tungsten"; Powder Metallurgy, pp 113-135, Leszynski, 1960 Interscience Publishers.

23. Graham, J. W.; "Development of Stabilized Porous Tungsten Ion Emitters" Final Report NASA Contract NAS 3-2513, January, 1964

24. Ritter, H. L., and Drake, L. C.; "Pore-Size Distribution in Porous Materials" Industrial & Engineering Chemistry - Analytical Edition - Vol. 17, No. 12, pp 782 - 786, December, 1945

25. LaChance, M., Kuskevics, G., and Thompson, B.; "Porous Ionizer Development and Testing", Final Report NASA CR 54016 Contract NAS 3-2519, May, 1964, p 4-23

26. Uhlig; "Corrosion Handbook", John Wiley & Sons, Inc., 1963

27. McIntyre, R. D.; "The Effect of HCl-H_2 Sintering Atmosphere on the Properties of Compacted Tungsten Powder", Trans. A.S.M., Sept. 1963, pp 468-476

28. Cotton, Text Book of Inorganic Chemistry

DISTRIBUTION LIST FOR FINAL REPORT
Contract NAS3-4115

	Addressee	Number of Copies
1.	NASA Headquarters FOB-10B 600 Independence Avenue, Northwest Washington, D. C. 20546 Attn: RNT/James Lazar	2
2.	Aeronautical Systems Division Wright-Patterson Air Force Base, Ohio Attn: Lt. Vickers AFAPL (APIE)	2
3.	NASA-Lewis Research Center 21000 Brookpark Road Cleveland, Ohio 44135 Attn: W. Rayle	1
4.	NASA-Lewis Research Center Spacecraft Technology Division 21000 Brookpark Road Cleveland, Ohio 44135 Attn: J. H. Childs	2
5.	NASA-Lewis Research Center Spacecraft Technology Division 21000 Brookpark Road Cleveland, Ohio 44135 Attn: A. E. Anglin	12
6.	Hughes Research Laboratory 3011 Malibu Canyon Road Malibu, California Attn: Dr. George Brewer	1
7.	NASA-Lewis Research Center Technology Utilization Office 21000 Brookpark Road Cleveland, Ohio 44135	1
8.	NASA-Lewis Research Center Spacecraft Technology Procurement Section 21000 Brookpark Road Cleveland, Ohio 44135 Attn: John H. DeFord	1

	Addressee	Number of Copies
9.	Jet Propulsion Laboratory 4800 Oak Grove Drive Pasadena, California Attn: Mr. J. J. Paulson	1
10.	NASA-Langley Research Center Technical Library Langley Field, Virginia	1
11.	General Electric Company Flight Propulsion Laboratories Cincinnati, Ohio 45215 Attn: R. N. Edwards	1
12.	Thompson Ramo Wooldridge, Inc. New Devices Laboratory 7209 Platt Avenue Cleveland, Ohio Attn: Dr. Park French	1
13.	Space Technology Laboratories 8433 Fallbrook Avenue Canoga Park, California Attn: Dr. D. Langmuir	1
14.	North American Aviation, Inc. Rocketdyne Division 6633 Canoga Avenue Canoga Park, California Attn: Dr. Clayton McDole	1
15.	The Marquardt Corporation Astro Division 16555 Saticoy Street Van Nuys, California	1
16.	Headquarters - USAF Air Force Office of Scientific Research Washington, D. C. 20025 Attn: Dr. M. Slawsky	1
17.	Aerojet-General Nucleonics Division San Ramon, California Attn: Mr. J. S. Luce	1

	Addressee	Number of Copies
18.	NASA-Marshall Space Flight Center Huntsville, Alabama Attn: Mr. Henry Martin	1
19.	NASA-Marshall Space Flight Center Huntsville, Alabama Attn: Dr. E. Stuhlinger	1
20.	NASA-Lewis Research Center Library 21000 Brookpark Road Cleveland, Ohio 44135	2
21.	Aerospace Corporation Technical Documents Group P. O. Box 95085 Los Angeles, California 90045	1
22.	Westinghouse astronuclear Laboratories Electric Propulsion Laboratory Pittsburgh, Pennsylvania 15234 Attn: Mr. H. W. Szymanowski	1
23.	AFWL Kirtland Air Force Base, New Mexico Attn: Capt. C. F. Ellis/WLPC	1
24.	NASA-Lewis Research Center Electric Propulsion Laboratory 21000 Brookpark Road Cleveland, Ohio 44135 Attn: W. R. Mickelsen	1
25.	NASA-Lewis Research Center Electric Propulsion Laboratory 21000 Brookpark Road Cleveland, Ohio 44135 Attn: W. E. Moeckel	1
26.	Space Technology Laboratories One Space Park Redondo Beach, California Attn: Dr. Heywood Shelton	1

	Addressee	Number of Copies
27.	NASA - Scientific & Technical Information Facility Box 5700 Bethesda 14, Maryland	6
28.	NASA-Lewis Research Center 21000 Brookpark Road Cleveland, Ohio 44135 Attn: Reports Control Office	1
29.	Defense Metals Information Center Battelle Memorial Institute 505 King Avenue Columbus 1, Ohio	1